Enhancement of Perception with the Application of Stochastic Vestibular Stimulation

by

Raquel Galvan-Garza

B.S. Aerospace Engineering
The University of Texas at Austin, 2009

S.M. Aeronautics and Astronautics
Massachusetts Institute of Technology, 2012

SUBMITTED TO THE DEPARTMENT OF AERONAUTICS AND ASTRONAUTICS IN PARTIAL FULFILLMENT OF THE REQUIREMENTS FOR THE DEGREE OF

DOCTOR OF PHILOSOPHY IN AERONAUTICS AND ASTRONAUTICS
AT THE
MASSACHUSETTS INSTITUTE OF TECHNOLOGY

June 2016

Signature of Author: Signature redacted

Raquel Galvan-Garza
Department of Aeronautics and Astronautics
May 19, 2016

Accepted by: Signature redacted

Paulo C. Lozano
Associate Professor of Aeronautics and Astronautics
Chair, Graduate Program Committee

Enhancement of Perception with the Application of Stochastic Vestibular Stimulation

by

Raquel Galvan-Garza

DOCTOR OF PHILOSOPHY IN AERONAUTICS AND ASTRONAUTICS
AT THE
MASSACHUSETTS INSTITUTE OF TECHNOLOGY

Certified by: Signature redacted

Charles M. Oman
Senior Research Engineer, Senior Lecturer
Department of Aeronautics and Astronautics
Massachusetts Institute of Technology
Thesis Committee Chair

Certified by: Signature redacted

Torin K. Clark
Assistant Professor
Aerospace Engineering Sciences
University of Colorado
Thesis Committee Member

Certified by: Signature redacted

Ajitkumar P. Mulavara
Senior Scientist
Universities Space Research Association
Neuroscience Lab at NASA Johnson Space Center
Thesis Committee Member

Certified by: Signature redacted

Leia A. Stirling
Assistant Professor
Department of Aeronautics and Astronautics
Massachusetts Institute of Technology
Thesis Committee Member

Enhancement of Perception with the Application of Stochastic Vestibular Stimulation

By
Raquel Galvan-Garza

Submitted to the Department of Aeronautics and Astronautics on
May 19, 2016 in Partial Fulfillment of the Requirements for the Degree of
Doctor of Philosophy in Aeronautics and Astronautics

Abstract

Astronauts experience sensorimotor changes during spaceflight, which may degrade their operational capabilities. A sensorimotor countermeasure that mitigates these effects would improve crewmember safety and decrease mission risk. The goal of this research was to investigate the potential use of electrical stochastic vestibular stimulation (SVS) as a sensorimotor aid to lower vestibular thresholds and improve manual control. We hypothesized that low-level, subsensory bandlimited white noise (±200 - ±700 μA peak, 52 - 182 ±5% μA RMS) passed between surface electrodes located on the mastoid bone behind each ear would enhance perceptual sensitivity to physical motions due to the phenomenon of stochastic resonance (SR). The goals of this research were to 1) demonstrate that SVS can significantly reduce vestibular direction recognition thresholds, 2) investigate whether the SR phenomenon involves stimulation of the semicircular canals, otoliths or both, and 3) demonstrate that SVS can improve perception-based manual control performance in a task relevant to piloting during planetary landing, docking, or other vehicle maneuvers.

In a first experiment, upright roll tilt direction recognition thresholds, which elicit responses from both the semicircular canals and otoliths, were measured with varying levels of SVS applied. Upright roll tilt direction recognition thresholds exhibited characteristic SR dependency on current level that was statistically significant in 6/12 subjects. However, SR repeatability across days was found to be weak, only present in 3/12 subjects.

In a second experiment, supine roll rotation (primarily stimulating the semicircular canals) and inter-aural translation (primarily stimulating the otoliths) direction recognition thresholds were measured with varying levels of SVS applied. SR was exhibited in inter-aural translation (6/11 subjects) but not supine roll rotation (1/12 subjects), suggesting that stimulation of the otolith organs may be vital to vestibular perceptual SR. Simulations of the experimental test procedure were used to create a dataset of direction recognition thresholds with several predefined underlying SR exhibition levels. A comparison of the results form Experiment 1 and 2 to the simulated datasets allowed us to more confidently draw conclusions from data that are prone to the existence of false positives.

In a third experiment, subjects used vestibular information to null out pseudo-random vehicle disturbance in a manual control task. SVS (±300 μA) improved the group mean position variability when motions were near threshold and extended the range of frequencies in which motions could be nulled out.

The results of this thesis are consistent with the concept that SVS is able to extend the operating range of the vestibular perceptual system in some individuals. In the context of human spaceflight, results from this research further our understanding of how SVS may be implemented in the future as a component of a comprehensive spaceflight countermeasure plan.

Thesis Advisor: Dr. Charles Oman
Title: Senior Research Scientist

Acknowledgments

This work was made possible with the generous funding support from a NASA Space Technology Research Fellowship #NNX13AM68H, the National Space Biomedical Research Institute through NASA NCC9-58, Universities Space Research Association, the Office of the Dean for Graduate Education at MIT, and the department of Aeronautics and Astronautics at MIT.

Thank you to my MIT advisor and Thesis Committee Chair, Chuck Oman. You have been such a steady voice of reason throughout my time at MIT and I am so thankful for the incredible opportunities that you have provided to me. Your infinite enthusiasm and passion for science has been a huge inspiration. Thank you Torin Clark for your endless patience, help, and willingness to talk through anything. This work would not have been possible without your insight and your unbelievably valuable advice and I am so appreciative of the time that you devoted to helping me with this project. Your ability to always stay calm and find a solution to any problem is something that I aspire to have. Thank you Leia Stirling for your help throughout and for your insightful and spot-on questions and comments. Thank you Ajit Mulavara for allowing me to join you in your fascinating stochastic resonance work. You have always made yourself available and have generously helped me every single step of the way with your patient guidance. I am so extremely grateful to you for all of your help. Thank you to Jacob Bloomberg for being my NASA mentor, for your valuable insight, and constant support.

Thank you to everyone in the Jenks Vestibular Physiology Lab at the Massachusetts Eye and Ear Infirmary, for letting me join your family for the past few years and for being such an amazingly supportive group of people. Thank you to Dan Merfeld for your feedback as a thesis reader, for allowing me to come into your lab and do these experiments, and for letting me build on the significant work that you and your lab have accomplished. Thank you to Faisal Karmali for being an insightful thesis reader and for your amazing advice and mentorship on this project and others.

Thank you to everyone in the Man Vehicle Lab at MIT, past and present. It has been a privilege to be a part of such a smart, passionate, and fun group of people and I'm so thankful for the life long friends that I've gained. Thank you David Sherwood for all the good times running these experiments and thank you Liz Zotos for helping me in a million different ways.

Thank you to my friends. Abhi, I'll be eternally thankful that we got to go through this together, and I'm so happy for you and all of your successes that I know are still to come. We slay. Maddie, Jacob, Ben, Phil, Ana, Alexandra, Marissa, Dustin, Aaron, Andie, Sathya, Allie, Ally, and Allie, ... what would I have done without you? Thank you.

Thank you to my family, Ana and Al Galvan, Jessica and Ty Albers, and Martina Galvan. You have always believed in me and built me up even when I wasn't so sure myself. I love you.

Thank you to my absolutely incredible husband, Joel Garza. You have given me the kind of love and support that just seems unreal. Thank you for moving across the country to be with me through all of this and for being the most caring, giving, funny, and ridiculous partner during this amazing chapter of our lives. Más.

Table of Contents

List of Acronyms

CNS – Central Nervous System
EVA – Extravehicular Activity
GVS – Galvanic Vestibular Stimulation
JSC – Johnson Space Center
JVPL – Jenks Vestibular Physiology Laboratory
KSS – Karolinska Sleepiness Scale
MEEI – Massachusetts Eye and Ear Infirmary
MIT – Massachusetts Institute of Technology
DR Threshold – Motion Recognition Threshold
NASA – National Aeronautics and Space Administration
OTTR – Otolith Tilt-Translation Reinterpretation
PVM – Position Variability Metric
PVT – Psychomotor Vigilance Test
RMS – Root Mean Square
ROTTR – Rotation Otolith Tilt-Translation Reinterpretation
SPM – Scalar Performance Metric
SR – Stochastic Resonance
SCC – Semicircular Canal
SVS – Stochastic Vestibular Stimulation
VOR – Vestibular Ocular Reflex

List of Figures

List of Tables

1 Introduction

Astronauts experience sensorimotor changes due to gravity transitions that occur during spaceflight (Figure 1). These sensorimotor changes are known to cause decrements in functional performance such as spatial disorientation, postural and gait instability, motion sickness, visual performance changes, and impaired motor control (Reschke et al. 1998, Paloski et al. 2008). The mission phase in which astronauts return to Earth after spaceflight, or land on another planetary surface after time in microgravity, is of particular concern in the context of sensorimotor adaptation. This is because degraded functional performance associated with the transition from microgravity to Earth's gravity or the gravity on another planet could hinder the ability of the astronauts to perform critically important tasks such as the actuation of controls and visual monitoring of displays typically associated with landing operations. Mission success may be particularly affected during an emergency scenario in which an astronaut is required to perform a task that heavily relies on sensorimotor function such as an off-nominal landing or an unplanned or unassisted vehicle egress before having an adequate amount of time to adapt to the new gravity environment. An emergency Extravehicular Activity (EVA) on another planetary surface too soon after landing would be particularly risky because of the impossibility of assistance from a ground crew.

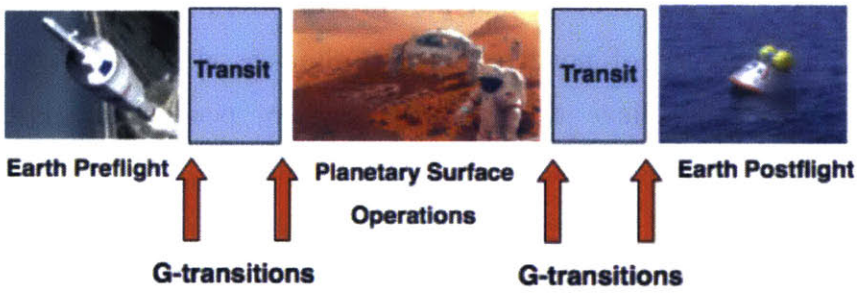

Figure 1. G-transitions that could occur during a planetary exploration mission.

Currently, time is the primary aid in driving sensorimotor function back to normal, allowable levels after exposure to altered-gravity. The time to recover depends on time in microgravity, the specific task being tested, and individual differences but for locomotor performance, has been measured to range from 2-15 days (Bryanov et al. 1976, Paloski et al. 1992, Mulavara et al. 2010, Bloomberg and Mulavara 2003, Courtine and Pozzo 2004). Astronaut safety and mission

success could be substantially improved if there existed a sensorimotor countermeasure that could enable astronauts to more quickly adapt to the new environment. Critical to sensorimotor adaptation in altered gravity environments is the vestibular system (Young 1984, Parker 1985). Located in the inner ear, the vestibular system senses information about one's position and movement in space to the brain. While not the only sensory system for orientation perception and control (e.g. visual, proprioceptive, somatosensory, etc.), the vestibular system is a logical system to focus on for the development of a sensorimotor countermeasure. Although not yet used in practice, the application of subsensory electrical stochastic vestibular stimulation (SVS) has been identified as a method for improving sensorimotor function via the phenomenon of stochastic resonance (SR), in which the response of a non-linear system to a weak input signal is optimized by the presence of a particular non-zero level of noise (Moss 1994, Collins et al. 1995, 2003, McDonnell and Abbott 2009). SVS is a specific type of Galvanic Vestibular Stimulation (GVS), which electrically stimulates the vestibular afferent neurons (Goldberg 1984, 2000), and has been used to study the responses to vestibular stimulation for almost 200 years (Purkyne 1819). Although not defined as such, GVS typically refers to the application of current to the vestibular system at levels high enough such that the person who is being stimulated perceives an illusory self-motion. In contrast, the SVS used in this research is limited to current levels that are relatively low and noisy such that they elicit no such motion perception on their own. The SR phenomenon is based on the concept that the flow of information through a system can be maximized by the presence of nonzero noise (Collins et al. 2003). Therefore, with the application of SVS, we believe that vestibular system performance is improved by an enhancement in the transfer of vestibular sensory information.

Interestingly, SR theory originated from the desire to explain the Earth's periodic glacial variations over time. It was reasoned that the planet's glacial state changes could be attributed to small fluctuations in the eccentricity of the Earth's orbit compounded with the presence of environmental noise (Benzi et al. 1981, 1982, Nicolis 1981, 1982). SR using various sources of non-vestibular noise has since been shown to exist in a variety of physiological systems, including vision (Ward et al. 2001, Simonotto et al. 1997), tactile sensation (Collins et al. 1996a, 1996b, 1997), hearing (Zeng et al. 2000), and balance (Priplata et al. 2002, 2003, Gravelle 2002). SR via the specific application of SVS has been shown in ocular reflexes in response to whole-

body tilts (Geraghty et al. 2008), postural balance in Parkinsonian patients (Pal et al. 2009) as well as healthy individuals (Mulavara et al. 2011, Goel et al. 2015), and locomotor stability (Mulavara et al. 2015).

In the context of improving sensorimotor function after G transitions during spaceflight, Bloomberg and colleagues (2015) have suggested that SVS might be best used as an aid in a pre-flight sensorimotor adaptability training program. They suggest that pre-flight training with SVS could benefit post-flight performance without SVS (an offline application). They reason that for a visually dependent subject, the enhancement of vestibular information from SVS in pre-flight training may promote the use of multiple sensory sources, rather than relying primarily on visual information. They believe this strategy of more equally weighing multiple sensory inputs may enhance one's capacity for adapting to sensory discordant environments and may therefore benefit post-flight adaptation in a novel sensory environment. As a clinical online application it has been suggested that a patch-type SVS stimulator device could be worn by people with disabilities due to aging or disease in order to improve functional balance and locomotion (Mulavara et al. 2011). Whether SVS would indeed be beneficial if implemented as an online patch-type wearable device during a spaceflight mission, for example upon landing on another planet, has not yet been determined. There may be complex interactions between vestibular adaptation to G-transitions and effects of SVS on the vestibular system that are not well understood. Thus it is difficult to predict what the effect of SVS could be on a microgravity adapted astronaut returning to Earth or partial gravity. The goal of this work was to look for stochastic resonance in vestibular performance and to begin to answer fundamental questions related to how and when vestibular SR occurs. The findings from the research will help direct future vestibular SR research, particularly for human spaceflight and clinical applications

This thesis first reviews the relevant literature, and then presents the results of three studies. The first study aimed to definitively show the exhibition of SR in vestibular perception, a basic component of sensorimotor performance and adaptation. The second study investigated whether the phenomenon of vestibular SR is specific to the semicircular canals or otoliths, the two organs of the vestibular system. This study was a first step in better understanding the fundamental requirements of SR exhibition in the vestibular system, a phenomenon that is still very much

viewed as an output characteristic of a black box system. Lastly, the third study aimed to investigate whether vestibular SR could be measured in a less clinical, more operationally relevant manual control task that has similarities to some piloting operations. Research involving the application of stochastic vestibular stimulation to invoke vestibular SR is in its early stages and there remain many unanswered questions that warrant further study. Therefore, this thesis concludes with ideas for future research involving SVS.

2 Background

2.1 Post Spaceflight Sensorimotor Function

Sensorimotor control requires central nervous system (CNS) integration of multiple sensory inputs including information from the visual, proprioceptive, tactile and vestibular systems. When function of even just one of these sensory systems is altered, sensorimotor control is altered and adaptation must occur to regain normal control of movement. During spaceflight G-transitions, the stimulation patterns of the vestibular system go through considerable changes. Primarily affected are the otolith organs, normally sensitive to gravity and linear accelerations, which become unloaded in microgravity and reloaded upon return to Earth. Both transitions require an adaptation period; however it is the transition from microgravity back to Earth gravity (or another planet's gravity) that causes sensorimotor issues that are particularly concerning for astronaut safety.

One of the most evident post-flight sensorimotor decrements is in balance and locomotion. Even after short duration flight, astronauts often have difficulty maintaining their balance and making typical motor movements. For example, compared to pre-flight, astronaut gait is wider and slower, and head movements are generally reduced post spaceflight (Bloomberg et al. 1997). Additionally, astronauts have less reliable motion perception post-flight (Clement and Wood 2014). Previous studies of motion thresholds, which can be thought of as motion perception sensitivity, measured post spaceflight have had mixed results. Thresholds of perception of whole-body 0.3 Hz linear oscillations, measured using a staircase procedure, were elevated post-flight in one Spacelab crew in the x- (anterior-posterior) and y- (medial-lateral) body axes but were lowered in another crew in the x-, y-, and z- (superior-inferior) axes (Benson et al. 1986).

Thresholds of the recognition of the direction of linear motions (direction recognition (DR) thresholds), measured using discrete linear movements more similar (but not identical) to those used in this research (Experiments 1 and 2) were found to be significantly higher in all axes than the pre-flight test on the first and second post-flight days. Thresholds continued to fall but did not return to pre-flight baseline within 7 days after returning from the German (D-1) Spacelab mission (Benson and Wetzig 1987). A study with similar procedures however found no post-flight impairment in thresholds to linear motion (Steinz 1980). A different method was used by Arrott et al. (1987) and Arrott and Young (1986) to estimate vestibular sensitivity. They used a time to detect task in which subjects had to signal the direction of motion (linear accelerations) as quickly as they could. There was no statistically significant difference in the time to detect metric between pre- and post-flight tests however the data showed that in four Spacelab-1 astronauts, estimated y-axis thresholds and variability increased post-flight. Another study showed that the time to detect linear accelerations in the y- and z-axes were significantly increased in three out of four astronauts who flew on the 14 day Spacelab Life Science-2 mission (Merfeld et al. 1996). The authors suggested that increased sensitivity to linear accelerations during spaceflight caused post-flight subjective confusion from the overly sensitive system on how to interpret signals from the graviceptors in the vestibular system, thus resulting in longer times to detect motion directions. This suggested subjective confusion might also account for the varying accounts of both decreased and increased motion thresholds post-flight across the studies discussed in this section. However, the same study also found that two of three subjects were significantly better at nulling their linear self-motion in the y- and x-axes suggesting an improvement in the ability to sense and respond to linear motions. These seemingly contradictory and findings were addressed by Merfeld et al. (1996) who suggested that the difference might be related to a difference in the magnitude of the linear accelerations in each task. The peak accelerations in the time to detect task were generally smaller than those in the linear manual control nulling task such that cues in the time to detect task might be primarily linear accelerations while in the nulling task, the brain may also interpret motions as tilts. Similar to the linear motion nulling task used in Merfeld et al. (1996), Merfeld (1996) measured the ability of returning Spacelab astronauts (14-day mission) to null out roll tilt motions in order to study the effect of spaceflight on tilt perception. Two astronauts tested on landing day had significant decrements in their nulling performance when tested in the dark, suggesting that the

CNS is unable to merge and interpret sensory cues into a single estimate of motion and orientation as well as pre-flight.

Some have speculated that the otolith unloading during spaceflight ultimately results in increased end organ sensitivity. Evidence of this has been found in the end organs of toadfish post flight (Boyle et al. 2001) and in rapid synaptic plasticity of rat otolith organs during spaceflight (Ross et al. 2003). Changes in vestibular system function appear to also occur at the level of central processing. The otolith tilt-translation reinterpretation (OTTR) hypothesis suggests that without otolith stimulation resulting from head tilts in microgravity, all otolith cues are reinterpreted by the CNS as linear acceleration, which causes misperceptions of tilt and translation post-flight (Young et al. 1984, 1986, Parker et al. 1985, 1986). The rotation otolith tilt-translation reinterpretation hypothesis (ROTTR) elaborates on OTTR by noting that rotational cues are normally important in decoding ambiguous otolith information, so that gravitational and acceleration cues can be distinguished. It suggests that the neural networks that are responsible for these types of calculations deteriorate in microgravity such that post flight, rotational cues are used incorrectly to perceive orientation with respect to gravity (Merfeld 2003).

It is important to note that the vestibular system is not the only input to the central nervous system in regards to sensorimotor function and performance. Other inputs include visual and proprioceptive information. Because otolith information is altered in microgravity, sensory integration seems to more heavily weigh visual inputs during flight. This has been shown through increased sensations of circular vection while in a rotating dot-patterned drum (Young et al. 1986) and linear vection when immersed in a virtual visual environment (Oman et al. 2003). An increase in linear vection has also been shown to occur in parabolic flight (Liu et al. 2002). The proprioceptive system also adapts in microgravity. More specifically, it has been shown that post flight there is a decrease in dynamic motor responses to proprioceptive stimulation and a reduction in vibration-induced illusions with ankle muscle stimulation. The perceptual responses were not different with neck muscle stimulation (Roll et al. 1998).

Time spent in microgravity can lead to reweighting of visual, proprioceptive, and vestibular components of central sensorimotor processing of body orientation and posture (Mulavara et al.

2012). Although multiple systems are likely affected, it has been suggested that the change in the vestibular system function and processing during spaceflight has the largest detrimental effect on sensorimotor function, including posture and balance (Buckey 2006).

2.2 Sensorimotor Adaptation

Consistent with the two stage adaptation process described in a review paper by Bastian (2008), adaptation to a novel gravitational environment has been described to occur in two stages: (1) a fast, "within-session" improvement that can be induced by a limited number of trials on a time scale of minutes and (2) a slowly evolving, incremental performance improvement, triggered by practice but taking hours to become effective (Karni and Bertini 1997). Performance by astronauts after long duration spaceflight on a functional mobility task that required navigation through an obstacle course (Figure 2A) was found to be severely degraded compared to pre-flight performance. Early motor adaptation, related to changes in strategy for completing the task, occurred immediately post-flight (Figure 2C) and was found to positively correlate to long-term recovery (Figure 2B, Mulavara et al. 2010). These results suggest that the initial strategic adaptation processes reinforces long-term learning.

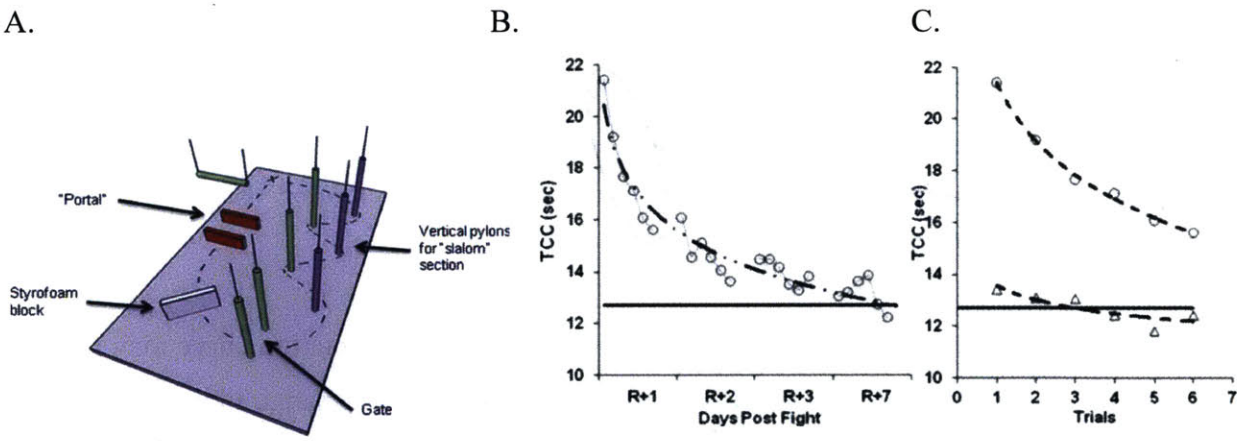

Figure 2. Functional Mobility Test used to assess post-flight locomotor function in astronauts. A: Schematic of obstacle course. B: A single crewmember's time to complete the course for all trials during multiple sessions. The curve illustrates long-term recovery. C: Enlarged view of trial times 1 day post-flight. The curve represents short-term recovery. Horizontal line in A and B represented pre-flight baseline performance (from Mulavara et al., 2010).

Using a visuomotor task which included complex optical rotations, Landi et al. (2011) found a correlation between the change in gray matter concentration over the hand area of the

contralateral primary motor cortex measured immediately after a one week training period to improvements in the speed of learning one year later. This study was the first to show that early structural changes in the brain can predict behavior long term.

The goal of quickening adaptation could potentially be accomplished in several ways, exemplified in Fig. 3, which shows a nonspecific performance measure that is elevated immediately post-flight and gradually adapts back to baseline over time. The decrement in post-flight performance can be approximated by a decaying exponential characterized by a magnitude and a recovery slope (Figure 3, blue circles). If the goal is to reduce the post-flight decrement to some set criterion level, this could be achieved either by a steepening of the recovery slope (Figure 3, purple squares), a discrete reduction in the magnitude of the decrement (Figure 3, red triangles), or some combination of the two (Figure 3, green stars).

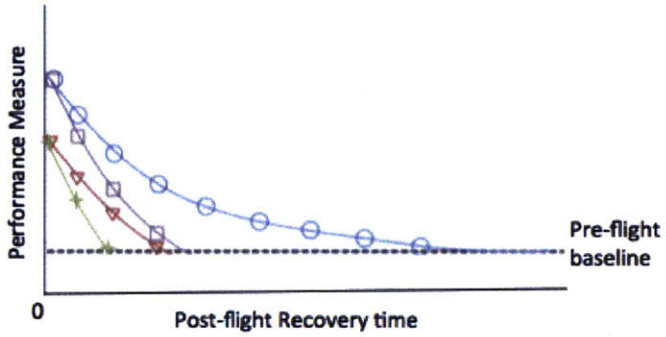

Figure 3. Theoretical adaptation curves for a generic performance measure that decreases with adaptation time. As a generic example of post spaceflight adaptation, the x-axis represents post flight recovery time and the dashed line represents the measured performance pre-flight.

The shift from the blue curve to the red curve represents what the adaptation curve may look like with a post-flight countermeasure in place that causes an immediate change in performance. As mentioned earlier, whether the application of SVS can be used as an effective sensorimotor countermeasure for spaceflight is yet to be validated. However if it or a different performance enhancing countermeasure were to be used, it is important to note a quicker return to pre-flight baseline performance could be achieved without necessitating a steepening of the adaptation curve. As discussed earlier, Bloomberg et al. (2015) speculate that SVS may be most appropriately used as a pre-flight training aid and not during a post-flight phase. In that capacity,

the aim would be to accomplish a steepening of the adaptation curve post-flight (purple squares) via residual pre-flight training effects. As mentioned by Mulavara et al. (2011) a patch-type wearable SVS device might be appropriate in a clinical setting. Perhaps in the non-spaceflight context of clinical rehabilitation, adaptation with SVS could resemble the shifted (Figure 3, red triangle) or shifted and steepened (Figure 3, green stars) curves.

2.3 The Vestibular System

The vestibular system senses motions of the head in space. It is located in the inner ear and is made up of two types of sensors, the semicircular canals (SCCs) and the otoliths. The SCCs are sensitive to angular acceleration (Reisine et al. 1988), however due to the fluid mechanics of the canals, the SCC neural output actually closely matches angular velocity (Fernandez and Goldberg 1971, Hullar et al. 2005, Hullar and Minor 1999, Sadeghi et al. 2007). There are three roughly orthogonal canals, the horizontal, superior, and posterior SCCs which sense angular velocities in the approximately yaw, pitch, and roll motion planes. The otolith organs are sensitive to gravito-inertial linear accelerations (Fernandez and Goldberg 1976a, 1976b, 1976c) and include the utricle and saccule, which relative to the head are approximately in the horizontal and vertical plane aligned anteroposterior, respectively. Because the otoliths are accelerometers, they are unable to differentiate between changes in inertial and gravitational accelerations (Einstein's equivalency principle, Einstein 1945) so they cannot distinguish between linear translation and tilt without additional information and processing from the CNS.

Most SCC and otolith primary afferent neurons have a resting discharge that allows the neurons to respond to accelerations and decelerations through an increase or decrease in firing rate. The SCCs on either side of the head are symmetric and therefore, each provides the same but opposite signals, working together in a push-pull manner to effectively sense motions in both positive and negative directions. Each otolith organ has hair cells lined up in approximately opposite directions across a midline named the striola. This cell arrangement causes both excitation and inhibition within a single otolith organ in response to a linear acceleration in a single direction.

2.4 Galvanic Vestibular Stimulation

In the late 1700's Luigi Galvani, an Italian physicist and biologist, was studying the nervous system of the frog and discovered that distant electrical discharges of the lumbar nerve would cause the muscles of a dead frog's legs to contract (Galvani 1791). This first display of bioelectricity became known as galvanism and has been used extensively since then to study the form and function of the nervous system.

Galvanic vestibular stimulation (GVS) has since been defined as the transcutaneous delivery of electric currents to the vestibular afferents (for review see Fitzpatrick and Day 2004). Spike recording experiments in animals stimulated by in vivo GVS have been conducted to understand the resulting vestibular neuron activation. GVS activates primary otolith and semicircular canal afferent neurons (Kim and Curthoys 2004) and is believed to probably act at the spike trigger zone of the primary afferents (Goldberg et al. 1982, Goldberg 1984), bypassing the transduction mechanism of the hair cells (Fitzpatrick and Day 2004). A few studies, using isolated guinea pig vestibular hair cells, showed that the presence of an extracellular alternating current field evoked fast length changes of the cell "neck", suggesting that the electricity may also affect the hair cell itself (Zenner and Zimmerman 1991, Zenner et al. 1992). Whether GVS applied to the skin of humans is only affecting the vestibular afferent spike trigger zones or the mechanical responses of the vestibular hair cells, or both, is unsettled. The most popular opinion in the literature is that the spike-trigger zone is likely the affected site.

A steady nonzero level of current increases the firing rate of the vestibular afferents on the cathodal side (depolarization) and decreases the firing rate of the vestibular afferents on the anodal side (hyperpolarization) (Goldberg 1984, 2000). Irregular vestibular neurons are more sensitive to GVS than regular neurons (Goldberg et al. 1984, Kim and Curthoys 2004) with an increase in firing rate about 20 times greater in irregular than regular units (Smith and Goldberg 1986, Goldberg et al. 2012). When galvanic current is applied, the shift in the mean voltage trajectory is only slightly shifted up for the regular units and results in a small increase in firing rate (Figure 4, A and C). However in the irregular unit, a similar shift results in a considerable increase in firing rate because of the many peaks that were already quite close to the firing threshold (Figure 4, B and D). Although the galvanic current affects the firing rate of the

irregular neuron, it does not change the shape of the afterhyperpolarizations, which are still deeper and slower in the regular unit compared to the irregular unit.

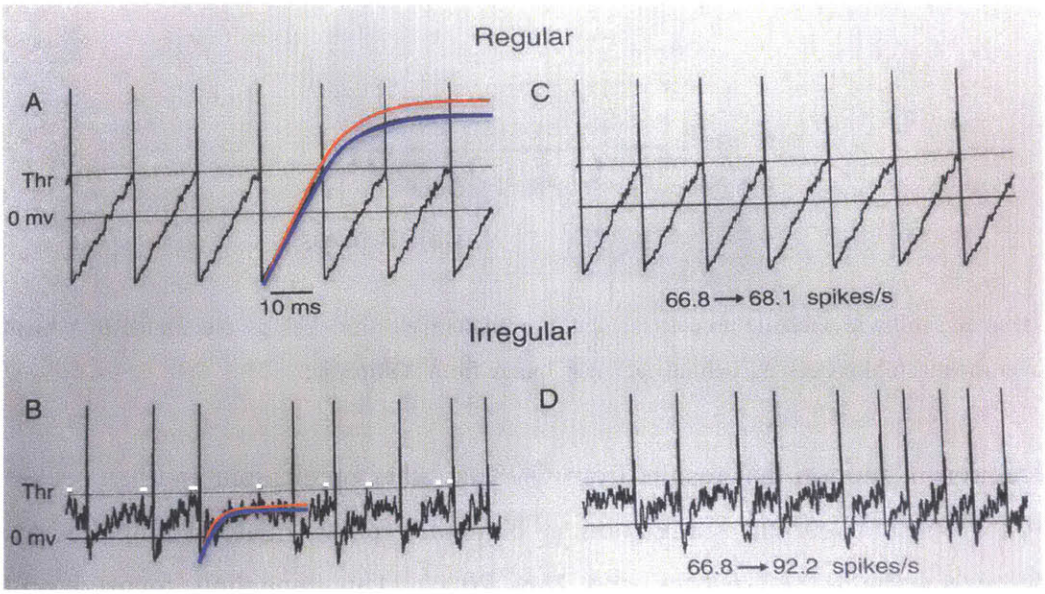

Figure 4. Simulated representation of the stochastic model of repetitive discharge for a primary regular neuron (A) and irregular neuron (B). Random timing of quanta (miniature excitatory post synaptic potentials) introduce synaptic noise in both cases. However, the quantal size is larger in the irregular unit. Thick blue lines represent the mean voltage trajectory and thin red line represents the effects of galvanic current. The effects of 1-mV depolarization on the firing rate are shown for the regular (C) and irregular (D) unit in an increase in firing rate. The white dots above the threshold line in subplot B mark peaks in the trajectory that are within 1 mV of threshold, which when crossed triggers an action potential or neuron fire. (Figure modified from Goldberg et al. 2012, Based on Smith and Goldberg 1986).

In human studies, GVS has typically been applied through surface electrodes placed on the skin of each of the mastoid processes with the cathode on one side and anode on the other (i.e., bilateral bipolar GVS, see Figure 5). Less common GVS configurations include bilateral monopolar GVS in which the electrodes on each mastoid (behind each ear) are both of the same polarity and an electrode of the other polarity is located at a distant location, and unilateral monopolar GVS in which an electrode is placed behind only one ear. In guinea pigs, the transmission of the signal through the head is such that if applying current to the skin surface over the mastoid, ten times as much current is needed to create the same change in firing rate accomplished by applying current to the tensor-tympanic muscle, which is very close to the end organs (Kim and Curthoys 2004).

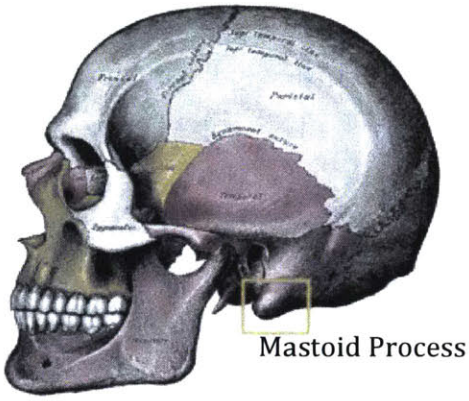

Figure 5. Human skull with mastoid process labeled. For bilateral electrode setups, electrodes are typically placed on the skin over the mastoid processes, behind each ear. Image from Wikipedia.

The perception of motion that results from GVS is rather predictable and has been extensively modeled for constant current stimulation in bilateral bipolar, bilateral unipolar, and unipolar electrode arrangements (Fitzpatrick and Day 2004). This modeling focused on predicting perceptual responses based on the geometry of the vestibular anatomy and responses were not defined for specific current levels or electrode sizes. Because of the catch-all nature of GVS stimulation, all of the semicircular canal and otolith afferents are stimulated, resulting in a firing pattern that has no equivalent natural stimulation (i.e. stimulation from physical motion). However, for bilateral bipolar GVS application (most commonly used), the model predicts a primary signal of acceleration toward the cathodal electrode and tilt response toward the anode (Figure 6A). Whole body responses to GVS seem to be organized by the balance system that interprets the GVS-induced afferent firing as a real head movement in space resulting from an unplanned body movement. The greater the stimulus level, the greater the virtual tilt that the subject feels. However, the compensatory physical tilt evoked depends on the available feedback from nonvestibular sensory systems (i.e., the visual, tactile, and proprioceptive systems), such that physical tilt is greatly reduced when other nonvestibular sensory feedback is available. Also, in normal subjects, stimulation causes a dynamic tilt that eventually reaches a steady tilt level, most likely due to the interference from other sensory cues. For example, a patient with loss of large-fiber somatosensory afferent input from his body below the collarbone was tested seated, with eyes closed. For him, tilt did not reach a steady level but instead continuously increased throughout the stimulation period (Day and Cole 2002).

The perceptual body tilt and resultant motion in the opposite direction is dependent on the location of the head on the trunk such that tilt always occurs parallel with the direction of electrical current flow (Figure 6B) (Fitzpatrick and Day 2004). This head direction influence on sway has also been shown with the addition of corresponding electromyography (EMG) analysis of trunk and lower limb muscles (Ali et al. 2002).

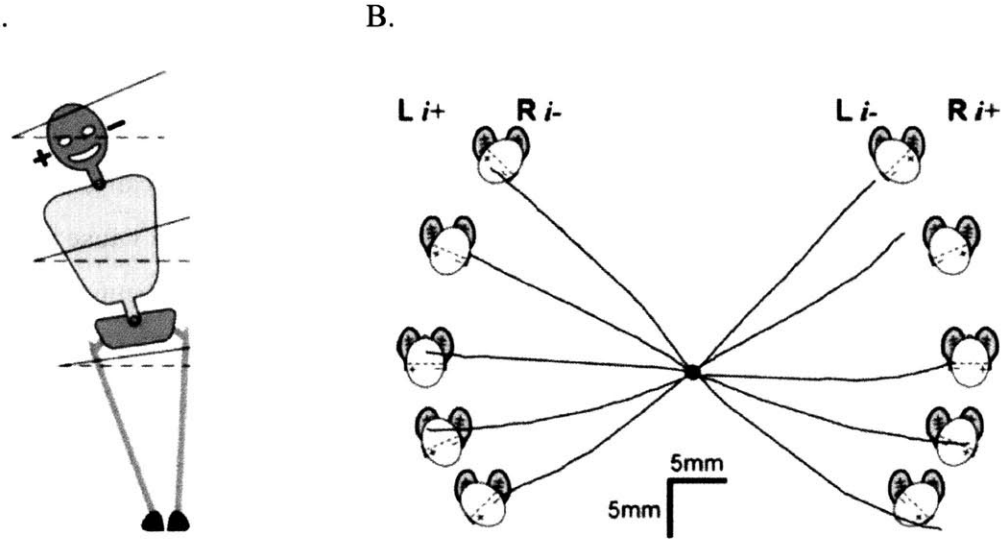

Figure 6. Body responses to GVS. A: Depiction of whole body tilt as a result of bilateral bipolar GVS (from Day et al., 1997). B: Sway responses to bilaterial bipolar GVS (0.5 mA, applied for 2s, using 3 cm diameter elctrodes). Subjects stood still at the central point with the head turned in yaw in 1 of 5 positions (R45°, R22°,0°, L22° L45°, where R is right and L is left), but with the feet always pointing straight ahead (represented by grey ovals under white oval). The whole-body sway trajectories were always along the head interaural line and towards the anodal electrode. Direction of sway induced by bilateral bipolar GVS is dependent on head position (from Fitzpatrick and Day 2004, redrawn from Pastor et al. 1993).

That GVS is non-specific in its target, and affects both SCC and otolith neurons is understood. However, whether GVS primarily stimulates the SCCs or otoliths in terms of behavioral and physiological responses has been a topic of debate that is still not considered settled. A recent review suggested that GVS likely induces behavioral responses that can be attributed to both the SCCs and otoliths depending on the context of the experiment (Curthoys and MacDougall 2012). Relevant studies have primarily focused on GVS stimulation (usually sinusoidal) and not SVS, the type of stimulation used in this research effort. Because this topic is the focus of Experiment 2, a more detailed review of SCC and otolith-specific GVS response behavior will be given in

Section 6.1.

Although not explictly defined as such, GVS applied to human subjects has historically been associated with suprathreshold stimuli, meaning that a perception of motion is present. Electrode size is a factor, but for most subjects and studies, this threshold is around 1 mA (Fitzpatrick et al. 1994, Wilkinson 2008, Cevette et al. 2012). Current levels around and above 1 mA can also elicit tingling and itching at the electrode site, depending on the size of the electrode, amount of elctrode gel used, and resistance across the electrodes. Increasing the stimulus level further, to around 2-3 mA, can cause moderate heating sensations on the skin at the location of the electrode and a metallic taste in the mouth, while levels around 4 mA can cause pain to the subject (Fitzpatrick et al. 1994, Lobel et al. 1998). GVS can be used to cause degradation in sensorimotor performance. For example, pseudo-random GVS has been used to create performance decrements in dynamic visual acuity during treadmill walking, time to complete an obstacle course (± 5 mA, Moore et al. 2006), simulated Shuttle landing performance (± 5 mA, Moore et al. 2011) and postural stability measured by sensory organization tests (± 5 mA, MacDougall et al. 2006), qualitatively similar to those observed in astronauts after return to Earth gravity. GVS has also been shown to degrade postural control to a similar extent as the postural performance of a vestibulopathic patient population and astronauts on landing day (MacDougall et al. 2006). None of these studies mention subject discomfort from high amplitude stimuli but they do state that their use of large area electrodes allowed them to use higher stimulus amplitudes than before. For reference, Fitzpatrick et al. (1994) used electrodes 6-8 cm^2, Moore et al. (2006) and MacDougall et al. (2006) used larger 10 cm^2 electrodes, and Mulavara et al. (2011), used electorodes with a 50 cm^2 area. Lastly, it has also been found that suprathreshold GVS (>1 mA) can cause degradation in some cognitive measures (Dilda et al. 2012).

2.5 Stochastic Resonance

Stochastic resonance is a phenomenon in which the response of a non-linear system to an input signal is benefited by the presence of a particular non-zero level of noise (for reviews see Gammaitoni et al. 1998, Collins et al. 2003, Moss et al. 2004, McDonnell and Abott 2009 and Aihara et al. 2010). In general terms, SR can be thought of as "helpful randomness" or "noise

benefit" (McDonnell and Abbott 2009). The signature of SR is some type of performance curve that has a pseudo-bell shape with a peak at some optimal noise level associated with optimal system output (Moss, 2004). In its original conception, SR was defined as pertaining to bi-stable dynamical systems. Later, in the mid 1990s the concept of threshold or non-dynamical SR began to appear in the literature. Both forms are described below.

2.5.1 Classic Dynamical Stochastic Resonance

The history of SR began in the early 1980s and grew out of the desire to explain Earth's glacial variations over time. It was realized that glacial-interglacial transitions have an average period of 10^5 years with seemingly random variability superimposed (Figure 7). The time scale of these transitions is quite large but it was recognized that the eccentricity of the Earth's orbit around the sun had a similar time scale. The perturbation in the eccentricity of the Earth's orbit does affect the total amount of solar energy on the Earth but the magnitude is very small, about 0.1%. The desire to explain how such a small perturbation could have such a large effect resulted in the theory of SR and it was reasoned that in this case, it was only possible because of the environmental noise that exists along with the weak "signal" or change in solar energy transmitted. Therefore the original SR case was the bi-stable system defined by glacial and interglacial states that somehow capture the periodicity of the weak astronomical perturbation signal (Benzi et al. 1981, 1982, Nicolis 1981, 1982).

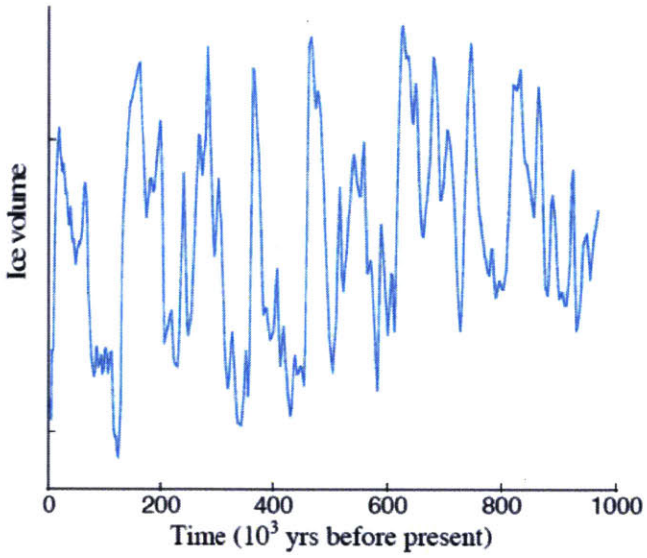

Figure 7. Ice volume variations over the last million years showing the transitions between glacial and interglacial states (Rouvas-Nicolis and Nicolis 2007).

In the SR literature, there has been a substantial effort to form mathematical equations to describe the SR phenomena. One such set of equations describes the amplitude of the periodic component of the response of a bi-stable system subjected to both noise and a weak periodic forcing for differing noise variance levels. All equations and explanations summarized in this section are from Rouvas-Nicolis and Nicolis (2007) and Gammaitoni et al (1998). This model of SR originates from a system with overdamped motion of a Brownian particle in a bi-stable potential well system in the presence of noise and periodic forcing. The equation for this system is of the form:

$$\dot{x}(t) = -U'(x) + A_0 \cos(\omega_0 t + \varphi) + F(t) \tag{1}$$

where

$$U(x) = -\frac{\lambda x^2}{2} + \frac{x^4}{4} \tag{2}$$

U(x) describes the symmetric quartic potential shown below:

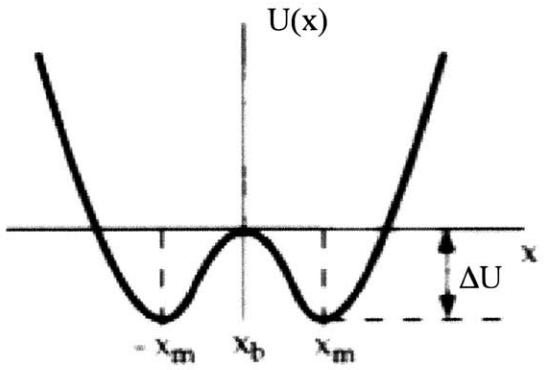

where

$$x_{\pm} = \pm\lambda^{1/2} \tag{3}$$

$$\Delta U = \frac{\lambda^2}{4} \tag{4}$$

In Equation 1, the second term represents the weak periodic forcing and the third term, F(t), is the random force, or noise in the system (internal and external). This is classically Gaussian white noise with zero mean and strength equal to q^2. This random force in the absence of externally applied periodic forcing can cause jumps of the Brownian particle between the potential wells with a rate described by the Kramer's rate equation:

$$r(q^2) = \frac{1}{\sqrt{2}\pi}\lambda \exp\left(-\frac{\lambda^2}{2q^2}\right) \tag{5}$$

When external periodic forcing is applied, U(x), the symmetric quartic potential, changes shape such that it becomes easier or harder for the particle to jump between wells, or more specifically, for the particle to jump to the more globally stable well. The potential well system with externally applied periodic forcing is described by Equation 6 and visualized in Figure 8:

$$W(x,t) = U(x) - A_0 x \cos(\omega_0 t) \tag{6}$$

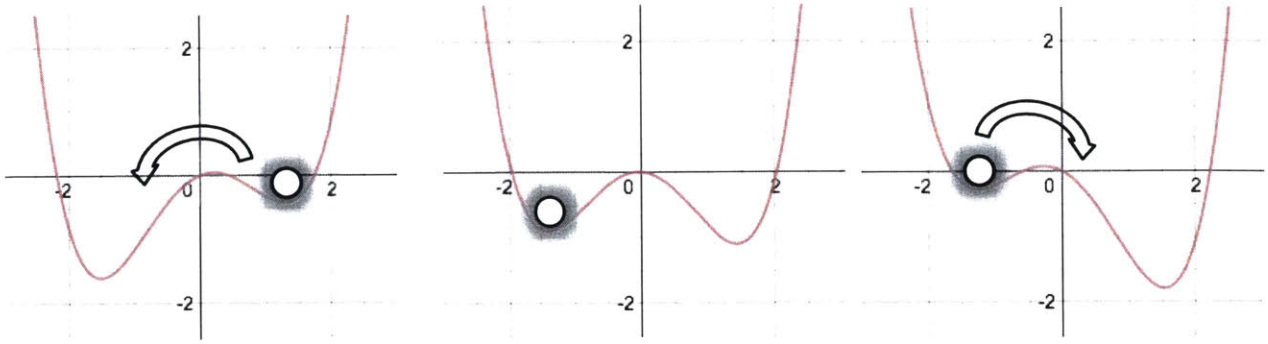

Figure 8. Graphical representation of the double potential well system, for increasing t=1.0, 1.5, 2.0 (left to right), with λ=2, A_0=1, ω_0 = 1. Notice how the globally stable well changes with applied periodic forcing. In the left plot, the circle, representing the Brownian particle, may tend to move into the leftward, more globally stable, potential well. Figure created by this author as a visualization aid.

In the presence of periodic forcing, Equation 1 becomes a Fokker-Plank equation that can be reduced to a closed equation for the attraction probability of the each well, with a solution given by the following periodic response:

$$\langle x(t) \rangle = x \cos(\omega_0 t - \phi) \tag{7}$$

with amplitude:

$$A = A_0 \frac{\lambda}{q^2} \frac{r(q^2)}{(4r(q^2)+\omega_0^2)^{1/2}} \tag{8}$$

and parameters:

A_0 = Amplitude of weak periodic forcing

ω_0 = frequency of weak periodic forcing

λ = quartic potential parameter (related to depth and spread of potential wells)

The shape of this amplitude of the periodic response can be seen in Figure 9.

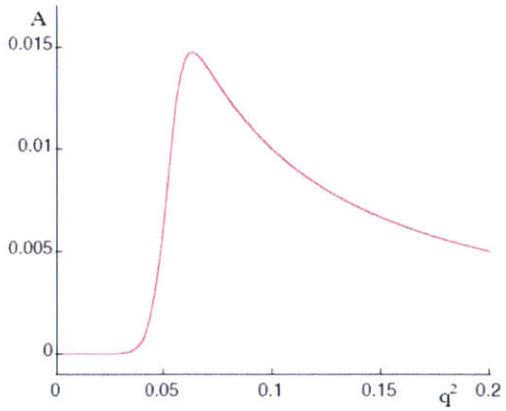

Figure 9. The amplitude of the periodic response of the system against the noise strength q^2 (Rouvas-Nicolis and Nicolis 2007).

The amplitude response includes the typical characteristics of SR: a sharp increase and peak with a more gradual return as noise continues to increase. The result is that with some particular level of noise, the motion of the Brownian particle between potential wells is best synchronized with the externally applied periodic forcing and the amplitude of the periodic response to the weak signal is maximized (Rouvas-Nicolis and Nicolis 2007). A theoretical concept for how this classic SR theory could relate to DR thresholds as measured in this work is discussed in Appendix 10.1.

2.5.2 Threshold or Non-Dynamical Stochastic Resonance

A simpler form of SR known as threshold or non-dynamical SR was first suggested in 1995 and required only a threshold, a subthreshold stimulus, and system noise (Gingl et al. 1995). An example can be seen in Figure 10, which gives an example of tactile detection responses to a weak (subthreshold) physical stimulus in the presence of increasing physical noise added to the signal. When the noise added to the signal is too low, the system does not experience any performance gains; the weak input signal remains undetectable. If the noise level is too high, the system may become saturated, rendering it unable to distinguish between signal and noise and again performance is not improved. With an appropriate level of noise, information from the weak signal can be optimally obtained (See Figure 10).

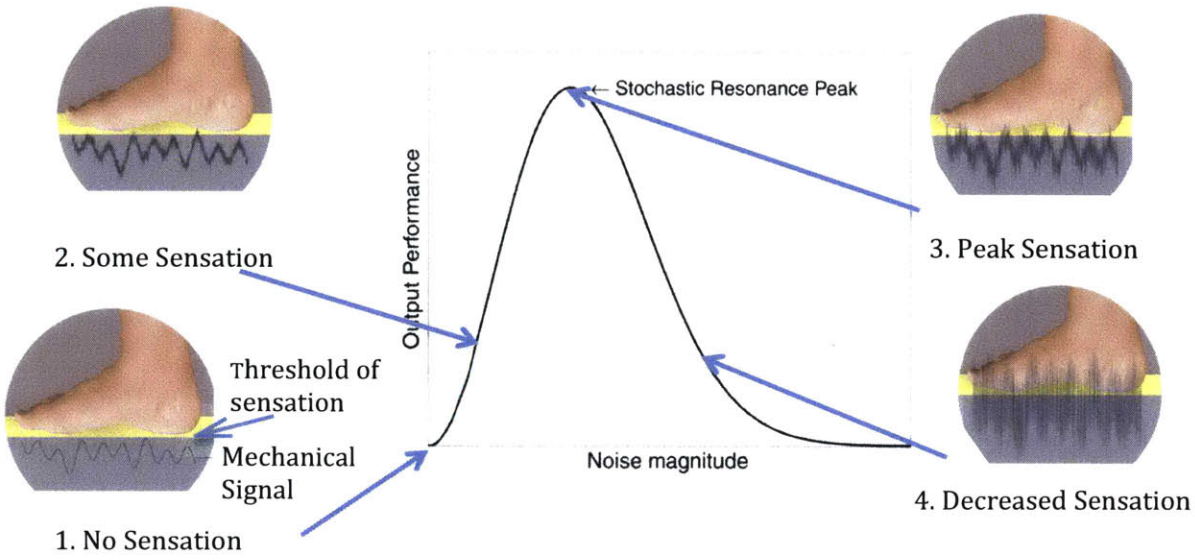

Figure 10. Typical SR curve of output performance, in this case discrimination index, vs. noise magnitude demonstrating the phenomenon of stochastic resonance. The example shows the change in physical sensation of a mechanical stimulus when various levels of noise are present (Adapted from McDonnell and Abbott 2009, Harry et al. 2005).

The classic example of threshold SR affecting the transfer of sensory information and output behavior comes from experiments done with juvenile paddlefish that showed that weak electrical noise of optimal amplitude applied to the water around the fish increased the spatial range that the fish could detect and feed on its prey (Russell et al. 1999).

2.5.3 Stochastic Resonance in Physiological Systems

We will not distinguish dynamical from non-dynamical SR in the next few sections but will instead use SR to broadly describe the exhibition of "noise benefit". This more inclusive definition is suggested and discussed thoroughly by McDonnell and Abbott (2009). SR has been demonstrated in a variety of human body systems, typically through psychophysical experiments. The application of stochastic noise to sensory input has been shown to improve visual contrast sensitivity and detection (Figure 11A), (Ward et al. 2001, Simonotto et al. 1997), letter recognition (Piana et al. 2000), perception of ambiguous figures (Riani and Simonotto 1994), and visual depth perception (Ditzinger et al. 2000). SR has also been observed in human hearing (Zeng et al. 2000, Jaramillo and Wiesenfeld 1998), and has been identified as an

important component in cochlear coding strategy (Morse and Evans, 1996). SR in tactile sensation has been demonstrated in the response to weak mechanical stimuli in healthy individuals (Figure 11B) (Collins et al. 1996a, 1996b, 1997, Richardson et al. 1998) and stroke survivors (Enders et al. 2013). The application of subsensory mechanical noise to the feet has been shown to improve balance through the reduction of sway in young and elderly subjects (Priplata et al. 2002, 2003, Dettmer et al. 2015) and in patients with diabetes and stroke (Priplata et al. 2006, Figure 11C) and gait variability in elderly fallers (Galica et al. 2008). Similarly, mechanical noise applied to ankle muscles can improve double-legged and single-legged balance in patients with functional ankle instability (Ross et al. 2013). Electrical noise applied to the back of the knee has also been shown to improve balance (Gravelle 2002). The application of whole body vibration over many days was shown to be an effective therapy to improve postural stability in Parkinson's disease patients (Kaut et al. 2016).

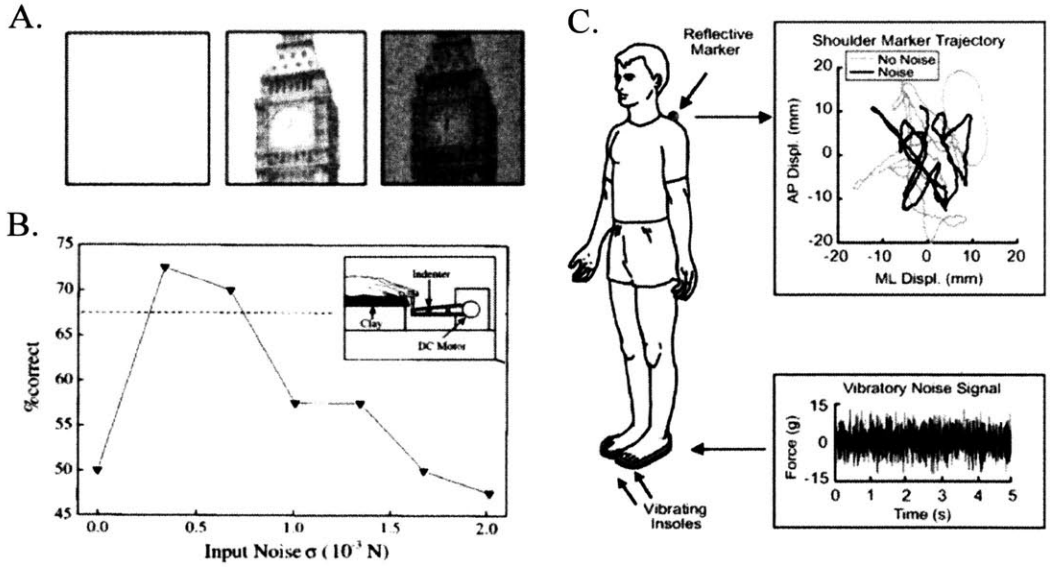

Figure 11. Stochastic resonance examples including A: vision tasks in which noise is added to each pixel of an image revealing an optimal noise level for image detection (from Simonotto et al. 1997), B: tactile sensation testing in which mechanical noise is added to a weak mechanical stimuli increasing the sensitivity of the subject to detect the stimuli (from Collins et al. 1996b), and C: balance measurements when mechanical noise is applied to the feet, improving balance performance (from Priplata et al. 2006).

2.6 Stochastic Vestibular Stimulation

The technique of using a suprasensory stochastic or pseudo-random waveform to stimulate the vestibular system instead of using a more traditional square-wave or sinusoidal galvanic signal has largely been examined through body responses in posture, balance, and gait (Fitzpatrick et al. 1996, Pavlik et al. 1999, Scinicariello 2003, MacDougall 2006, Moore 2006). Studies have also begun to focus on low stimulus amplitudes, which are either set to a fixed set of amplitudes (for example in Pal et al. 2009), or set at a certain level below, or at a certain percentage of a subject-specific threshold stimulus level. For example, Lobel et al. (1998) set their stimulus level 0.5 mA below each subject's pain threshold while Geraghty et al. (2008) used 90% of sensory threshold (in their case was the level at which nystagmus began), and Yamamoto et al. (2005) used 60% of nociceptive threshold. Samoudi et al. (2015) used the lowest level of SVS with which subjects exhibited rhythmic sway measured by a force plate.

Using subsensory stimulus levels, SVS has been found to improve ocular stabilization reflexes in response to whole-body tilt (Geraghty et al. 2008) and postural balance performance on an unstable compliant surface in Parkinsonian patients (Pal et al. 2009, Samoudi et al. 2015). SVS has also been shown to improve autonomic and motor responsiveness in neurodegenerative patients with multi-system atrophy or Parkinson's disease (Yamamoto et al. 2005). The subject-specific optimal level of SVS identified by exposing subjects to a range of stimulus levels and identifying which resulted in optimal performance, has been found to improve stability during balance and walking tasks in normal, healthy subjects (Goel et al. 2015, Mulavara et al. 2011, 2012, 2015, Figure 12).

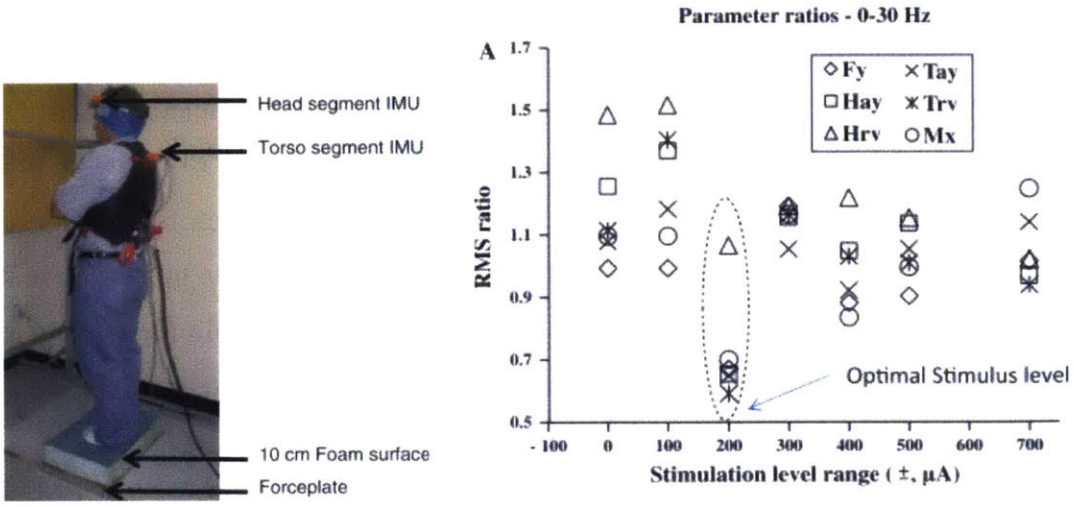

Figure 12. Example of balance measured with SVS applied. RMS ratios of six postural response parameters vs. applied SVS intensity level (right panel) for a subject tested standing on medium density foam with feet together, arms crossed, head facing forward, and eyes closed (left panel). Here, SVS was bandlimited (0-30 Hz) white noise, at peak-peak amplitudes shown. The root mean square (RMS) ratios compare responses during the stimulus period with those in a prior baseline (no stimulation) period, averaged over 3 trials. Note that this subject's RMS ratios were dramatically lower at the, 200 μA stimulus level. This optimal level varied across 18 subjects but resulted in an average response parameter improvement ranging from 11-25%. Postural responses measured included: Fy: Mediolateral shear force, Hay: Mediolateral linear accelerations for the head segment, Hry: Roll angular velocity for the head segment, Tay: Mediolateral linear accelerations for the trunk segment, Trv: Roll angular velocity for the trunk segment, Mx: Roll moments (from Mulavara et al. 2011).

Mulavara et al. (2011) compared the effects of SVS on postural balance using both narrow band (1-2 Hz) and wide band (0-30 Hz) frequency ranges. The two frequency ranges were tested in separate test sessions and were found to be similarly effective in improving an average of six RMS sway measures. The optimal SVS level as determined from individual trials, varied depending on which stimulus spectrum was used (0-2 or 0-30 Hz). Additionally, an optimal SVS level could not be determined for 12 out of the 30 test sessions. For two of the 18 subjects, the optimal level could not be determined in either session using either stimulus. Mulavara et al. (2011) discussed that at high amplitudes, a 1-2 Hz stochastic signal has been shown to induce postural sway indicating an effect of stimulation at this frequency range on body stability (Pavlik et al. 1999, Nashner et al. 1989). At high amplitudes, a 0-30 Hz signal has been shown to stimulate lower limb muscles indicating an effect on vestibulo-spinal function (Dakin et al. 2007). Additionally, Songer and Eatock (2010) have shown that saccular hair cells have average

cutoff frequencies ranging from 3 to 9 Hz. Mulavara et al. (2011) therefore reasoned that the 0-30 Hz signal should encompass the frequencies of stimulation that have been shown to be effective in eliciting body responses. Mulavara et al. (2011) evaluated subject response at a range of low stimulation levels (±100 - ±700 μA peak) using a bandlimited 0-30 Hz white noise signal and were able to identify the stimulation level for each subject at which best performance was achieved (typically in the range of ±100 - ±400 μA) over multiple trials in a given test session. Pal et al. (2009) also found improvements in standing balance with amplitudes as low as 100 μA using a similar task of standing on compliant foam, but with a bicathodal electrode setup (i.e. two cathodal mastoid electrodes and one anodal C7 electrode).

3 Specific Aims

The long-term goal of research in this area is to develop methods to augment sensorimotor function and accelerate adaptation after G-transitions as a sensorimotor countermeasure for astronauts. Use of SVS in pre-flight training or during the post-landing period has been suggested. The objective of this thesis is to investigate the use of stochastic vestibular stimulation as a tool to enhance vestibular system performance and to better understand details associated with SVS use to inform future studies and SVS implementation. The specific aims and associated hypotheses of this research were as follows:

Experiment 1:

1) To determine if the stochastic resonance phenomenon can be demonstrated in vestibular perceptual thresholds.

Hypothesis: Stochastic resonance can be demonstrated in vestibular direction recognition thresholds, with a characteristic improvement in threshold at a specific SVS current level.

Experiment 2:

2) To determine if the stochastic resonance phenomenon can be demonstrated in vestibular perceptual thresholds that are primarily related to semicircular canal or otolith stimulation.

Experiment 3:

3) To determine if stochastic vestibular stimulation can improve manual control nulling ability in a simple but operationally relevant piloting-type task.

Hypothesis: Performance in a manual control task that is dependent on vestibular perception can be improved by use of SVS.

4 Methods Used In Multiple Experiments

Methods employed in more than one experiment are described in this section. Methods unique to each individual experiment will be described in later chapters. Experiments 1 and 2 both involved measurements of GVS thresholds and direction recognition (DR) thresholds with the application of varying SVS levels. Experiment 3, which investigated manual control performance with the application of SVS, did not measure GVS or DR thresholds. However a comparison between manual control performance and DR thresholds is discussed in the Experiment 3 results.

4.1 Study Approval and Facilities

Approval from the Institutional Review Boards of the Massachusetts Institute of Technology and the Massachusetts Eye and Ear Infirmary (MEEI) were obtained prior to conducting experiments on human subjects. All subjects signed informed consent forms before participating in each experiment. Subjects also filled out an online health screen questionnaire that was managed using REDCap electronic data capture tools hosted at the MEEI (Harris et al. 2009). REDCap (Research Electronic Data Capture) is a secure, web-based application designed to support data capture for research studies, providing: 1) an intuitive interface for validated data entry; 2) audit trails for tracking data manipulation and export procedures; 3) automated export procedures for seamless data downloads to common statistical packages; and 4) procedures for importing data from external sources. The health screen questionnaires were reviewed by an IRB approved lab mate in the JVPL and when necessary, were reviewed by an IRB approved MEEI physician (Appendix 10.17). Those selected were females and males ages 18-35 in good health with no reported vestibular defects or conditions. All experiments took place at MEEI in the Jenks Vestibular Physiology Laboratory (JVPL).

4.2 Setup and Application of Electrical Vestibular Stimulation

The galvanic stimulation device and data acquisition system used in this research was obtained on loan from the Neuroscience Laboratory at NASA Johnson Space Center (JSC) (See Mulavara et al. 2011 for more details). Bilateral bipolar electrical stimulation was generated using the

constant current stimulator with subject isolation and delivered via leads connected to 2" by 4" (5.1 by 10.2 cm) UltraStim Electrodes (Axelgaard Manufacturing Co., LTD.) placed on each of the mastoid processes as previously described (Mulavara et al. 2011). Before electrodes were placed, the surface of the skin was lightly scrubbed using Nuprep skin prep gel. Alcohol wipes were used to clean the skin before and after the application of the scrub. Although the electrodes were manufactured to include a layer of Multistick gel, an additional, generous layer of Signagel electrode gel (Parker Labs) was added to the electrodes before adhering to the subject's head for improved conductivity and to ensure subject comfort (e.g. avoiding tingling, itching, or pain during stimulation) (Figure 13 Left). To keep the electrodes in place, micropore surgical tape was placed around the edges of the electrodes. Additionally, foam pads on each electrode and a head wrap were used to secure and protect the electrodes for the duration of the experiment (See Figure 13 for final setup). To promote consistency between stimulation applications, we required that the impedance between the two electrodes be less than 1 kΩ before applying stimulation. After electrode application, many subjects met this requirement immediately. For those who had higher impedances, we either allowed for some time to pass or gently pressed the electrodes on the subject's head until the impedance was low enough to begin testing. Measured impedance values from Experiment 1 are included in Appendix 10.2. The total setup time including electrode application and time waiting for the impedance to reach an acceptable level was approximately 30 minutes.

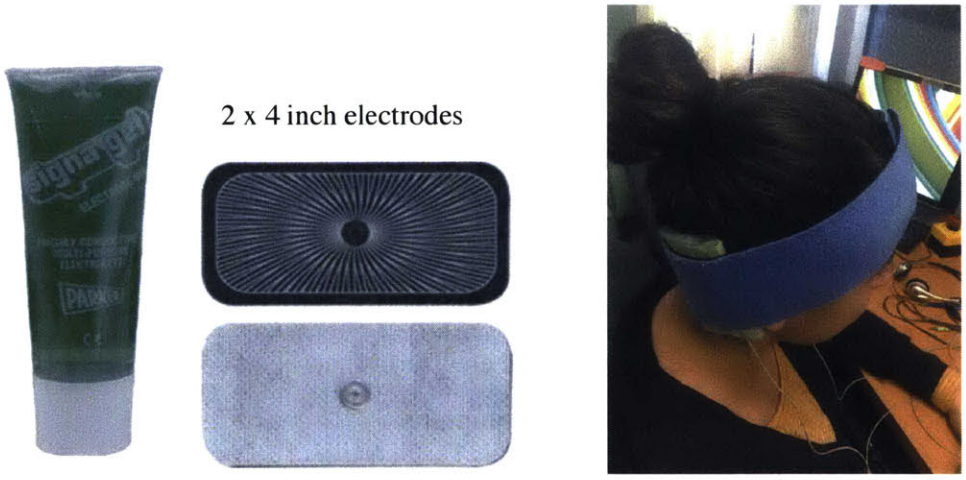

Figure 13. Electrode supplies and application. Left: Signa gel electrode gel and Axelgaard electrodes used in all experiments. Right: Final electrode setup with foam pads and head wrap securing the electrodes in place behind each ear.

4.3 Galvanic Vestibular Stimulation Motion Detection Threshold Test

Motion detection thresholds to sinusoidal (i.e. non-stochastic) GVS stimuli were measured to quantify each subject's perceptual sensitivity to electrical current using a method previously developed by a collaborator (Jeevarajran and Mulavara, personal communication, Goel et al. 2015). These thresholds measured the lowest sinusoidal GVS level that the subject could reliably perceive as self motion. They did not measure whether the subject was able to correctly identify a leftward from a rightward GVS stimulus. The current stimulus consisted of a 1 Hz sinusoidal signal in 15 sec duration bursts spaced at 20 second intervals. The peak-to-peak amplitude of each successive burst was varied downward and then upward in staircase fashion as shown in (Figure 14A). The successive order of peak-to-peak sinusoidal amplitudes was: ±2000, ±1500, ±1100, ±700, ±500, ±300, ±100, ±200, ±400, ±600, ±900, ±1300 μA. During the test, subjects sat with eyes closed upright in a chair without using the back or arm supports (to reduce and standardize nonvestibular cues). Subjects were asked to use a joystick on a game controller to indicate their perceived self-motion due to the sinusoidal GVS stimulation (Figure 14A). It was stressed to the subjects that their priority was to move the joystick when they felt self-motion, even if they were not certain of which direction they were moving. The most common perception of motion was of an alternating upright roll tilt, as expected with a 1 Hz bilateral bipolar sinusoidal signal centered about zero. The GVS amplitude range (±0 to 2000 μA) was sufficient such that all subjects reported some sensations. The percentage of time that the subject indicated a perceived motion (in any direction) during a particular stimulation amplitude level was calculated and along with the stimulation level, was fit with a generalized linear model, using Matlab's glmfit function with the logit link function specified (Figure 14B). We defined the GVS threshold as the stimulation burst amplitude at which the fit to the self-motion perception percentage (normalized to maximum response time percentage) reached 50%. The GVS threshold test was done at the beginning of each test session after electrodes had been placed on the subject, once the impedance between the electrodes had been confirmed to be less than 1 kΩ. This task took approximately 8 minutes to complete.

A.

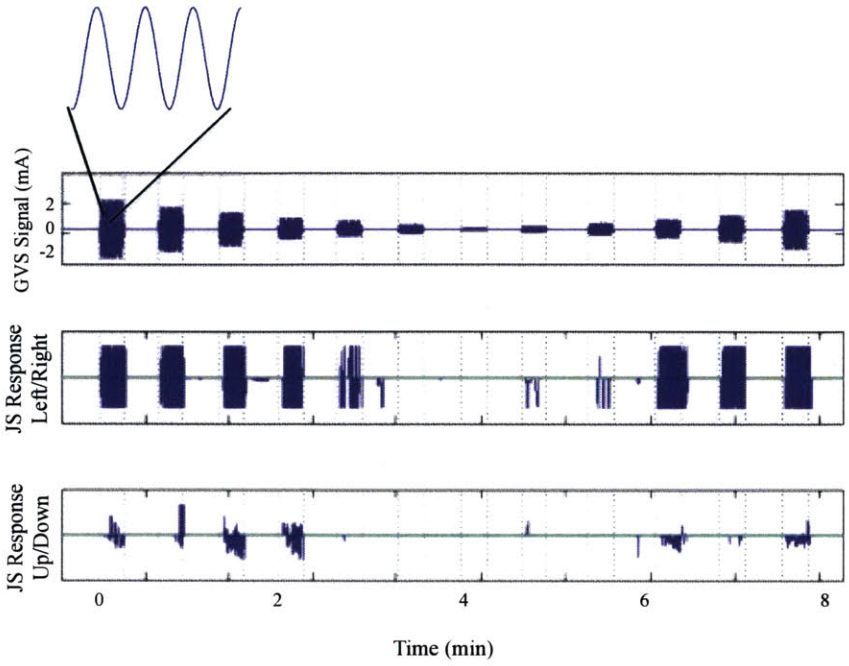

B.

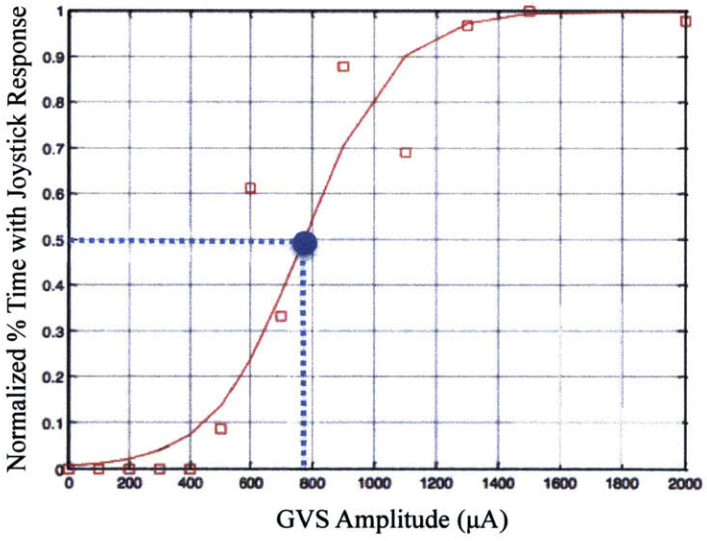

Figure 14. GVS threshold method. A: Top row indicates the GVS signal amplitude applied to the subject during the down/up staircase test. Detail of the sinusoidal burst is shown in the inset picture. Middle and bottom row show one subject's joystick responses in the left-right and up-down directions, respectively. B: The percentage of time during a single GVS level that the subject indicated that they were moving normalized to the maximum indicated percentage time plotted by GVS level. Red line is a logit fit to the data. Blue dotted line and circle marker indicate 50% of the logistic fit at which the GVS threshold was defined (770 μA in this example).

4.4 Measuring Motion Recognition (DR) Thresholds

Linear and angular direction recognition (DR) thresholds and bias were measured using a method previously developed by Merfeld and colleagues (Merfeld 2011, Chaudhuri and Merfeld 2013). Subjects were seated in a chair mounted on a motion device. They were held securely in place by a quick release five-point harness and an adjustable head restraint that was tightened snuggly, but comfortably, around their head. Testing was done in darkness in a room completely free of light leaks. Subjects wore headphones that played white noise during all motions in order to mask auditory cues and a microphone that allowed for constant communication between the subject and operator. Each trial consisted of single cycle acceleration motion to either the left or right (Figure 15A). Motions were in the upright roll tilt and inter-aural translation, and supine roll rotation motion directions (Figure 15 B and C).

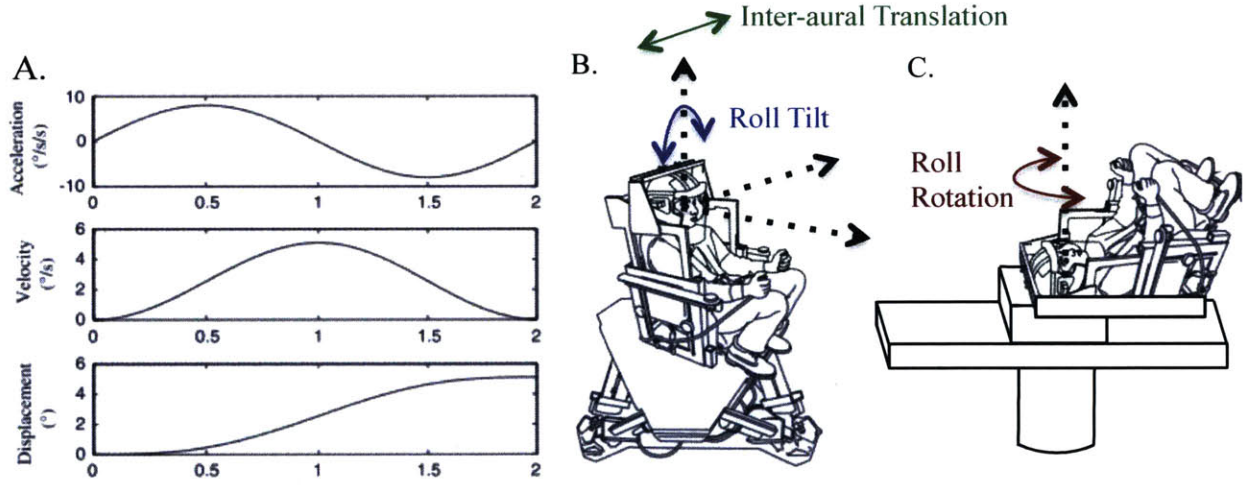

Figure 15. Direction recognition threshold test description. A. Motion profiles for acceleration, velocity, and displacement for a single left or right forced-choice direction recognition threshold trial using the B. Moog 6DOF2000E motion platform, and C. the Eccentric Rotator device. Upright roll tilt motions stimulate both the SCCs and otoliths, while inter-aural translation primarily stimulates the otoliths and supine roll rotation primarily stimulates the SCCs. Note that whether the subject is upright or supine depends on the motion being tested. Figure modified from Grabherr et al. 2008. See Appendix 0 for photographs of the Moog and Eccentric Rotator in the configurations used for DR threshold testing.

After each motion, subjects were tasked with indicating which direction they perceived their motion to be, by tapping either the left or right side of an iPad tablet computer touch sensitive display, or by pressing either a left or right handheld button. The next trial then began following

a pause of at least three seconds to allow for any transient motion sensations to subside. Although the frequency of the motions was held constant across trials within a session such that each motion took the same amount of time, the velocity of the motions varied using an adaptive staircase procedure to sample stimuli levels near threshold. Initially, the motion magnitudes were determined using a 2-down, 1-up staircase (i.e., two motion directions had to be correctly identified in a row in order for the next trial's magnitude to decrease). If the direction indicated by the subject was incorrect, the magnitude increased and the staircase switched to a 3-down, 1-up staircase (Figure 16A) with a 90% correct motion direction target (Chaudhuri and Merfeld 2013, Karmali 2015), which allowed us to determine the lowest velocity motion that a subject could reliably detect left form right 90 % of the time. This sampling approach was selected for the present experiments to enhance efficiency (i.e. a very precise estimate of threshold for a given number of trials). In this thesis, DR thresholds will be presented in terms of velocities (angular for upright roll tilt and supine roll rotation, and linear for inter-aural translation). DR thresholds could also be presented in terms of an angular or linear displacement and are sometimes in the literature. Due to the nature of the motion stimulus, the velocity and displacement are proportional to each other. At least 110 trials were completed for each individual DR threshold measurement (For additional details on number of trials in each test see Appendix 10.6). Subjects were given short breaks during each test and were also allowed to get out of the motion chair between tests. Directions of motions, frequencies, and devices used are detailed in Table 1 and Figure 15B,C. Both motion devices were located in the JVPL at the MEEI.

Table 1. Details of all Motion Recognition Threshold Tests Conducted

Experiment	Motion	Frequency	Stimulation	Device
1	Roll Tilt	0.2 Hz	SCC and otolith	Moog
2	Roll Rotation	0.2 Hz	SCC	Eccentric Rotator
2	Inter-aural Translation	1 Hz	otolith	Moog

The decision to test upright roll tilt DR thresholds at 0.2 Hz in the present experiments was based on previous data (conference abstract, Lim et al. 2009) that suggested, although the exact crossover frequency (the frequency at which the DR threshold for pseudo-static tilt equals that for supine roll rotation) varies across subjects, 0.2 Hz was a reasonable frequency in which both SCC and otolith inputs were approximately equally weighted as sensory inputs for a majority of subjects. After completion of Experiment 1, we were able to collect additional data (see Appendix 10.3) indicating that the mean crossover frequency across subjects is actually slightly higher than previously thought, at 0.57 Hz. However, we note that the SCC / otolith contribution does not abruptly start and stop at a single frequency. Instead, there is a range of frequencies in which both SCCs and otoliths substantially contribute to vestibular upright roll tilt perception. For upright roll tilt DR thresholds as tested in this study, this range has at least begun at 0.2 Hz for 12/14 subjects tested in the more recent data collection effort. Therefore, even with this new evidence that points to a higher crossover frequency than was previously estimated, we still believe that for the majority of subjects, perception of 0.2 Hz upright roll tilt motions should include contributions from both SCCs and otoliths. It is however likely that the otolith contribution is larger than the SCC contribution at this frequency. More detail on the frequency of the supine roll rotation and inter-aural translation motions will be given in later relevant sections.

Each DR threshold dataset consisted of at least 110 trials (motions and responses, example of first 50 trials shown in Figure 16A) that were analyzed by fitting with a bias reduced generalized linear model fit MATLAB function (brglmfit.m) developed by Chauduri and Merfeld (2013). The bias reduced fit accounts for an inherent bias in the threshold measure due to the adaptive sampling procedure. Within this method, a cumulative Gaussian psychometric curve was applied, such that the mean and standard deviation correspond to the "vestibular bias" and one-sigma DR threshold, respectively (Merfeld 2011) (Figure 16B).

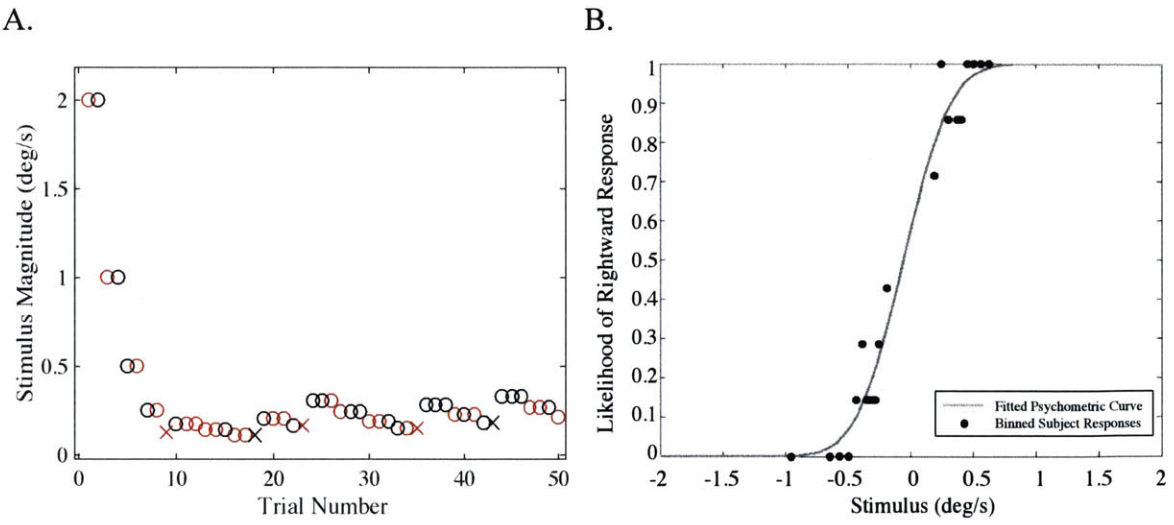

Figure 16. Direction recognition threshold data example. A: An example of the first 50 trials of a single DR threshold test. Red and black circles represent correctly identified rightward motions and leftward motions, respectively. X's represent incorrectly identified motions. B: Example of a psychometric curve fit to the dataset. The sign of the stimulus corresponds to leftward (-) and rightward (+) motions. Data points represent subject responses grouped by sets of seven neighboring stimulus levels. In the example shown, the standard deviation of the cumulative Gaussian psychometric curve fit was 0.2 deg/s, which corresponds to the DR threshold for this specific test.

Before determining the DR threshold, lapse detection was applied to each data set to identify and remove outlier subject reports (lapses) using a delta-deviance, or consistency, method (Clark and Merfeld, unpublished). Briefly, the deviance of the full data set – a quality-of-fit statistic - was calculated through the brglmfit.m function. For the data set with N trials, the deviance was then calculated N times leaving a single trial out of the data set each time. The difference between the deviance calculated using the full dataset and that with a single trial removed is termed the delta-deviance. The delta-deviances have a Chi-squared distribution with one degree of freedom, which we then statistically checked for outliers, using a conservative p-value of 0.01. If there were multiple outliers, we allowed only one outlier to be removed at a time. With the single outlier removed from the dataset, the lapse detection process was then repeated, but with a "Bonferroni-like multiple comparison" correction in which the p-value set for identifying outliers was divided by the iteration number, thus making it more difficult to statistically identify outliers with each successive iteration (Clark and Merfeld, unpublished). See Appendix 10.6 for

details on the number of outliers detected and removed by this lapse detection method in the experimental data.

Using a jackknife resampling method (Tukey, 1985), the standard error of each DR threshold was calculated using $SE = \sqrt{\frac{N-1}{N}\sum_{i=1}^{N}(\hat{\sigma}_i - \bar{\sigma})^2}$, in which $\hat{\sigma}_i$ was the estimated DR threshold obtained by deleting a single trial from the data set and $\bar{\sigma}$ was the estimated DR threshold using the full dataset. A flow chart showing the general process just described is shown in Figure 17.

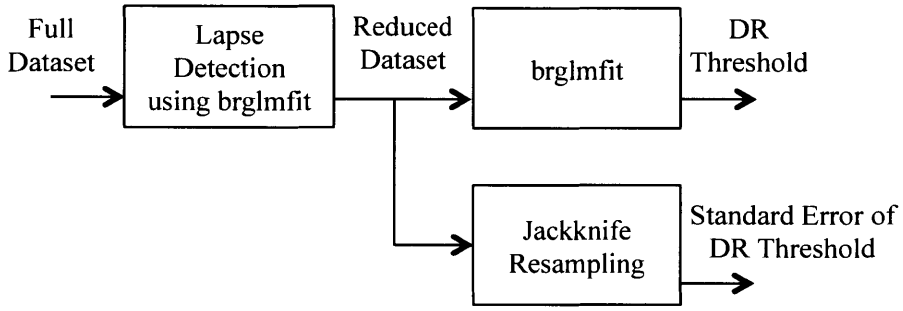

Figure 17. Flow chart of DR threshold data processing

To determine if one estimated DR threshold was statistically significantly higher than another, we conducted one tailed t-tests using a MATLAB function in the form of tcdf(t, df, 'upper'). The t-statistic was calculated as $t = \frac{\hat{\sigma}_1 - \hat{\sigma}_2}{\sqrt{SE_1^2 + SE_2^2}}$. The number of degrees of freedom for the t-test was calculated using a Satterthwaite approximation (Satterthwaite 1941) described by $df = \frac{\left(\sum_{k=1}^{2} SE_k^2\right)^2}{\sum_{k=1}^{2} \frac{SE_k^4}{df_k}}$, in which k is the case number of each estimated DR threshold. The parameter df_k is calculated using the following equation $df_k = \left(3.16 - \frac{2.77}{\sqrt{N}}\right)\left[\frac{\left(\sum_{j=1}^{N}(\hat{\sigma}_{jk} - \hat{\sigma}_k)^2\right)^2}{\sum_{j=1}^{N}(\hat{\sigma}_{jk} - \hat{\sigma}_k)^4}\right]$ (Johnson and Rust 1992b), in which N is the number of trials within a single DR threshold estimate, $\hat{\sigma}_{jk}$ is the estimated threshold with a single trial (j) removed, and $\hat{\sigma}_k$ is the estimated DR threshold using all N trials for each case k. This method does not necessarily allow a degree of freedom for each squared difference term, $(\hat{\sigma}_{jk} - \hat{\sigma}_k)^2$. Instead the effective degrees of freedom will be

closer to the number of dominant squared difference terms. With this process, we were able to use standard error calculated by a jackknife resampling method to conduct a t-test between two estimated DR thresholds to determine if one was significantly lower than another. See Appendix 10.7 for more on methods for calculating confidence intervals with DR threshold data.

5 Experiment 1: Demonstration of Stochastic Resonance in Vestibular Perception

The primary goal of this experiment was to definitively demonstrate the existence of SR in vestibular direction recognition thresholds due to the application of SVS. The secondary goal was to investigate the repeatability of the SR phenomenon in vestibular perception by repeating the test on the same subject on a separate test day. Since the subject's measured upright roll tilt direction recognition (DR) threshold was to be the dependent variable, a preliminary experiment was conducted as a control without SVS to establish the test-retest repeatability of DR thresholds across days in individual subjects. The stability of DR thresholds over time had not previously been determined.

5.1.1 Motion Recognition Threshold Repeatability Experiment

This experiment measured the repeatability of 0.2 Hz head-centered upright roll tilt DR thresholds of four subjects without the application of SVS. Subjects (2 female, ages 25, 27, 28, 34) had normal vestibular function according to a clinical vestibular screening that took place in the JVPL at the MEEI. Subjects were tested nine times within a single day and once a day across eight days (Figure 18). Each threshold test consisted of 75 trials. A 3-down, 1-up adaptive staircase was used with an initial motion of 2 deg/s. Subjects were allowed to take breaks between tests at their discretion. Most subjects chose to get out of the chair and stretch every two or three tests during the test session with nine repeated tests. To address the concern that drowsiness induced by sitting in a darkened test room for long periods could influence the results subjects we collected subjective sleepiness ratings at the beginning and end of each test session. Subjects reported verbally using a paper version of the Karolinksa Sleepiness Scale (KSS) as reference, a scale from 1 (very alert) to 9 (fighting sleep) (Akerstedt and Gillberg 1990). We also collected an objective measure of sleepiness, using a short version of the Psychomotor Vigilance Test (Dinges and Powell 1985) implemented through an iPhone app, Sleep2Peak (Gartenberg and Parasuraman 2010).

The upright roll tilt DR thresholds of these four subjects, were remarkably consistent, and free of outlier thresholds. Across multiple days, none of the four subjects had any single DR threshold

that lay outside of the 95% confidence interval of the mean of their DR thresholds (Figure 18A). Within a single day, two of the four subjects had no DR thresholds different than the mean. However, subjects PS2 and PS4 had two tests and one test, respectively, outside of the mean 95% confidence interval (Figure 18B). The probability of two or more outliers in a binomial distribution is 7.1% (calculated using the probability mass function), which is slightly higher than the 5% expected by chance to be outside of the 95% confidence interval. Similarly, the probability of one or more outliers is 37%, again higher than a 5% chance, suggesting that these outlier measurements are somewhat expected and do not necessarily indicate a change in underlying DR threshold (Clark et al. in preparation). This repeatability study measured DR thresholds with only 75 trials in each estimate. We would expect the variability in the estimate to decrease as the number of trials increases. We therefore chose to measure DR thresholds with at least 110 trials in each test in Experiments 1 and 2, to be discussed.

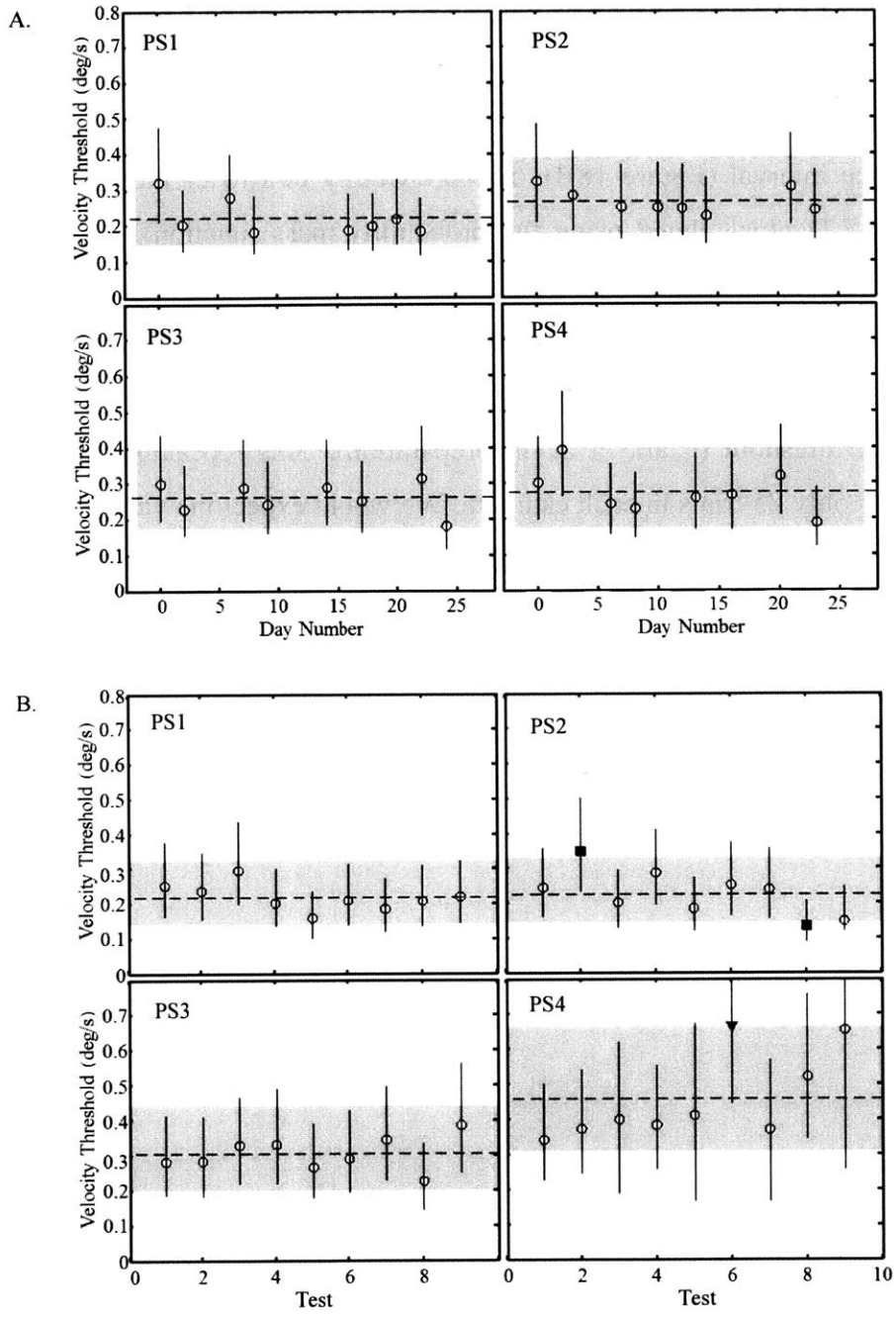

Figure 18. Preliminary repeatability test data. A: DR thresholds of four subjects for eight tests across 25 days and B: for nine repeated tests within a single day Shaded region represents the 95% confidence interval of the mean across tests. Error bars represent 95% confidence intervals of each individual measurement. Each estimate is made using 75 trials.

Analysis of sleepiness data (24 tests taken over 12 weeks) showed that subjects subjectively felt sleepier after a test than before; however being sleepier did not correspond to an increase in DR

threshold, which remained fairly consistent. Furthermore, although subjects subjectively reported feeling sleepier, their performance on the objective sleepiness task did not worsen (See Appendix 10.8 for more details). We believe that although sleepy, subjects were able to maintain their performance because of the discrete nature of the task and because they were not under any extreme sleep pressures such as chronic or acute sleep deprivation.

We concluded from this four subject repeatability study that upright roll tilt DR thresholds were stable and exhibited little variability over timescales of minutes and days. Small changes in measured DR thresholds are to be expected as a result of minor attention factors or variability associated with the estimation method. Lastly, we found that even when subjects indicated that they felt sleepier, their measured DR thresholds did not significantly worsen. The results of this preliminary study gave us confidence that DR thresholds are sufficiently stable such that we could identify potential impacts due to the application of varying levels of SVS.

5.2 Stochastic Resonance Demonstration Experiment Methods

5.2.1 Subjects

Fourteen participants were recruited for the SR demonstration experiment. All were healthy, with no history of vestibular disorders and met our inclusion criteria (Section 4.1). However, two were subsequently dropped. One was hypersensitive to the suprathreshold GVS stimulation applied in the GVS threshold task and reported uncomfortable tingling at the electrode site even though the skin preparation, electrode attachment, and stimulation levels appeared normal. Testing was discontinued. A second subject reported tilt sensations consistently in only one direction during the GVS threshold test, whereas all the other subjects reported tilts in both directions. This does not necessarily indicate a vestibular sensory anomaly, and indeed this subject's baseline tilt DR threshold measurement was within the normal range. Conceivably some benign anatomical factor might have made the galvanic current stimulus asymmetric. The remaining 12 subjects (6 female) were 25.8 ± 2.7 (SD) years old.

5.2.2 SR Demonstration Experiment Procedures

Subjects were tested in two separate test sessions, separated by 6-14 days. At the beginning of each test session, after electrode application, subjects' perceptual threshold to 1 Hz sinusoidal GVS was measured. The GVS threshold was measured at the start of each test session, and used to normalize the "optimal" SVS current level condition uses in the subsequent session, scaling the stimulus up or down to account for possible variations in the subject's GVS perceptual threshold that possibly occur between sessions simply due to differences in electrode placement or some other uncontrolled physiologic factor. We expected that if the subject's threshold to GVS stimulation increased, the optimal level of subthreshold SVS stimulation would increase also.

The SVS signals used were modified from those created and used by Mulavara et al. (2011). These signals were generated in LabVIEW using a Gaussian white noise generator and then filtered using a 10^{th} order low-pass Butterworth filter with a cutoff frequency of 30 Hz and were checked for zero mean (± 1%) and RMS ([26 μA RMS/ 100 μA) ± 5%] as previously described (Mulavara et al. 2011, 2015). In this thesis, only the 20.5 second stimulus period of Mulavara et al. (2011) stimulation profile was used, which did not include the two seconds in which a start and end ramp filter had been applied. This 20.5 second SVS profile was simply repeated continuously to achieve SVS for the duration of testing in our three experiments. In this thesis, SVS level (±0 - ±1500 μA) refers to the (±) peak of the signal over the 20.5 second stimulation profile duration. Table 2 below gives the minimum, maximum, mean, and RMS for each of the SVS profiles used in this thesis.

Table 2. SVS details

±SVS	Min	Max	Mean	Calculated RMS
200	-200	178	1.56	54.4
300	-258	300	-1.14	81.6
500	-500	481	4.12	136
700	-655	700	-4.41	190.4
800	-669	800	6.81	218.1
900	-900	864	-3.48	244.6
1500	-1144	1500	-4.16	407.9

In the first test session, subjects' 0.2 Hz head-centered upright roll tilt motion thresholds were measured five times. Within the first session, each test included the application of five different, and randomly ordered, SVS levels: ±0, ±200, ±300, ±500, or ±700 μA. During the second test session, subjects were tested at ±0, ±1500 μA, and ± the SVS level that was determined to be their optimal level from test session 1, normalized by their GVS threshold on each day. The high level (±1500 μA) of SVS was included in this test session to populate a data point in the right tail of the SR curve. Prior to testing, it was unknown whether ±1500 μA would improve or worsen DR thresholds relative to baseline (±0 μA SVS). In the second test session, the order of which the 0 and optimal SVS levels were given was counterbalanced across subjects, however the higher level of ±1500 μA SVS was always given last in the second test session. There is no literature to suggest that a relatively high level of SVS should affect subsequent responses to lower SVS levels, however we wanted be cautious and therefore we always applied ±1500 μA SVS last. Some subjects felt a sensation of stimulation when ±1500 μA was applied while others did not. No subjects reported discomfort due to the stimulation, which was not started until the subjects were in complete darkness. Each test consisted of 150 upright roll tilt trials and the SVS was delivered continuously during testing such that it was on during the motion, the subject response, and the delay until the next motion. Subjects were allowed to take as many self-paced breaks as desired. These always occurred between tests and SVS was not administered during these breaks. A single DR threshold measurement took approximately 40 minutes to complete. The whole Test Session 1 took approximately 4-5 hours including setup, testing, and subject breaks.

5.2.3 SR Equation Fitting Method

In an effort to better visualize "SR exhibition" in our experimental data, the dataset for each subject, which included a DR threshold for each of the 5 SVS levels applied, (±0, ±200, ±300, ±500, or ±700 μA) was fit with an equation from the SR literature discussed in Section 2.5.1 (Equation 8): $A = A_0 \frac{\lambda}{q^2} \frac{r(q^2)}{(4r(q^2)+\omega_0^2)^{1/2}}$. The three parameters discussed in Section 2.5.1 were included as free parameters in the fit: A_0 = Amplitude of weak periodic forcing, ω_0 = frequency of weak periodic forcing, and λ = quartic potential parameter (related to depth and spread of

potential wells). An additional shifting parameter was included that allowed the baseline, or starting point, of the curve to vary depending on the subjects baseline DR threshold and the equation was made negative, corresponding to a dip, rather than peak, in the data. The fit was done using Matlab's bounded minimum search function, fminsearchbnd. This search method finds the minimum of a scalar function of several variables, starting at an initial estimate (Matlab documentation) and allows for bounds to be placed on the individual parameters. Initial values for each parameter were required for the fit and each parameter was given a lower bound of zero, forcing only positive fit values. See Appendix 10.9 for the Matlab scripts used. In Experiment 1 (and Experiment 2), successful fits using the method just described, could not be accomplished for every subject. In these cases, the fits either resulted in a flat line, a curve that decreased but never increased again within the range of the data, or a curve in which the inflection point was negative.

5.2.4 Simulations

To rigorously assess the possibility that the observed SR in vestibular upright roll tilt perception occurred by chance (i.e., appears to occur without an underlying SR phenomenon existing), we compared our experimental results to Monte Carlo simulations of our threshold test protocol (Chaudhuri and Merfeld 2013, Karmali et al. 2015). In brief, the input to each simulation is an underlying DR threshold and the output is a measured or estimated DR threshold. Each estimated DR threshold varies slightly from the underlying DR threshold due to simulated randomness associated with the sampling procedure and imperfect subject perception. We simulated 348 "test subjects" with known underlying levels of SR exhibition and gave these data plots along with the Experiment 1 data plots to three human judges, who were asked to subjectively judge whether each plot resembled SR. Our goal was to see how accurately the three judges could classify the known levels of SR in the simulated data, as well as how consistently they classified the experimental data. Because the design and use of the simulations was so heavily based off of our experimental results, extensive detail on the simulation methods is given in Section 5.3.4, after Experiment 1 results have been presented.

5.3 Results for Experiment 1 and Simulation Details

SR will be discussed in two main ways. The first is in terms of the proportion of subjects that were subjectively identified as exhibiting SR (i.e. did human judges think that the data looked like a characteristic SR curve?). The second method uses a more strict criterion, and asks whether subjects were both identified as subjective SR exhibitors and had a statistically significantly lower than baseline minimum threshold. The data is also normalized and averaged across the group of subjects and the SVS effect is discussed in terms of mean changes as well. The experimental data will be discussed in comparison to the simulated data sets that were judged by 3 independent judges.

5.3.1 Session 1 SR results

As our primary finding, vestibular perceptual SR was subjectively exhibited in 10/12 subjects (Figure 19, subplots with blue curve fit). In these subjects, the DR thresholds decreased with increasing SVS, reached a minimum value and then increased to a value generally below the baseline, or the 0 μA SVS threshold. We fit our data with a defined SR equation from the SR literature (Method discussed in Section 5.2.3 above and Appendix 10.9). The resulting curve fits can be seen overlaid on the experimental data in Figure 19. We do acknowledge that this equation comes from the classical form of SR, namely a bi-stable dynamical system that may not be a perfect analog to the vestibular perceptual system being tested in this experiment. However, the goodness of fit from visual inspection further solidifies the belief that SR is indeed being exhibited in the vestibular system as measured by our perceptual threshold task. Out of the 10 subjects that exhibited SR subjectively, 6 also had a statistically significantly lower ($p<0.05$) minimum threshold compared to their baseline threshold (t-test and indicated in Figure 19). Including all 10 subjectively identified SR exhibitors, the decrease in threshold due to the "optimal" level of SVS ranged from 0.02 deg/s (SF) to 0.41 deg/s (SI), with a percent change from baseline ranging from -5.4% (SF) to -47% (SK), and an average percent change of -30%. Including only the 6 subjects that also had statistically significant lower thresholds with SVS, the smallest decrease was 0.10 deg/s (SB), the smallest percent change from baseline was -26% (SJ), and the average percent change was -39%.

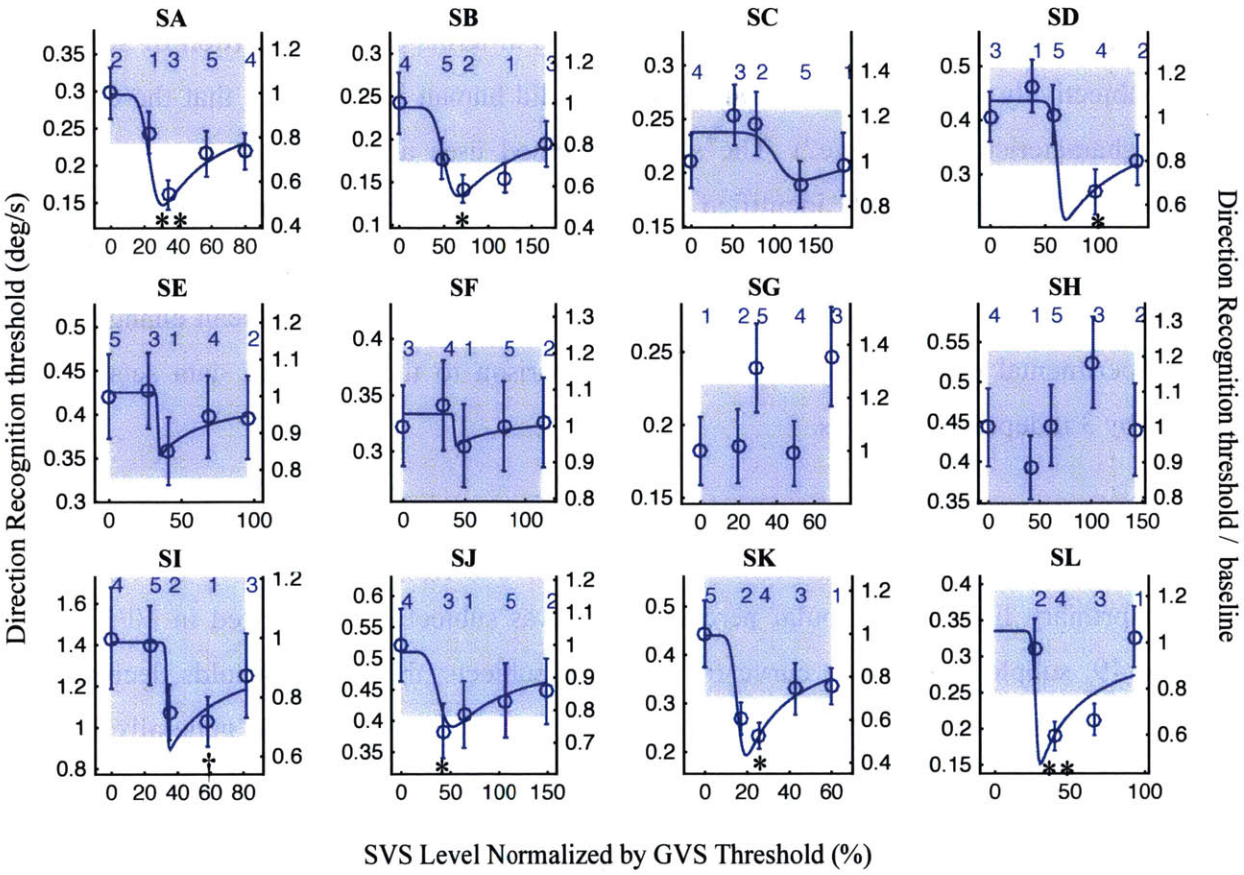

** p<0.005 , * p<0.05, † p=0.078

Figure 19. Upright roll tilt DR thresholds (0.2 Hz) from the first test session vs. SVS level normalized by the individual subject's GVS threshold on the same day. Left axis indicates the 50% DR threshold in deg/s. Right axis indicates the threshold normalized by the baseline measure (0 μA SVS). Each threshold was calculated using a 3 – down 1-up 90% target staircase method. Error bars indicate standard error. Lapse detection was applied. Blue shaded areas indicate the 95% confidence interval of the baseline (0 μA SVS) threshold measure, calculated with the same jackknife procedure. The blue line is the fit SR curve for each individual subject, when a successful fit was possible. Blue numbers above data points indicate the order that the SVS level was given, which was randomized for each subject. Applied SVS levels were 0, 200, 300, 500, and 700 μA for every subject and correspond to the data points in that order for each subplot from left to right. p-values refer to a statistically significantly lower DR threshold compared to the baseline motion threshold (one-tailed t-test).

The percentage of subjects exhibiting subjective SR behavior (75%) in this data set is similar or higher, than the percentage of subjects that are typically identified as SR exhibitors in other SR studies. For example, with 90% sensory threshold SVS applied, 8/17 (47%) subjects had increased ocular counterroll in response to whole body tilts (Geraghty et al. 2008). With some

level of SVS between ±0-700 μA SVS, 10/15 (67%) and 8/15 (53%) subjects had improved balance performance with 0-30 Hz, and 1-2 Hz SVS, respectively (Mulavara et al 2011). With some level of SVS between 0 and 400% of perceptual threshold, 32/45 (71%), 30/45 (67%), and 22/45 (49%) of subjects had reduced sway in the medio-lateral, anterior-posterior, and combined directions, respectively. These studies did not require the characteristic SR shape to be present in the individual data sets, nor did they require that there be statistically significant differences between the 0 and optimal SVS conditions with an individual subject.

The percentage of subjects exhibiting subjective SR and a statistically significantly lower than baseline minimum DR thresholds was 50% in our data set. This percentage is slightly lower than other studies that have reported individual statistical results. Yamamato et al. (2005) did find statistically significant differences within individuals, showing that with 60% nociceptive threshold SVS, 4/7 (57%) and 9/12 (75%) subjects had significantly smaller scaling exponents for GVS, a measure that corresponded to heart rate dynamics and trunk activity dynamics of healthier individuals, respectively. Finally, Collins et al. (1996) recorded directly from cutaneous SA1 mechanoreceptor neurons and still did not find 100% SR exhibition (aperiodic SR, discussed later in Section 7.1) although the exhibition rate was very high with 11/12 neurons (92%) showing the characteristic SR shape behavior over a range of input noise levels.

The exhibition of vestibular perceptual SR for 0.2 Hz upright roll tilt motions was clear when looking at data from certain individual subjects and this remained the case when we averaged across subjects (Figure 20). When all 12 subjects were included, the two lowest average motion thresholds were achieved at the 500 and 300 μA SVS levels, with a normalized change from baseline of 16.7% and 16.0%, respectively (Figure 20A). There was a statistically significant decrease of 0.086 deg/s from the 0 to 300 μA SVS group means (paired $t(11)=2.530$, $p=0.014$). Similarly, the decrease was 0.082 deg/s between the 0 and 500 μA SVS means (paired ($t(11)=2.377$, $p=0.019$). The normalized change was 25.6% between the group average baseline and minimum threshold when the optimal SVS level was allowed to vary between subjects (Figure 20B). There was a statistically significant decrease of 0.118 deg/s between the baseline and minimum threshold group means (paired $t(11)=3.706$, $p=0.002$). With the two non-SR exhibitors (SG and SH) removed from the dataset, the group optimal SVS level was 300 μA with

a motion threshold normalized change of 22.4% between baseline and optimal SVS (Figure 20C). There was a statistically significant decrease of 0.109 deg/s between the 0 and 300 μA SVS group means (paired t(9)=3.005, p=0.008). When allowing for varying optimal SVS levels by subject, the normalized change between the average group baseline and optimal was 29.5% (Figure 20D) and there was a statistically significant decrease of 0.136 deg/s between the group baseline and minimum threshold means (paired t(9)=3.856, p=0.002).

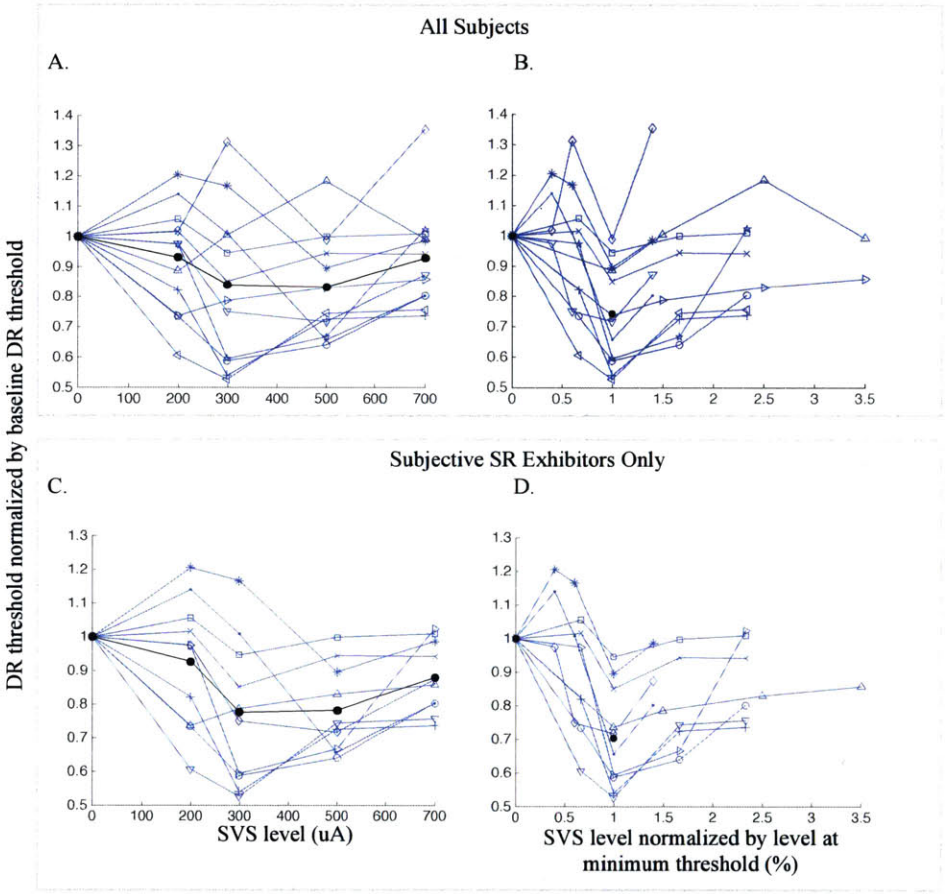

Figure 20. Group upright roll tilt DR thresholds. A: In blue, upright roll tilt DR thresholds connected by simple line for each individual subject normalized by their baseline threshold vs. SVS level delivered. Thick black data points represent the average threshold across all subjects. B: DR thresholds normalized by baseline vs. SVS level normalized by each subject's optimal SVS level, or that which resulted in the lowest motion threshold. Thick black dots represent average thresholds at group baseline and optimal. C and D match A and B except that the two "non-SR exhibitors" (Subjects G and H) have been removed from the group.

5.3.2 GVS Threshold Variation between Sessions 1 and 2

Average GVS 1 Hz current detection thresholds (described in Section 4.3) varied considerably across subjects, ranging from 380 to 1,165 μA during Test Session 1 and 365 to 1,185 μA during Test Session 2. Motion thresholds were minimized at 300 μA SVS for six out of the 10 SR-exhibitors, at 500 μA SVS for three subjects, and at 200 μA SVS for one subject (Figure 19).

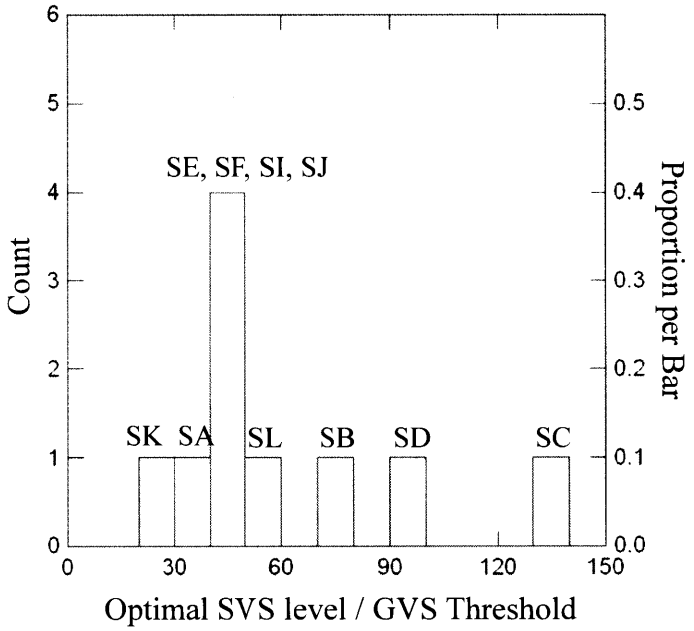

Figure 21. Histogram of SVS level that resulted in the minimum motion threshold normalized by each subject's individual GVS threshold. Subject numbers in each bin are labeled above respective bars.

An examination of optimal SVS levels normalized by individual GVS thresholds shows that for 4 out of 10 SR exhibitors normalized optimal SVS level was between 40-50 %. The remaining normalized optimal SVS levels ranged between 25% and 132% (Figure 21).

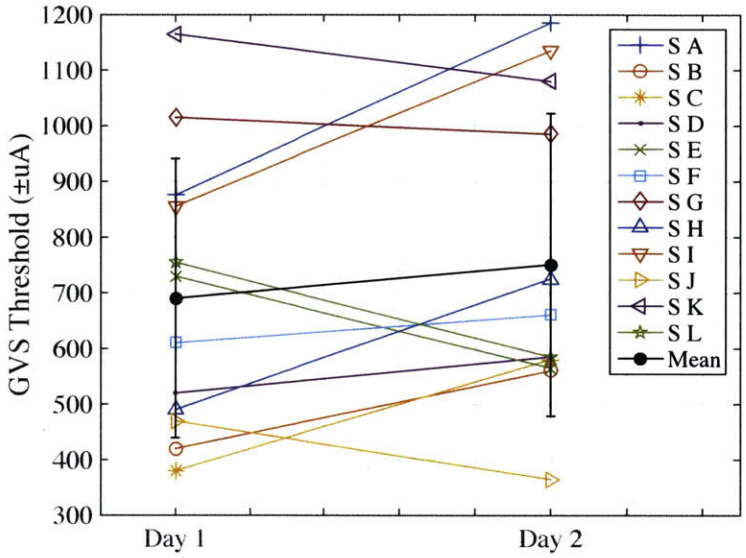

Figure 22. GVS thresholds for all 12 subjects in upright roll tilt DR group for Test Session 1 and Test Session 2. Group mean GVS threshold and standard deviation are shown in black.

GVS thresholds varied more between subjects than within individual subjects across test sessions (Figure 22). The absolute difference in GVS thresholds between Test Session 1 and 2 ranged from 30-280 μA within individual subjects, while the difference across subjects was 785 and 820 μA for Test Session 1 and 2, respectively. There was no statistically significant difference in the group means of GVS thresholds between Test Session 1 and Test Session 2 (paired $t(11) = -1.213$, $p = 0.251$). Additionally, a significant slope was found between the GVS thresholds measured on Test Session 1 and 2 ($F(1,10)=16.024$, slope = 0.724, $p = 0.003$), with $R^2 = 0.616$ suggesting that GVS thresholds were correlated across test days. From observation, there were differences between subjects in the size of the phase lag between the applied sinusoidal GVS stimulation and their reported motion perception due to the stimulation. It's unclear whether this lag was physiological, cognitive perhaps in the decision-making pathway, or due to motor response delays.

To ensure that we were in principle applying the same optimal SVS level from Test Session 1 during Test Session 2, we adjusted the optimal SVS level from Test Session 1 by multiplying by the ratio of GVS thresholds from Test Session 2 and 1. All GVS threshold tests were

accomplished prior to motion threshold tests and therefore the optimal SVS level to be applied in Test Session 2 was determined after the GVS threshold was measured on that day.

5.3.3 Session 2 SR Repeat Test Results

To investigate the repeatability of the Test Session 1 SR results, we retested the DR threshold 6-14 days after the first test session. Motion thresholds were measured using three SVS stimulus levels: none, the subject's optimal SVS level from test session 1 (normalized by GVS threshold measured on the repeat test day), and 1500 μA. These data are shown in red in Figure 23. For ten of the subjects, retesting was accomplished in a single session. For two others, two retesting sessions were required due to scheduling conflicts (data points identified in Figure 23 using black diamond data points).

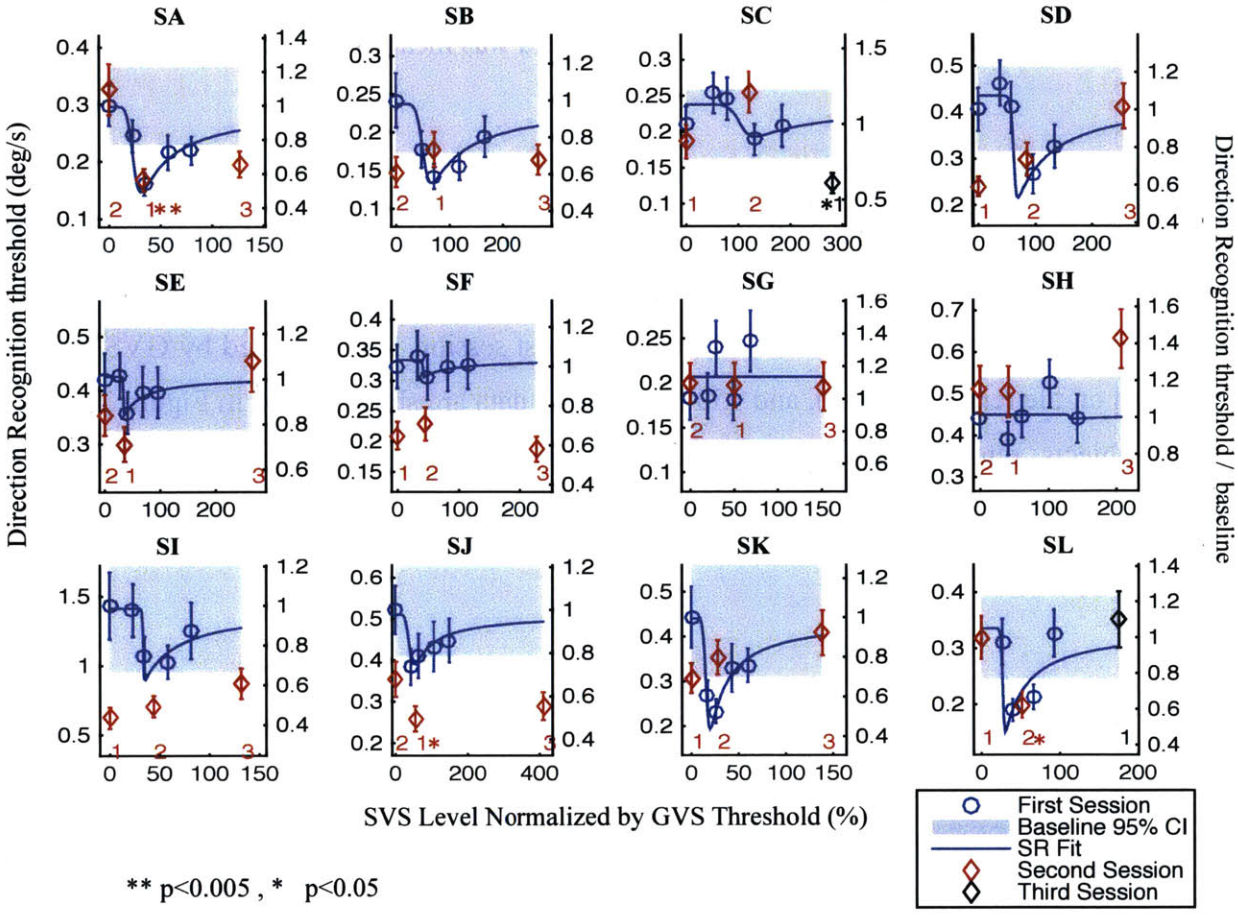

Figure 23. Upright roll tilt DR thresholds for Test Sessions 1 and 2. Data and features in blue as explained in Figure 19. Red diamond data represent the DR thresholds measured during Test Session 2 for each individual subject. Due to scheduling conflicts, two subjects completed their testing on a third test session (identified with black diamond data points). All subjects were tested at 0 and 1500 μA SVS regardless of their GVS threshold. The middle SVS level was individualized based on the subject's data from Test Session 1. Red (and Black) numbers indicate the order of which the SVS level was given within Test Session 2. 1500 μA was always given last while 0 and "optimal" SVS levels were counterbalanced between subjects. p-values refer to a statistically significantly lower DR threshold compared to the baseline DR threshold both measured during Test Session 2 (one-tailed t-test).

Four out of the ten SR-exhibitors (SA, SE, SJ, SL) showed repeatability of the SR exhibition, in that on Test Session 2 when their adjusted optimal SVS level was applied, their motion threshold was lower than their baseline motion threshold on Test Session 2. Three out of those four subjects (SA, SJ, SL) had statistically significantly lower thresholds with optimal SVS than with no SVS (t-test, labeled in Figure 23) in both the first and second test sessions. The remaining six

SR-exhibitors (SB, SC, SD, SF, SI, SK) did not indicate SR repeatability. However, it is worth noting that five of these subjects (SB, SD, SF, SI, SK) did not exhibit SR repeatability, not because of inconsistent DR thresholds at optimal SVS, but because of a decrease in their motion threshold in the baseline (0 SVS) condition. In fact, 6 out of the 12 subjects had statistically significantly lower baselines in Test Session 2 than Test Session 1. This was an unexpected result based on the consistency of DR thresholds across days in our preliminary study of motion threshold repeatability.

The DR thresholds with 1500 μA SVS in Test Session 2 were consistent with the SR fit in Test Session 1 in four out of the ten SR-exhibitors (SD, SE, SK, SL). The remaining six subjects had lower motion thresholds when given 1500 μA SVS than were expected based on Test Session 1 results. With all 12 subjects included, there were no statistically significant differences between group means (0, optimal, and 1500 μA SVS) of log transformed motion thresholds as determined by a repeated measures ANOVA ($F(2,22) = 0.553$, $p=0.583$). There were also no statistically significant differences when only the 10 SR-exhibitors From Test Session 1 were included ($F(2,18)=0.372$, $p=0.695$) (Figure 24). Because the drop in baseline on Test Session 2 was so unexpected, a comparison was also made between the Test Session 2 optimal SVS test and pooled baseline (SVS = 0) data from Test Session 1 and Test Session 2. Pooling the baseline data from both test sessions, still only 3 out of the 12 subjects had a significantly lower DR threshold when the normalized optimal SVS level was applied on Test Session 2 (see Appendix 10.10 for more details).

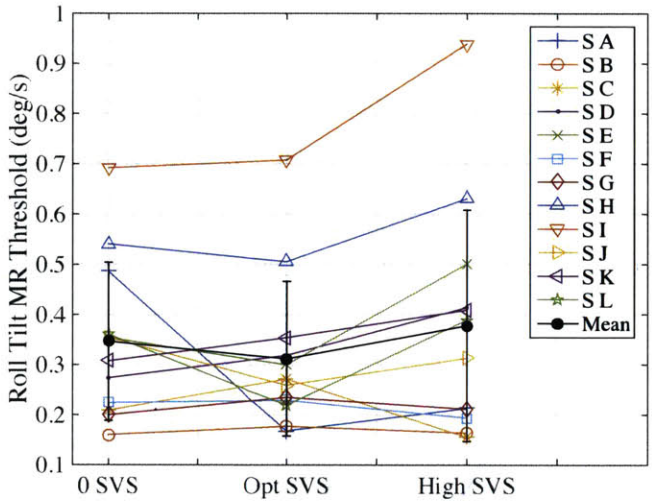

Figure 24. Test Session 2 data for the 10 SR-exhibitors from Test Session 1. Black data points and error bars represent the mean of all subjects and the standard deviation.

5.3.4 Comparison to Simulations

To provide a wide spectrum of possible outcomes, three simulation cases were considered: 1) Strong underlying SR exhibition, 2) Weak underlying SR exhibition, and 3) No underlying SR exhibition. Cases 1 and 2 were defined using actual SR curves fit to subject data from Experiment 1, Test Session 1. The SR curve representing strong SR was defined by the fit to SA's data and was characterized by an optimal level at 300 μA SVS and an improvement in DR threshold from baseline to optimal of 46%. The Weak SR case was defined using the SR curve fit to SE's data, of which had an optimal level of 300 μA and a change from baseline to optimal of 14.9%. Case 3 was defined by constant threshold of 0.34 deg/s (i.e. no improvement in threshold as a function of SVS level), which was the arithmetic mean DR threshold for the 10 SR exhibitors, excluding SI who had a relatively high threshold compared to the group. Case 3 utilized the same underlying DR threshold for the simulation of each "SVS level" and thus quantified the inherent measurement variability in the *estimated* DR thresholds. Specifically, Case 3 demonstrates that multiple simulations (or repeated empirical tests) of the same *underlying* DR threshold will yield different *estimated* DR thresholds due to measurement and perceptual variability. In all simulations the underlying bias was set to zero for simplicity.

A single simulated subject data set was constructed as follows. The SR curve from one of the three simulation cases was used to define the underlying motion threshold at each of the 5 SVS levels (set to be the same as those tested: ±0, 200, 300, 500, and 700 μA) (Figure 25A). With the bias (μ) set to zero, each individual motion threshold (σ) was input to the experiment simulation. A cumulative distribution function (CDF('norm',X, μ, σ)) with X equal to the range of motion stimuli was then fully defined (Figure 25B). One trial at a time, the simulation then calculates a subject response to a single motion stimulus (initial motion amplitude was set to 2 deg/s, matching the experiment). The subject response (left or right) and whether the response was correct or incorrect, was determined by calculating the probability of a rightward response for the specific motion stimuli (using the Gauss error function to solve the CDF) and then assessing whether a random number selection, from 0 to 1, falls above or below the calculated probability (Figure 25C). This random element corresponds to human perceptual processing, modeled using signal detection theory (Green and Swets 1966) in that subjects will not always choose the same response even if given the identical motion stimuli many times. For example, although the probability for responding correctly may be high (e.g. 74%) for a relatively large motion stimulus, there is still a chance (e.g. 26%) that the subject's perception of the motion will result in an incorrect response. It is from this random component of the simulation that the output, estimated motion threshold (and bias) varies even when the same underlying motion threshold (and bias) is used as an input. In the simulation once the subject response was determined, the next motion stimulus was defined using the same adaptive 3-down, 1-up 90% target with an initial 2-down, 1-up phase method, as was used experimentally. This process was repeated until all 150 trials had been simulated, resulting in a set of 150 motion stimuli and their associated simulated subject responses for each underlying motion threshold.

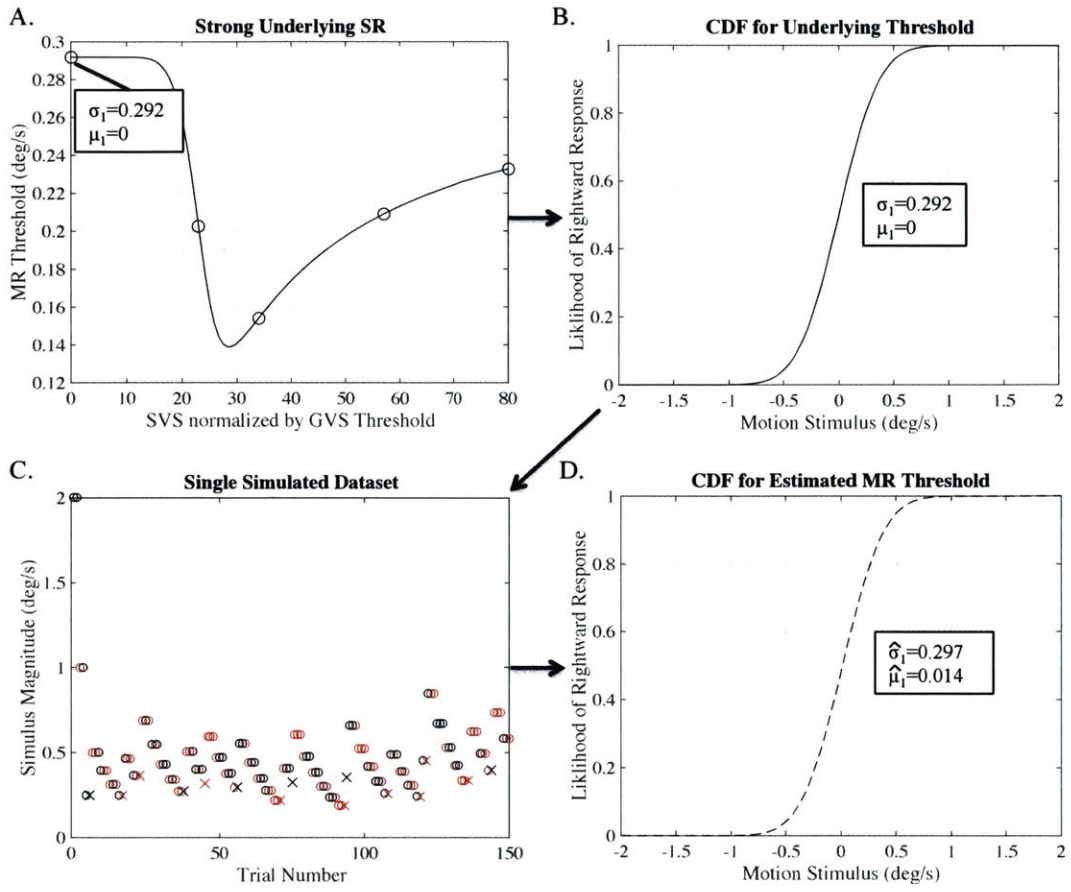

Figure 25. Example of the simulation steps for calculating an estimated DR threshold with strong underlying SR. This example is for the first threshold at 0 SVS. A: Strong underlying SR curve with the underlying thresholds for each SVS level (normalized by GVS threshold) shown. B: Cumulative Distribution Function (CDF) defined by the first underlying threshold with the bias set to zero. C: Simulated data set for the underlying threshold. Red and black circles represent correctly identified rightward motions and leftward motions, respectively. X's represent incorrectly identified motions. D: CDF fit to the simulated data defined by the estimated DR threshold $\hat{\sigma}_1$ and bias $\hat{\mu}_1$.

The data set was then fit using a bias-reduced glm fit (Chaudhuri and Merfeld 2013), again matching the experimental fitting approach, defining a new CDF for the estimated DR threshold (Figure 25D). Lapse detection and standard error calculations were done in the same manner as well and the result was an estimated motion threshold at each SVS level (blue data points, Figure 26). To simulate Test Session 2 (red data points, Figure 26) for each subject, two additional simulations were performed corresponding to the 0 SVS threshold level and the SVS level at which the minimum estimated DR threshold occurred during "Test Session 1". For these, we used the underlying threshold of the original underlying SR curve (thus assuming perfect

"repeatability" from simulated Test Session 1 to simulated Test Session 2). Finally an SR curve was fit to each individual "subject" and was overlaid on the Test Session1 data along with baseline 95% confidence interval shaded box.

5.3.4.1 Independent Judges

In Figure 19 we subjectively identified 10/12 subjects that exhibited SR in upright roll tilt DR thresholds. However, we note random variability in threshold estimates, as well as potential biases in "seeing SR", may have caused us to subjectively identify SR exhibition even when none existed, or vice versa. To rigorously protect ourselves against this, and further quantify the proportion of SR exhibitors and magnitude of SR exhibition (i.e. large or small improvements relative to the 0 SVS level), we asked three judges (the author was one of the judges) to independently review simulated and experimental data for SR exhibition. Judges were blinded to underlying SR types (simulated Case 1, 2, 3, or experimental). A Matlab script was written to randomly simulate either Case 1, 2, or 3, and randomly group simulated subjects with real subject data from Experiment 1 into sets of 12 (An example is shown in Figure 26). Although the author wrote this Matlab script, she remained blinded to the underlying SR cases to be judged, just as the other two judges were. All three judges were familiar with the characteristic SR curve prior to participating in this judging process.

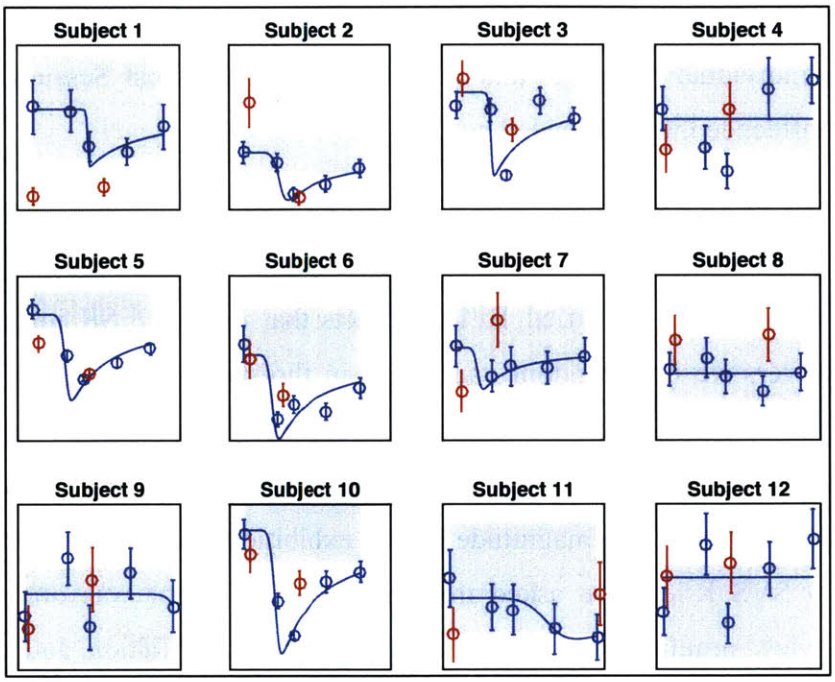

Figure 26. Example figure given to three independent judges for review. Blue data corresponds to Test Session 1 data and red data corresponds to Test Session 2. Subplots represent an individual subject who was either simulated using one of the 3 simulation cases or from the actual experimental data set. Presentation of these 4 possible groups was completely random within and across figures. This figure set consists of (in subject order) S, S, S, N, S, S, W, W, N, S, N, N with S = strong SR, W= weak SR, and N= No SR.

In total, 360 "subjects" (where each "subject" consists of a single subplot in Figure 26) were presented to the judges. These consisted of the 12 actual subjects from Experiment Test Session 1 and 348 simulated cases, 116 simulations of each of the simulated SR conditions: Strong SR, Weak SR, and No SR. Axes labels were purposefully left off of plots in order for judges to not be influenced by the magnitude of any differences between thresholds. Plots were given to the judges as Matlab figures and therefore judges could zoom in on each "subjects" data as they desired.

Judges were given written instructions and an Excel template to record their judgments. For each subplot, they were asked to indicate if 1) SR was exhibited and 2) if SR repeatability was achieved during Test Session 2. Judges were not instructed to prioritize either correct or incorrect classification. Instructions stated:

"SR is considered exhibited in Test Session 1 data if the baseline (leftmost blue data point) is highest or almost highest data point, and there is a dip followed by a gradual return to baseline. The 95% CI of the baseline data point is included in the plots for your reference however it is NOT necessary that the dip of the data be significantly different than the baseline (outside of the CI) for you to consider a subject to be exhibiting SR. Additionally, an SR curve has been fit to the Test Session 1 data for your reference. Since the goodness of fit is dependent on initial conditions, a good solution cannot always be found for these large-scale random simulations. Therefore it is possible for SR to be exhibited even though a good fit was not plotted. Please consider that case and zoom in when needed."

"Baseline and Optimal relationship is considered to be repeatable if the direction of the relationship is convincingly consistent between Test Session 1 and 2 (for example in both days the BL is higher than the Opt or vice versa). Do you believe that there is repeatability?"

Judges were also given this simple sketch to use as a reference for what typical SR exhibition looks like:

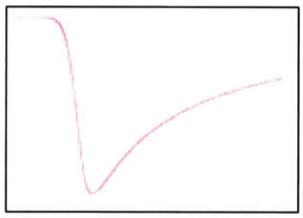

5.3.5 Comparison to Simulations Results

When split by group (3 simulation groups and experimental group), all three judges identified SR exhibition in a higher percentage of subjects for the Strong underlying SR case (mean=95.7%, stdev=2.3%) than for the Weak underlying SR case (mean=54.3%, stdev=11.4%) than for the No underlying SR case (mean=31.3%, stdev=13.7%)(Figure 27). The percentage of subjects identified as SR exhibitors by all three judges were 13.8, 39.7, and 93.1% in the No, Weak, and Strong underlying SR simulation groups, respectively. For the experimental data set, two of the

three judges identified 83.3% of subjects (the same 10 subjects) as exhibiting SR, matching the author's assessment in the previous section without the experimental subjects intermixed with simulated "subjects". Judge 2 was relatively more strict in their identification of SR exhibition across all groups and identified only 66.7% (8/12) of experimental subjects as exhibiting SR. We will refer to the average judge vote of 9/12 subjective SR exhibitors from now on. This proportion of SR exhibitors in upright roll tilt (75%) was statistically significantly higher than that of the simulation group with No underlying SR ($z=3.01$, $p=0.001$), not different from the Weak underlying SR ($z=1.38$, $p=0.084$), and lower than the proportion of SR exhibitors in the Strong underlying SR group ($z=-2.82$, $p=0.002$).

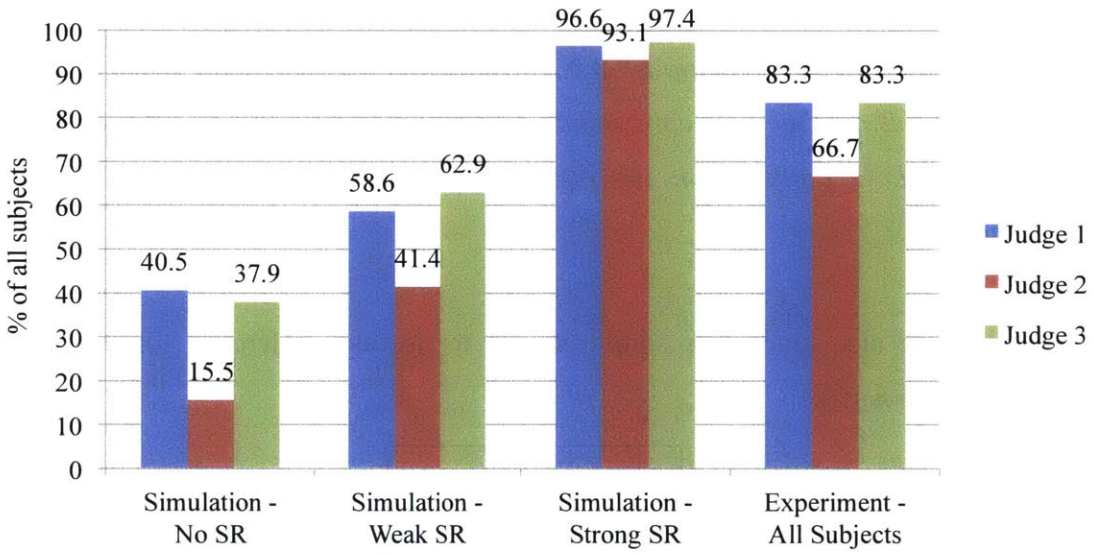

Figure 27. Percentage of subjects identified by three judges as subjective SR exhibitors, for each of the three simulated cases and for the experimental data set. N=116 in first three groups. N=12 in experiment group.

An important finding from the simulations was that even when there was absolutely No underlying SR (Case 3), the judges (incorrectly) identified an average of 31.3% of subjects as SR exhibitors. Thus the inherent variability in subject perception in combination with our experiment design could result in a relatively large number of false positives. Inversely, even with Strong underlying SR, there was an average of 4.3% of cases that were not identified as exhibiting SR. Therefore, our simulations make it clear that in our experimental paradigm, it is very possible for human judges to classify data as exhibiting SR when it is not actually present. It is also possible, although perhaps less likely, that a subject who actually has Strong underlying

SR may be judged not to. We conclude that this rigorous method using simulations was valuable in assessing the presence of SR (particularly in dealing with false positives).

From a signal detection theory perspective, the three judges participated in a psychophysical experiment by judging if SR exhibition was present in a large data set of negative and positive SR exhibitors. The resulting Receiver Operating Characteristic (ROC) curve for the Weak and Strong underling SR groups shows a clear difference in the sensitivity (or d') in judging between the Weak and Strong underlying SR groups (Figure 28).

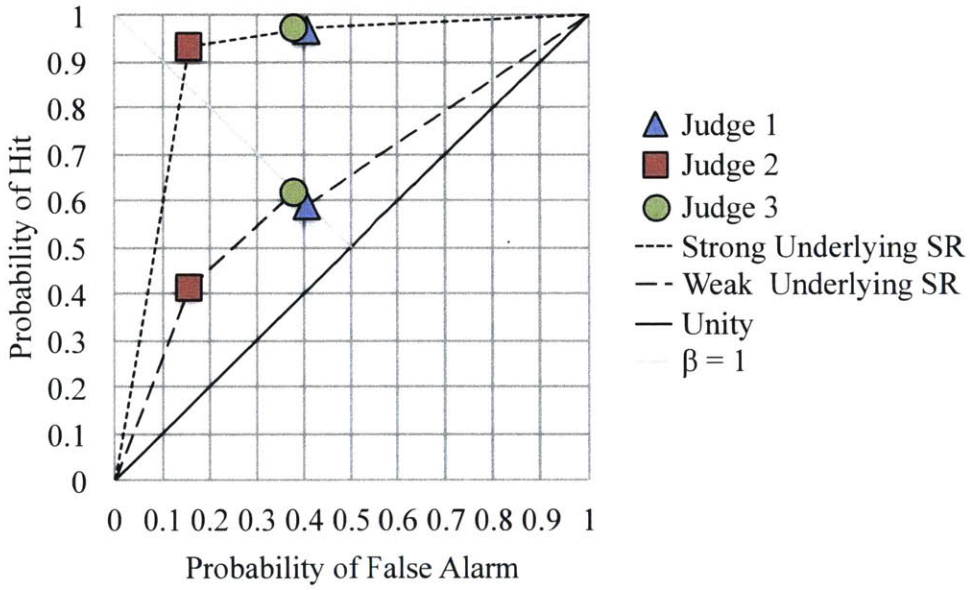

Figure 28. ROC curve plots for the SR Exhibition Judging decisions divided by the Weak and Strong underlying SR group simulations.

The ROC curve shows that it was more difficult to correctly identify negative and positive SR exhibitors when the underlying signal was weak. Judges 1 and 3 had similar response styles, with β approximately equal to one in the Weak SR group and β lower than one in the Strong SR group, consistent with a more liberal tendency to identify positive SR exhibition. Judge 2 differed in both SR groups, with a β close to one in the Strong SR group and a higher β than the other two judges in the Weak SR group suggesting that Judge 2 had the most conservative threshold for identifying positive SR exhibition. Within each simulation group, the judges'

responses were such that they reasonably lie on the same ROC curve (small and large dashed lines in Figure 28), suggesting that the judges' thresholds for detection were different but there was no fundamental difference in how they were completing the judging task. The Area Under the Curve (AUC) for the Strong and Weak SR groups including all three judges was 0.90 and 0.64, respectively.

Similar to our experimental data analysis, we also looked at the percentage of simulated subjects that were identified as subjectively exhibiting SR that also had a significantly lower than baseline minimum DR threshold. The percentage was higher for the Strong underlying SR case (mean=93.4%, stdev=1.8%) than for the Weak underlying SR case (mean=36.2%, stdev=2.3%) than for the No underlying SR case (mean=16.1%, stdev=3.5%) (Figure 29). For the experimental data set, all three judges identified 50% of subjects as exhibiting SR that also had a significantly lower than baseline minimum threshold, matching what was claimed in a Section 5.3.1. Using the unanimous judge vote of 6/12 SR exhibitors that also had statistically significantly lower than baseline minimum thresholds, the proportion in upright roll tilt (50%) was statistically significantly higher than that of the simulation group with No underlying SR ($z=2.83$, $p=0.002$), not different from the Weak underlying SR ($z=0.940$, $p=0.174$), and lower than the proportion in the Strong underlying SR group ($z=-4.72$, $p<0.001$). This suggests that the SR exhibition with statistically significantly lower thresholds seen in our experimental data likely did not happen by chance.

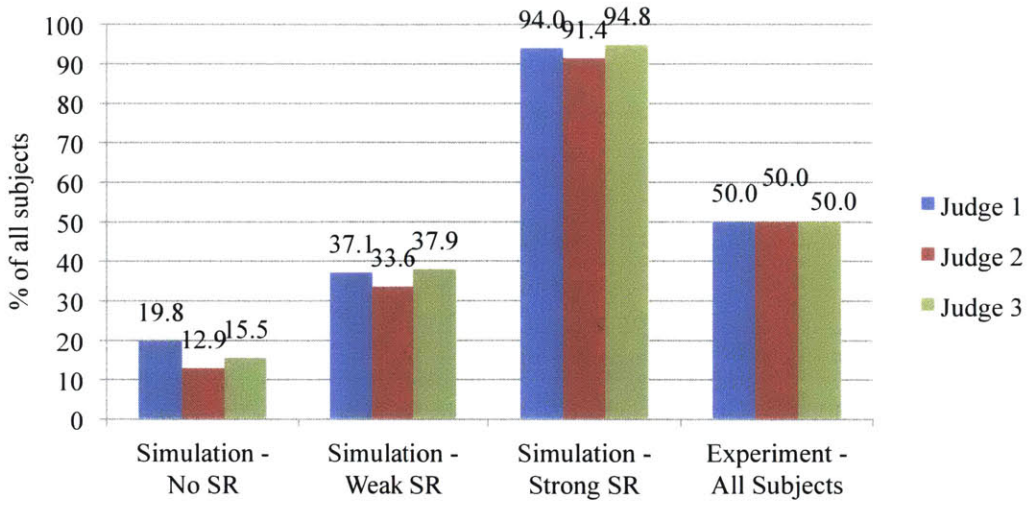

Figure 29. Percentage of subjects identified by three judges as subjective SR exhibitors that also had a significantly lower than baseline minimum DR threshold. N=116 in first three groups. N=12 in experiment group.

Independent of SR exhibition, judges were also asked to judge whether there was convincing repeatability of the relationship between the baseline and minimum motion threshold between Test Sessions 1 and 2. All three judges identified SR exhibition and between session repeatability in a higher percentage of subjects for the Strong underlying SR case (mean=93.7%, stdev=1.8%) than for the Weak underlying SR case (mean=31.3%, stdev=5.1%) than for the No underlying SR case (mean=12.7%, stdev=6.5%) (Figure 30). For the experimental data set, all three judges identified 4/12 or 33.3% of subjects as exhibiting SR on both test days, matching what was claimed in a Section 5.3.1. Using this unanimous judge vote of 4/12, the proportion in upright roll tilt (33.3%) was not statistically significantly higher than that of the simulation group with No underlying SR ($z=1.25$, $p=0.108$) or the Weak underlying SR ($z=0.188$, $p=0.429$), but was statistically significantly lower than the proportion in the Strong underlying SR group ($z=-6.14$, $p<0.001$). This suggests that there are experimental factors that tend to reduce the repeatability of SR exhibition compared to the idealistic simulations.

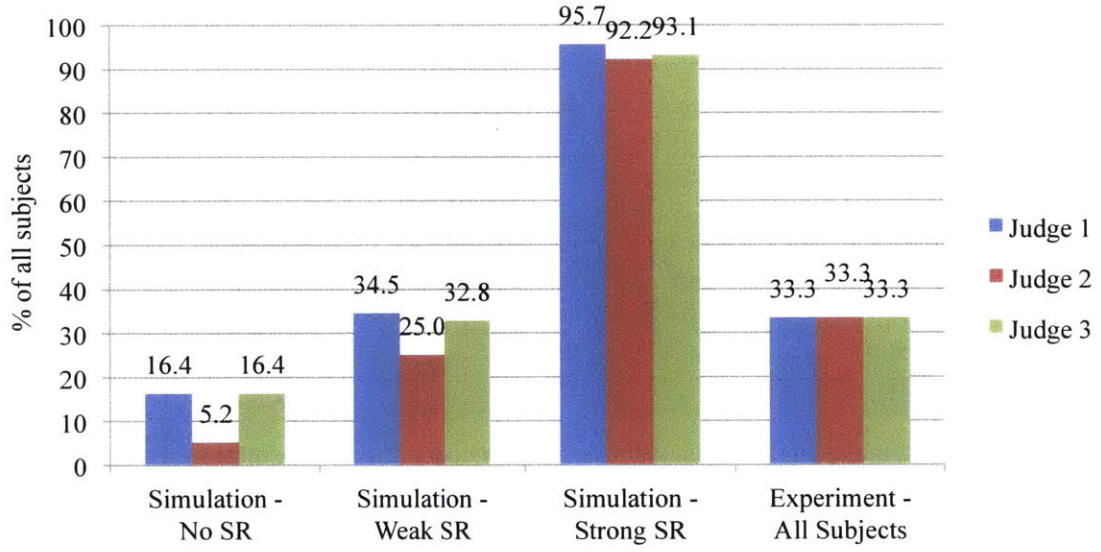

Figure 30. Percentage of subjects identified by three judges as having both subjective SR exhibition and between session repeatability. N=116 in first three groups. N=12 in experiment group.

5.3.6 Lack of correlation between GVS thresholds, DR thresholds, and optimal SVS levels

We also investigated whether there were any correlated or predictive variables in our data set that may be useful in future experiments or future implementation. Firstly, we know that both GVS and physical motion stimulates vestibular afferents. We therefore asked if there was a correlation between subjects' thresholds to GVS and thresholds to motion but found no correlation between GVS threshold and baseline DR threshold within our subjects. We also asked if the GVS threshold correlated with our estimates of subjects' optimal SVS level for motion thresholds. Could we have simply measured GVS threshold (~8 min task) to determine the optimal motion SVS level (~ 3 hours of testing)? We found no correlation between these variables in part due to the relatively large range of measured GVS thresholds (380-1165 μA) compared to the more narrow range of optimal SVS levels (40% of subjects were at 300 μA). There was also no correlation between GVS threshold and the difference or percent change in DR threshold between baseline and minimum, suggesting that a subject's sensitivity to GVS did not influence how effective SVS was in improving motion direction recognition. GVS thresholds also did not seem to relate to SR exhibition or SR repeatability in any way.

Lastly we asked if a subject's baseline motion threshold correlated to the improvement in threshold with SVS (baseline threshold – minimum threshold). For our 10 SR exhibitors we found a significant correlation between these two variables ($R=0.892$, $p=0.001$), suggesting that if a subject was relatively weaker at the task to begin with, they have more room for improvement and therefore experienced larger improvements in performance with SVS.

5.4 Summary of Results and Discussion

Through both a qualitative and quantitative analysis, we definitively showed the exhibition of stochastic resonance in vestibular perception using an external application of low-level electrical noise. Subjective SR exhibition was shown in 9/12 subjects while statistically significant SR exhibition, defined by both subjective SR exhibition and a significantly lower than baseline minimum DR threshold was found in 6/12 subjects. SVS elicited an improvement in upright roll tilt DR thresholds with a maximum percent change of 47% within an individual and a mean percent change of 30% and 39% for the subjective and statistically significant SR groups, respectively. These results indicate that with a nonzero level of SVS, at least half of the subjects were better able to correctly perceive passive body motion in the absence of visual cues. Further, the characteristic shape of the relationship between DR threshold and SVS level was quite consistent with classical SR theory (i.e. a decrease in threshold with increasing SVS level up to some optimal level and then a gradual increase back towards the baseline, no SVS, threshold). Similar to other physiological studies of stochastic resonance, we could not measure SR in every subject. It is possible that these non SR subjects (Subjective: 3/12, Statistically: 6/12) 1) indeed do not exhibit SR, 2) did exhibit SR, but because of experimental variability it was not measurable, or 3) could exhibit SR, but our experiment design was not conducive to measuring their SR exhibition due to inappropriate sampling (Figure 31).

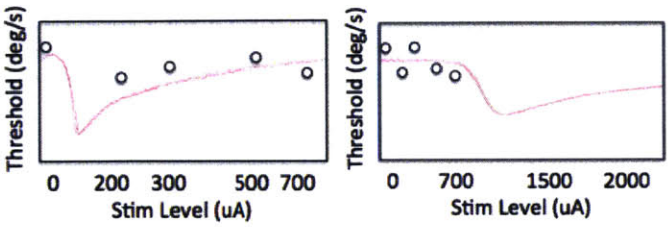

Figure 31. Possible scenarios in which underlying SR (represented by red line) would not be captured by our chosen sampling of SVS levels. The characteristic SR dip might be narrow and between two applied SVS levels (left) or occur outside of the range of SVS levels tested for an individual subject (right).

GVS thresholds (to sinusoidal signals) were more consistent across test sessions within individual subjects, than between subjects. This between subject variability may be explained by the following possibilities:

1) Subjects have different physiological sensitivities to the same applied GVS level.

    -Each subject's vestibular neurons likely did not receive the same level of stimulation due to inter-individual differences in the anatomy of the mastoid process and vestibular system.

2) Subjects have different perceptual sensitivities to the same GVS induced neuronal stimulation.

    -Perhaps the GVS actually delivered to the neurons was relatively similar between subjects, and the variability mostly occurred during perceptual and cognitive processing.

Differences in the measured GVS threshold across multiple test sessions within subjects may have been caused by slight differences in electrode placement, the amount of gel applied, or how the gel interacted with the skin. An individual's perceptual threshold for GVS may have also varied across test sessions. Future studies could investigate the repeatability of GVS thresholds with various methodologies, including a forced choice motion detection or motion direction recognition task, similar to how DR thresholds were measured.

It is intriguing that even though subjects varied considerably in their "sensitivity" to GVS as indicated by their perceptual threshold to sinusoidal GVS, they did not vary considerably in terms of what level of applied SVS was optimal or near optimal in terms of improving their motion threshold. Half of our subjects achieved their minimum motion threshold at 300 μA SVS and 8/12 subjects had lower DR thresholds than baseline with 300 μA SVS applied (Figure 20). This SVS level also corresponded to the minimum motion threshold when subjects' DR

thresholds were averaged together by SVS level, and suggests that inter-subject differences in GVS thresholds may be predominantly due to perceptual processing. We must be careful to remember that there is a fundamental difference in the nature of the electrical GVS signal in each task: 1Hz sinusoidal in the GVS threshold task vs. 0-30 Hz wideband white noise in the motion threshold task. Perhaps SVS thresholds if measured, would better relate to what level of SVS was most beneficial for an individual. In terms of practical use of SVS in the future, it would be beneficial if the range of helpful SVS levels was relatively small across subjects, such that the SVS level may not need to be tuned specifically for each individual in order to see an improvement in performance.

We investigated the repeatability of SR exhibition on a separate test day and found fairly poor SR consistency between test sessions (Subjective: 4/12, Statistically: 3/12 subjects). However in 5/12 subjects, this was due to inconsistent baseline motion thresholds (0 SVS) rather than inconsistent motion thresholds with nonzero "optimal" SVS reapplied. Recall that the threshold measurement has some inherent noise due to the nature of the forced-choice task. This inherent variability in the threshold task may have showed up in our results as outlier data points, however the inconsistency of the baseline data was unexpected since our preliminary repeatability experiment showed remarkable consistency of DR thresholds (without SVS) across days, weeks, and even months (not discussed). The improvement in baseline (0 SVS) DR threshold would be consistent with a learning effect from Test Session 1 to 2. However, we suggest this is unlikely, since it has previously been shown that learning is not strong in vestibular self-motion threshold tasks even when specifically trying to induce learning (Hartmann et al. 2013). Finally, it is possible the SVS had an effect on motion thresholds that persisted for up to 2 weeks after the initial application, and therefore showed up in our Test Session 2 data as lowered baseline motion thresholds. There is currently no evidence for longer duration effects of SVS, but this may be worth investigating further in the future.

We created and utilized a simulation of our experimental protocol so that we could better understand the likelihood of SR exhibition and repeatability in this type of data and compare to our experimental results. We performed a qualitative analysis using three independent judges. An important conclusion from our simulation results is that there is always a possibility that a

subject could seem to exhibit SR when there is actually no underlying SR, just as it is possible that a subject may not exhibit SR when in fact underlying SR is present. However, by comparing the blinded judgments of our experimental results to our simulation results, we conclude that the proportion of subjects exhibiting SR in Test Session 1 is considerably and significantly higher than what is expected to occur by chance (i.e. if there were no underlying SR phenomena). Similarly, the proportion of experimental subjects that had both subjective SR and a statistically significantly lower than baseline minimum DR threshold was significantly higher than what the simulations show occur with no actual underlying SR. The proportion of experimental subjects that had subjective SR on both Test Session 1 and 2 was however not different than what would be expected to happen by chance. Given these comparisons, we believe that the constancy of the SR exhibition, the tendency for the data to fit the shape of a characteristic SR curve, and the statistical analysis, gives ample evidence of the exhibition of true SR in the majority of our subjects on Test Session 1. However, the proportion of subjects exhibiting SR repeatability on Test Session 2 is weak and suggests that future studies should not assume between day repeatability and should pay careful attention to changes in the baseline, no SVS, measure.

We found no significant correlations using various relationships between our variables of GVS threshold, motion thresholds at baseline and optimal, and optimal SVS levels. However, we note that the motion thresholds measured in this study aimed for the lowest motion stimulus that the subject could reliably detect left from right (direction recognition), and GVS thresholds measured the lowest stimulus that the subject could reliably perceive motion or no motion (motion detection). We know that motion detection thresholds are smaller than DR thresholds and that the relationship between the two varies across subjects (Chauduri et al. 2013). There are a few possible solutions to alleviate this discrepancy. Firstly, future studies could measure thresholds to SVS instead of sinusoidal GVS. This measure may better correlate to performance measures with SVS applied since the nature of the GVS signal would have matched across the experiment (i.e. always stochastic 0-30 Hz). However, noisy GVS (SVS) signals are difficult to perceive due to the high frequency nature of the signal. Futures studies may have to test at much higher SVS levels to measure an SVS perception threshold, which might introduce more of the typical discomforts of high GVS such as tingling and metallic taste. Alternatively, futures studies could measure GVS motion direction recognition thresholds (i.e. identifying left vs. right)

instead of motion detection thresholds (identifying sensation of motion vs. no sensation of motion). Subjects often commented that with the sinusoidal GVS they felt that they were definitely moving but weren't sure in which direction. This uncertainty in motion direction likely comes from 1) the non-selective and therefore unnatural vestibular stimulation, 2) having to overcome contradictory vestibular and proprioceptive/tactile cues, and 3) a higher threshold for motion direction recognition than motion detection. A motion direction recognition threshold task for sinusoidal GVS stimulation may be useful to implement in the future, but would presumably require collecting larger sets of data (and therefore longer testing time) in order to minimize variability in reports. Additionally, there seemed to be differences between subjects in the size of the phase lag between their reported motion perception and applied sinusoidal GVS stimulation. It's unclear whether this lag is physiological, more cognitive and in the decision making path, or in motor response delays. Either way, varying phase lags to sinusoidal GVS may motivate the use of a different type of direct GVS signal (e.g. simple ramp) for use in GVS motion direction recognition threshold testing. Lastly, futures studies could test motion detection thresholds (to physical motion stimuli) instead of motion direction recognition thresholds to match the detection GVS threshold task. However, the Moog motion device used to measure motion thresholds is not without vibrations, which likely provide non-vestibular cues for detection thresholds (Chaudhuri and Merfeld 2014). Further, we believe direction recognition thresholds are more relevant to practical sensorimotor performance that requires direction specific reactions.

We did find a statistically significant correlation between baseline motion thresholds and the maximum improvement in threshold due to SVS. This result is consistent with similar findings from a study that measured differences in torsional ocular counter-roll in response to whole body tilts with and without SVS (Geraghty et al. 2008, Serrador et al. 2014) and shows that within a population, subjects who are relatively worse at the sensorimotor task have more room for improvement. These results suggest that an SVS device may be particularly useful in lowering DR thresholds for a patient population with sensorimotor dysfunction (presumably elevated vestibular perceptual thresholds such as in Valko et al. 2012).

This Experiment showed that SR is possible in the context of upright roll tilt DR thresholds that involve both the SCCs and otolith vestibular sensors. Remaining unanswered questions were whether SR was possible in other motions that use the SCCs and otoliths differentially and whether SVS could provide a benefit in a more operationally relevant aerospace task. These are the questions that are the focus of Experiments 2 and 3.

6 Experiment 2: Investigation of Vestibular Perceptual Stochastic Resonance with Isolation of Semicircular Canals and Otoliths

We have so far discussed SVS (and GVS) under the understanding that externally applied electrical stimulation is non-specific such that all of the vestibular afferents are stimulated. Presumably both SCC and otolith afferents are being activated by the SVS (or GVS); however there has been interest and disagreement regarding whether GVS induces SCC or otolith behavioral and physiological responses. A recent review concluded that the answer is likely a combination of both options; that behavioral responses can be attributed to both the SCCs and otoliths depending on the context of the experiment (Curthoys and MacDougall 2012). However the majority of recent studies have focused on only GVS stimulation (usually sinusoidal). It remains unknown whether the exhibition of SR due to SVS is specific to otolith- or SCC-driven responses, or whether both organs contribute or are necessary for the SR phenomenon to occur. The aim of this experiment was to determine whether vestibular perceptual SR was exhibited in DR thresholds for motions that stimulate the two vestibular sensors in isolation. We compared these results to the upright roll tilt motions in Experiment 1, which stimulated both the otoliths and SCCs.

6.1 Background Specific to Experiment 2

Most studies of SVS to date have focused on postural sway and balance (Mulavara et al. 2011, Goel et al. 2015), which involve both the SCCs and otoliths. A study of ocular counterroll in response to whole body upright roll tilts with SVS, found an increase in responses to sinusoidal upright roll tilts of ± 25 degrees at frequencies from 0.03 to 0.25 Hz (Serrador et al. 2014). Although discussed as an otolith specific response, the ocular counterroll in this study could be partially influenced by the SCC stimulation, specifically at the higher upright roll tilt frequencies tested. Experimental results to date support the existence of SR due to the application of SVS for both otolith + SCC stimuli. With limited experimental evidence for SVS induced SR specific to SCC vs. otolith stimulation, we will summarize the literature addressing the same question in the context of GVS.

It is well accepted that GVS applied by surface electrodes is non-specific in its target and that both SCC and otolith afferent neurons are stimulated (Goldberg et al. 1984). However this does not exclude the possibility that the SCC and otolith neurons are differentially affected such that the resulting behavior is more specific to either a SCC or otolith response. In 2012, an article titled "What does galvanic vestibular stimulation actually activate?" (Cohen et al. 2012) and two subsequent responses (Reynolds and Osler 2012, Curthoys and MacDougall 2012) highlighted conflicting scientific evidence. Cohen et al. (Jan 2012) first concluded that GVS, although activating the entire vestibular nerve, only induced neural and behavioral responses consistent with otolith stimulation and suggested that canal-related responses were inhibited due to quick habituation of rotation vestibular units to GVS stimulation. They pointed to evidence for an otolith only GVS response that included how humans experience sensations of rocking, head and/or body tilt, and ocular torsion when exposed to sinusoidal GVS. Additionally, they cited the orthostatic response of muscle sympathetic nerve activity to sinusoidal GVS as clearly otolith related (Yates 1992, Woodring et al. 1997, Kerman et al. 2003) and an experiment that showed the absence of GVS induced activation of the gene c-fos and resulting accumulation of protein c-Fos in the vestibular nuclei for regions associated with canal driven vestibulo-ocular or vestibulo-spinal reflexes in gerbils (Kaufman and Perachio 1994, Marshburn et al. 1997).

Soon after this paper was published, a response was written by Reynolds and Osler (June 2012) that took the opposing view, "that GVS is primarily interpreted by the brain as head roll, consistent with activation of semicircular canal afferents". They were less sure of any otolith related activation. They pointed to experiments in which GVS was applied concurrently with actual rotation and either induced a larger or smaller perception of rotation depending on the stimulus direction as evidence for SCC stimulation from GVS (Fitzpatrick et al. 2002, Day and Fitzpatrick 2005). They also cited studies that measured torsional eye movement and found that GVS induced eye motions were the same as eye movements produced by pure head rotations (i.e. torsional offset plus nystagmus) (Schneider et al. 2002).

Finally, a response by Curthoys and MacDougall (July 2012) opted to conclude that the effect of GVS is not restricted to only the SCC or only the otoliths, but that both SCC and otolith primary afferents are activated and that behavioral response are consistent with contributions from both,

particularly when reviewing the evidence with careful attention to detail. Discussing the c-Fos argument laid out by Cohen et al. (2012), they pointed out that other studies using the same method had shown that c-Fos does not always show in all brain regions that are known to be activated. This suggests that the lack of GVS induced c-Fos accumulation seen in SCC specific brain regions did not necessarily correspond to a lack of actual SCC activation. They cited technical advances in video recording frame rates for disparities between earlier studies that showed no ocular nystagmus (suggesting otolith only response) and later studies that clearly showed both horizontal and torsional nystagmus (suggesting a canal response). They also discussed the importance of the presence of vision in interpreting oculomotor responses to GVS and how in a normal healthy person, vertical nystagmus due to bilateral bipolar GVS should not occur because of a cancellation between the anterior and posterior canal stimulation. They stress that this absence of a response is not evidence of an absence of activation. In fact, vertical nystagmus in response to GVS was confirmed to occur in a patient with a dysfunctional posterior canal nerve and functional anterior canal (MacDougall et al. 2005). Further support that both otoliths and SCCs are affected includes the direction of the vestibular ocular reflex (VOR) in response to pulsed suprathreshold GVS (Aw et al. 2006) and by measured three-dimensional eye movements in response to subthreshold GVS (Severac-Cauquil et al. 2003).

Fitzpatrick and Day (2004) approached the question of how GVS should affect SCCs and otoliths from a modeling perspective. They considered the electrophysiology and anatomy of the vestibular organs including details on the location of the SCCs and otoliths within the head, and the orientation of the otolith maculae, hair cells, and striola. They used these details to develop a model that explains observed behavioral responses to GVS. They concluded that bilateral bipolar GVS creates large roll and small yaw SCCs signals and a small otolith acceleration signal. Each utricle is divided by the striola into the pars medialis and pars lateralis, which respond oppositely to the same stimulus. Fitzpatrick and Day, therefore, predict the net utricular acceleration to be small, however it is not perfectly cancelled due to the small size difference between the two regions. They state that "no form of GVS, monopolar or bipolar, unilateral or bilateral, can be expected to produce a large afferent signal from the otolith organs." This thorough and elaborate modeling effort provides strong evidence that although GVS stimulates both SCC and otolith primary afferent neurons, the behavioral response is consistent with primarily SCC neuron

activation.

With mixed evidence for the mechanism of GVS-induced perception of motion and limited data pertaining to otolith- and SCC-specific responses to SVS (i.e. only balance ocular torsion), we conducted an experiment specifically aimed at identifying the potential vestibular pathways for SVS induced SR-behavior. We studied the effect of SVS on vestibular perception specifically targeting motions that stimulated primarily otoliths (translation), primarily SCCs (rotation), and compared to perception that targeted both vestibular sensors (upright roll tilt at mid-frequency motions in Experiment 1). If we assume that a net stimulation of the vestibular sensor due to the electrical stimulation is necessary for SR exhibition, then the GVS literature (Fitzpatrick and Day 2004) suggests that SVS induced SR would be most prevalent in a predominately SCC-specific task than a primarily otolith-specific task. We must however acknowledge that whether subsensory SVS induced SR is actually related to GVS induced behavioral responses is not currently known. The limited SVS literature does not suggest that semicircular canals are necessary for SR.

6.2 Methods Specific to Experiment 2

6.2.1 Subjects

This study consisted of 12 participants (6 female) who were healthy, had no known vestibular disorders, and were of average (± one standard deviation) age of 26.6 ± 3.3 years. Seven of these subjects also participated in Experiment 1 (See Appendix 10.5 and Section 6.3.4 for additional details). The subjects who had been tested previously were not specifically selected for any reason; rather they were the subjects who remained available. Approximately a year had passed between the two experiments. The inter-aural dataset consisted of 11 out of the 12 subjects because one subject, after completing the supine roll rotation tests, became medically ineligible to participate after their supine roll rotation test day for unrelated reasons.

6.2.2 Testing Procedures

As in Experiment 1, Experiment 2 measured DR thresholds with the application of SVS ranging from ±0-700 μA. Testing methods were very similar to those in Experiment 1 Test Session 1, such that in each test session electrodes were applied, impedance compliance was assured, GVS thresholds were measured, and then 5 motion threshold tests were conducted, each with at least 110 trials and a single and continuous SVS level applied. The order that the varying levels of SVS were applied was random for each subject. The primary difference between this experiment and the previous was the axes of motion in which subjects' motion thresholds were measured. Recall that in Experiment 1, DR thresholds were assessed for upright roll tilt with 0.2 Hz trajectories, a task that requires the integration of SCC and otolith cues. Now, in Experiment 2, subjects were tested in two sessions. In one session, subjects were tested on a Moog Motion platform to create inter-aural y-translation motions at 1 Hz. In the other session, subjects were tested on the Eccentric Rotator Device in the supine position in supine roll rotation about the Earth-vertical axis (Figure 15B) with 0.2 Hz motions. The orders were counterbalanced, such that half of the subjects were tested in y-translation during the first test session. All motions followed the same single cycle acceleration profile as previously described. See Section 4.4 for additional detail on the Moog platform and Eccentric Rotator devices.

For supine roll rotation, the subject is gravitationally supine with their head on the axis of rotation, so the predominant vestibular cue is to the SCC (i.e. no head linear acceleration or tilt to stimulate the otoliths of the vestibular system). For inter-aural translation, the subject remains gravitationally upright, so the stimulus is predominantly to the otoliths (i.e. no head rotation to simulate the SCCs). We acknowledge that other somatosensory, proprioceptive, and tactile cues may also occur. However, the fact that these thresholds increase 1.3-56.8 x in total bilateral loss vestibular patients (Valko et al. 2012) suggests vestibular cues dominate the perception of motion thresholds. Supine roll rotations were performed at 0.2 Hz to enable a direct comparison to the upright roll tilt motion thresholds measured in Experiment 1, which were also done at 0.2 Hz. Inter-aural translation thresholds were assessed at a commonly tested frequency of 1 Hz (Grabherr et al. 2008, Valko et al. 2012, Lim and Merfeld 2012), instead of 0.2 Hz. As inter-aural thresholds at 0.2 Hz are higher and thus require larger motions than 1 Hz, it would not have been feasible to assess thresholds at 0.2 Hz given the limited range of motion of our Moog

motion platform. We further note that the otolith stimulation pattern during upright roll tilt is substantially different than that for inter-aural translation (upright roll tilt stimulates both the utricle and saccule with peak stimulation happening during the static tilt at the end of the trial, while inter-aural translation stimulates primarily the utricle with peak stimulation occurring during the dynamic translation motion, see Figure 36), such that even if the frequency was matched it would not replicate the stimulation profile.

In all DR threshold test sessions, subjects were encouraged to report if they were sleepy and "missed" a trial (it was then repeated with the direction re-randomized). Also subjects were allowed breaks between sessions. Lights were turned on and the subjects sat, stood upright, or walked around until they were ready to continue. Light breaks were also given within single test sessions if the subject desired.

6.2.3 Data Analysis

The data analysis for this experiment closely follows the data analysis from Experiment 1. DR thresholds measured with five levels of SVS were fit with the theoretical SR equation and subjectively identified as exhibiting or not exhibiting SR. Because the author's subjective judgment of SR exhibition in the upright roll tilt data from Experiment 1 closely matched the assessment of the other blinded judges, the judging of the supine roll rotation and inter-aural translation DR thresholds in this experiment were not blinded, and judged only by the author. Additionally, all individual datasets are shown to keep the author's subjective judging as transparent as possible to the reader. The proportion of SR exhibitors within each subject group was compared to the same set of simulations described in Experiment 1 in order to assess whether SR exhibition was present more or less than what be expected to occur by chance. Additionally, a comparison of the proportion of subjects that had significantly lower DR thresholds with SVS than without SVS is made across motion directions tested (upright roll tilt, supine roll rotation, and upright inter-aural translation) and group means are discussed.

6.3 Results Experiment 2

6.3.1 SCC - Roll Rotation

The author judged that vestibular perceptual SR was exhibited in only 3 out of 12 subjects (25% of subjects: S3, S6, S12) for DR thresholds in the primarily SCC supine roll rotation motion direction (Figure 32). The SR curves that had reasonably good fits were overlaid on the data in blue. Unlike in the upright roll tilt motion in (Figure 19), many subjects tested on the Eccentric Rotator with supine on-axis supine roll rotation showed signs of sleepiness such that their thresholds tended to increase as the session progressed (Appendix 10.11). The most extreme example was S7, whose threshold was approximately five times higher in the last test than in the previous four tests. No subjects reported any symptoms of motion sickness so we do not think sopite syndrome was causing sleepiness or drowsiness. An effort was made to account for sleepiness in this data set. Specifically, a linear fit of motion threshold by test number was first applied to the data. The data for the subjects that exhibited behavior consistent with what might be expected from sleepiness (i.e., had a positive slope to the fit of threshold vs. session number, 8/12 subjects) was then adjusted by subtracting out the linear increase by test number. Finally, the adjusted data was fit with the SR equation as usual. Using this adjusted data set, 4 out of 12 subjects showed subjective, albeit poorly fitted, SR trends (Appendix 10.11). Because the adjustment (by test number) did not notably improve SR exhibition and cannot be justified by actual measures of sleepiness, subsequent analysis will focus on the non-adjusted data.

Using the non-adjusted data, only 2 out of 12 subjects had a statistically significantly lower than baseline motion threshold in their test session (S3, S8, calculated using one tailed t-test and indicated in Figure 32), although for one subject (S8) the lower threshold was at the highest SVS level given and did not correspond to subjective SR exhibition. Also, although S3 was identified as a subjective SR exhibitor the SR fit method was particularly poor at dealing with DR thresholds at high SVS levels that were larger than the other DR thresholds in the set. The proportion of subjective SR exhibitors (3/12) in supine roll rotation was not statistically significantly different than that of the simulation group with No underlying SR ($z=-0.45$, $p=0.326$) and was statistically lower than those of the Weak ($z=-1.93$, $p=0.027$) and Strong underlying SR ($z=-7.47$, $p<0.001$) simulation groups. For the three subjective SR exhibitors, the

difference between minimum and baseline threshold using the non-adjusted data ranged from -0.55 deg/s (S12) to -2.65 deg/s (S3). In percent change from baseline, the range was -24.8% (S6) to -26.3 % (S3).

The proportion of subjects with subjective SR exhibition and a statistically significantly lower than baseline minimum DR threshold (1/12) was not statistically significantly different than that of the simulation group with No underlying SR (z=-0.71, p=0.239) and was statistically lower than those of the Weak (z=-1.95, p=0.025) and Strong underlying SR (z=-8.04, p<0.001) simulation groups. This suggests that the exhibition of SR (subjectively and statistically) in this supine roll rotation data set did not occur more than what would be expected to occur by chance.

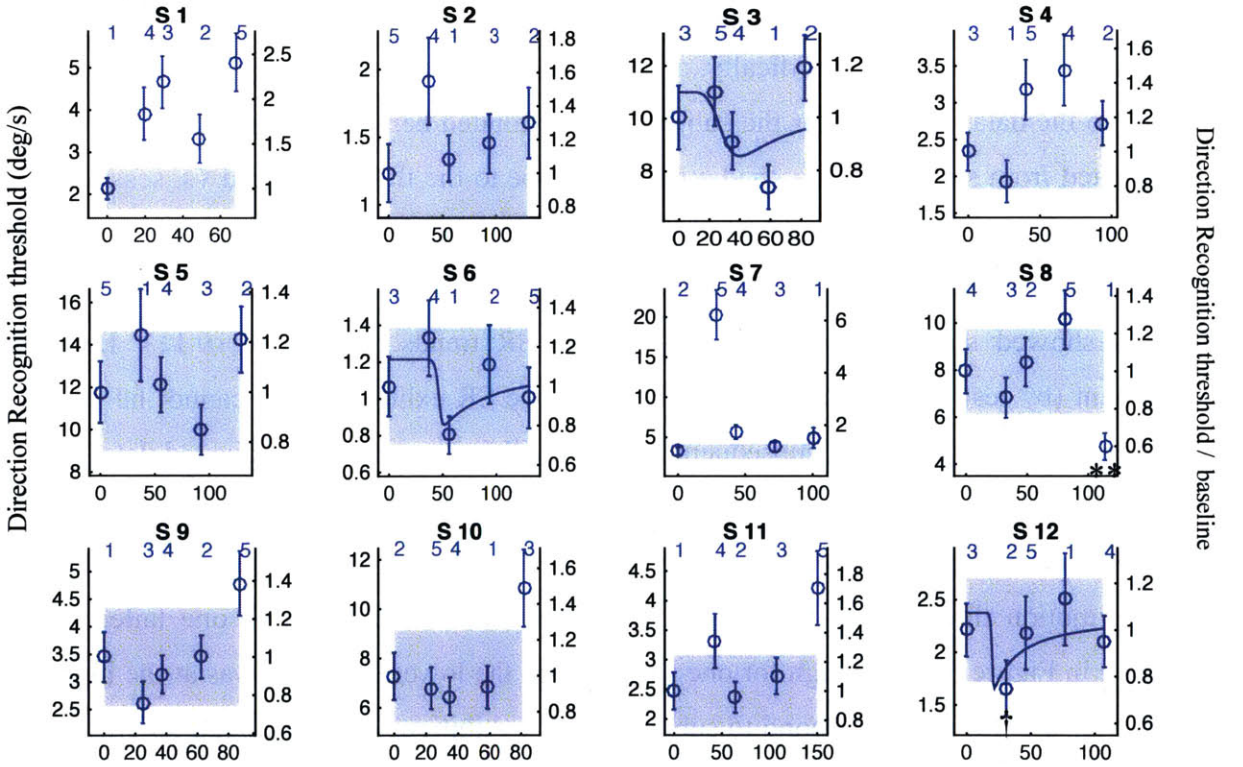

Figure 32. Supine roll rotation DR thresholds (0.2 Hz) vs. SVS level normalized by the individual subject's GVS threshold on the same day. Figure specifics are identical to those in Figure 19. SR curve fits are not shown for subjects that did not subjectively exhibit SR.

A general lack of SR exhibition is evident when looking at the group data in Figure 33.

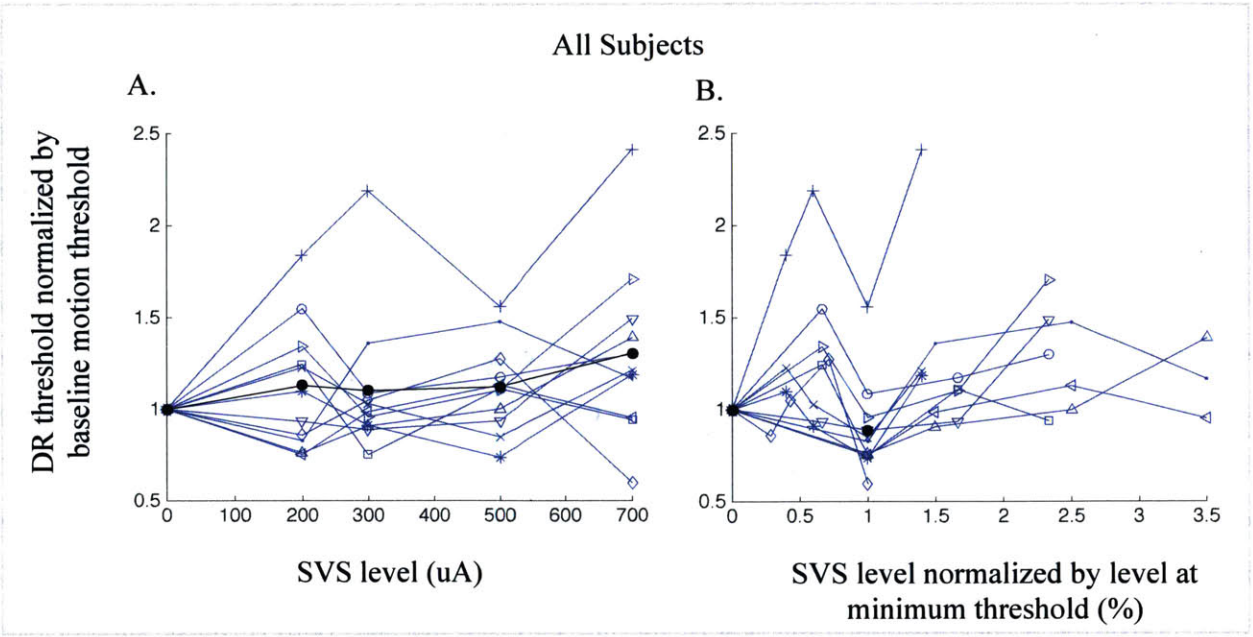

Figure 33. Group supine roll rotation DR thresholds. A: In blue, 0.2 Hz supine roll rotation DR thresholds connected by simple line for each individual subject normalized by their baseline threshold vs. SVS level delivered. Thick black data points represents the average threshold across all subjects. B: DR thresholds normalized by baseline vs. SVS level normalized by each subject's optimal SVS level, or that which resulted in the lowest motion threshold that was not the 0 SVS condition. Thick black dots represent average thresholds at group baseline and optimal. S7 is not included because of an extreme outlier in their dataset. Note that the minimum DR threshold was achieved with 0 SVS for two subjects. See Appendix 10.11 for the same figure with the sleepiness-adjusted data.

Across 11 subjects (S7 excluded because of extreme outlier test), the lowest average motion threshold occurred when 0 μA SVS was applied (Figure 33A). When the SVS level was normalized by the non-zero level at minimum threshold measurement, the normalized group average minimum was 11.2% less than the group baseline (Figure 33B). This decrease of 0.842 deg/s was statistically significant (paired $t(10)=2.220$, $p=0.025$), however there was still a lack of subjective SR exhibition per individual subject. This highlights the importance of not just comparing the "optimal" DR threshold to each subject's baseline, because with variable data, it is easy to have false positives. Additionally, two of the subjects shown in Figure 33 had their minimum DR threshold at the 0 SVS level. Therefore, we conclude that SR was not evident in the primarily SCC, supine roll rotation DR threshold data at 0.2 Hz.

6.3.2 Otolith – Inter-aural Translation

For DR thresholds in the primarily otolith inter-aural translation motion direction, vestibular perceptual SR was judged by the author to be subjectively present in 7 out of 11 (64%) subjects (S5, S6, S7, S8, S9, S10, Figure 34). Additionally, 6 out of the 11 subjects also had a statistically significantly lower than baseline minimum DR threshold (S3, S5, S6, S8, S9, S10, calculated using a one-tailed t-test and indicated in Figure 34). For the subjective SR exhibitor group, the change in threshold due to the "optimal" level of SVS ranged from -0.9 cm/s (S8) to -0.2 cm/s (S6) and in percent change from baseline, the range was -63.1% (S8) to -18.7% (S7), with an average of -42% . For the group of SR exhibitors that also had a significantly lower than baseline minimum DR threshold, the smallest difference from baseline and percent change were -0.17 cm/s (S6) and -28.5% (S6), respectively, with an average percent change of -46%. Additionally, across all subjects, out of all DR thresholds measured with SVS, only two (from S2 and S12) were above the 95% confidence interval of the no SVS baseline and both of these subject were identified as non-responders.

The proportion of subjective SR exhibitors in inter-aural translation was statistically significantly higher than that of the corresponding simulation group with No underlying SR ($z=2.16$, $p=0.015$), not different from that of the Weak underlying SR simulation group ($z=0.59$, $p<0.278$) and lower than that of the Strong underlying SR group ($z=-3.96$, $p<0.001$). The proportion of SR exhibitors that also had statistically significantly lower than baseline minimum DR thresholds (55%) was also statistically significantly higher than the corresponding simulation group with No underlying SR ($z=3.08$, $p=0.001$), not different than that of the Weak underlying SR group ($z=1.20$, $p=0.115$) and significantly lower than that of the Strong underlying SR simulation group ($z=-4.20$, $p<0.001$).

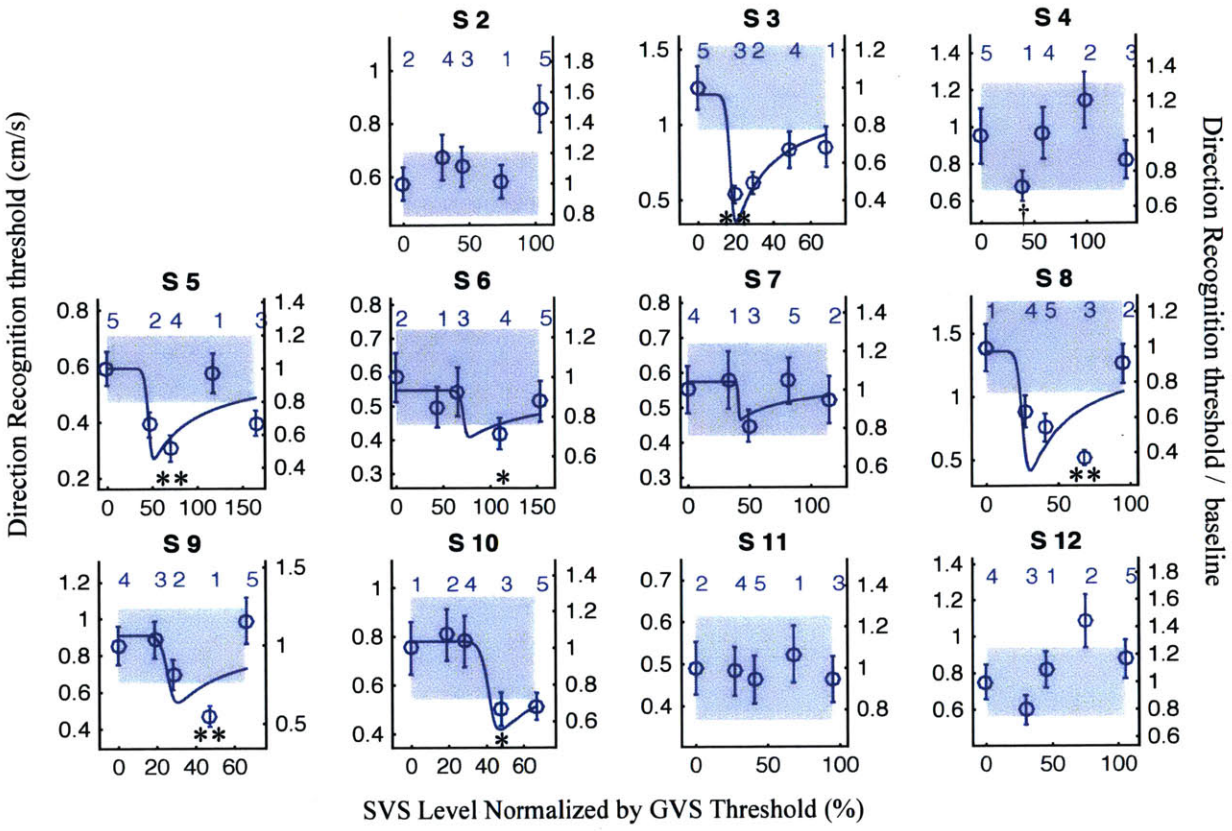

Figure 34. Inter-aural translation DR thresholds (1 Hz) vs. SVS level normalized by the individual subject's GVS threshold on the same day. Figure specifics are identical to those in Figure 19.

When the DR thresholds from all 11 subjects were averaged together, the lowest average motion thresholds were achieved at 300 μA SVS level, with a normalized change from baseline of 15.4% (Figure 35A). There was a statistically significant decrease from the 0 to 300 μA SVS group means of 0.2 cm/s (paired t(10)=1.894, p=0.044). The normalized change was 31.7% between the group average baseline and minimum threshold when the optimal SVS level was allowed to vary between subjects (Figure 35B). There was a statistically significant decrease of 0.318 cm/s from the 0 to nonzero optimal μA SVS group means (paired t(10)=3.238, p=0.005).

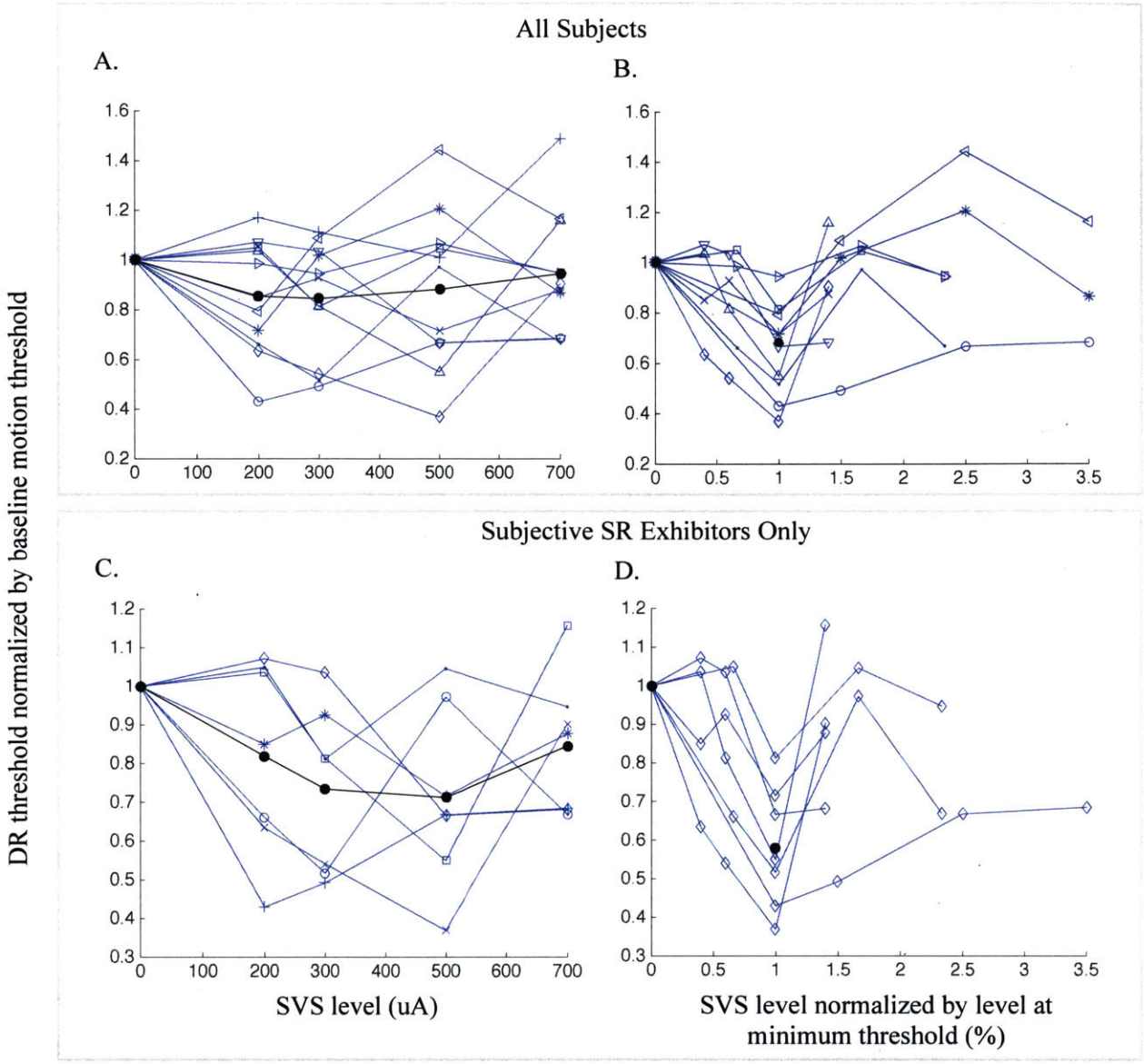

Figure 35. Group inter-aural translation DR thresholds. A: In blue, 1 Hz inter-aural translation DR thresholds connected by simple line for each individual subject normalized by their baseline threshold vs. SVS level delivered. Thick black data points represents the average threshold across all subjects. B: DR thresholds normalized by baseline vs. SVS level normalized by each subject's optimal SVS level, or that which resulted in the lowest motion threshold. Thick black dots represent average thresholds at group baseline and optimal. C and D match A and B except that the four "non-SR exhibitors" (Subjects 1, 3, 10, and 11) have been removed from the group.

With the four presumed non-SR exhibitors removed from the dataset, the group optimal SVS level was 500 μA with a normalized change of 26.6% from baseline to optimal SVS (Figure 35C). There was a statistically significant decrease of 0.34 cm/s from the 0 to 500 μA SVS group

means (paired t(6)=2.633, p=0.020). There was also a statistically significant difference of 0.30 cm/s between the 0 and 300 μA SVS group means (paired t(6)=2.305, p=0.031). When allowing for varying optimal SVS levels by subject, the normalized change between the average group baseline and minimum was -42% (Figure 35D), corresponding to statistically significant decrease of -0.44 deg/s (paired t(6)=3.282, p=0.009).

6.3.3 Relationships between Experimental Measures

Similar to Experiment 1 (Section 5.3.4), an analysis was done comparing various experimental measures to determine if there were any predictors of SR characteristics or relationships between baseline performance and improvement in performance. Concerning the inter-aural translation test session data, we found no correlation between subjects' detection thresholds to GVS and recognition thresholds to motion. There was also no correlation found between GVS threshold and optimal SVS level for motion thresholds. No correlation was found between GVS thresholds and the difference or percent change in motion threshold between baseline and minimum. Together, the above results suggest that the GVS threshold measured at the beginning of each inter-aural translation test session had no relation to motion thresholds or the SR characteristics due to SVS application.

With just the subset of the seven subjective inter-aural translation SR exhibitors, there was a significant correlation between baseline motion threshold and the improvement in thresholds with SVS (baseline threshold – minimum threshold) (R=0.958, p<0.001). Similarly, there was a statistically significant correlation between baseline motion threshold and the percent change in threshold between baseline and minimum thresholds (R= -0.795, p=0.003). Similar to our upright roll tilt results (Experiment 1), these results suggest that if a subject was relatively worse at the task to begin with, they had more room for improvement and therefore experienced larger beneficial effects of SVS (both absolute and normalized by the baseline).

GVS thresholds measured in the supine roll rotation test session were also compared to baseline supine roll rotation DR thresholds and no correlation was found. Lastly, there was no difference between GVS thresholds measured on the supine roll rotation and inter-aural translation test

sessions (paired t(10)=1.172, p=0.268). This was consistent with Experiment 1 results that showed no difference in GVS thresholds between test days, suggesting that the GVS threshold is a relatively consistent measure within a subject.

6.3.4 Within Subject Comparisons

In Experiment 2, the same subjects were tested in both supine roll rotation (primarily SCC) and inter-aural translation (primarily otolith) in order to enable a within subject comparison of SR exhibition across motion directions. The three subjects that exhibited SR in supine roll rotation were S3, S6, and S12. Within this group, only S3 and S6 exhibited SR in inter-aural translation as well (details in Table 3).

Table 3. Supine roll rotation and Inter-aural translation SR Exhibitors

Subject	Motion	GVS Threshold	Optimal SVS	Optimal SVS/GVS Threshold	% Change in Threshold
S3	Supine Roll Rotation	850	500	58.8%	-26.3 %
	Inter-aural Translation	1025	200	19.5%	-57.0 %
S6	Supine Roll Rotation	535	300	56.1%	-24.8 %
	Inter-aural Translation	455	500	109.9%	-28.5 %

With only these two subjects, there were no clear consistencies in the SVS level associated with lowest threshold measurement or the SVS level normalized by GVS threshold between the supine roll rotation (SCC) and inter-aural translation (otolith) tests. The percent changes in threshold were similar across tests, but were always at least slightly larger for inter-aural translation. With only two subjects it was difficult to reach firm conclusions from this comparison.

It was not an original goal of this research to compare SR exhibition across upright roll tilt (Experiment 1), supine roll rotation and inter-aural translation (Experiment 2) motion directions. However, there were seven subjects that were tested in both Experiment 1 and Experiment 2, and

we could therefore do a comparison for this subset of subjects (For Experiment 1, Test Session 1 Data is included, Table 4).

Table 4. Upright roll tilt, supine roll rotation, and inter-aural translation comparison

Subject Exp2, Exp1		Motion	GVS Threshold	Optimal SVS	Optimal SVS/GVS Threshold (%)	% Change in Threshold
S1	SA	Upright Roll Tilt	875	300	34.3	-46.0
		Supine Roll Rotation	1020	-	-	-
S6	SC	Upright Roll Tilt	380	500	131.6	-10.4
		Supine Roll Rotation	535	300	56.1	-24.8
		Inter-aural Translation	455	500	109.9	-28.5
S7	SD	Upright Roll Tilt	520	500	96.2	-34.3
		Supine Roll Rotation	695	-	-	-
		Inter-aural Translation	735	300	40.8	-18.7
S8	SE	Upright Roll Tilt	730	300	41.1	-14.8
		Supine Roll Rotation	615	-	-	-
		Inter-aural Translation	735	500	68.0	-63.1
S9	SF	Upright Roll Tilt	660	300	45.5	-5.4
		Supine Roll Rotation	800	-	-	-
		Inter-aural Translation	1055	500	47.4	-45.0
S10	SJ	Upright Roll Tilt	490	200	40.8	-26.4
		Supine Roll Rotation	855	-	-	-
		Inter-aural Translation	1050	500	47.6	-33.4
S12	SL	Upright Roll Tilt	755	300	39.7	-40.6
		Supine Roll Rotation	650	200	30.8	-24.9
		Inter-aural Translation	665	-	-	-

From the table above we see that there was one subject who was judged to have subjective SR in all three motion directions (S6). Five out of the six subjects that were tested in both upright roll tilt and inter-aural translation exhibited SR in both tests. Three subjects (S9, S10, S12) had

optimal SVS levels normalized by GVS thresholds that were consistent across tests (within 10 percentage points of each other) while three subjects (S6, S7, S8) did not. The percentage difference between baseline and optimal threshold in upright roll tilt and inter-aural translation tests was not positively correlated within subjects, suggesting that if SVS was relatively more effective in one motion direction, it was not necessarily equally as effective in the other motion direction. For example subject S9 had one of the largest differences in inter-aural translation, -45 %, but showed only a -5% change in the upright roll tilt test. Thus from this limited data set, we believe that whether a subject was a Strong, Weak, or non-exhibitor in one axis did not seem to determine their SR exhibition in another axis.

6.4 Summary of Results and Discussion

In Experiment 2, we investigated whether vestibular SR was exhibited during a predominantly SCC or predominantly otolith motion task in order to gain a better fundamental understanding of how vestibular SR occurs. As in Experiment 1, noise was added to the vestibular system via the application of subsensory bilateral bipolar electrical stochastic vestibular stimulation. For supine roll rotation (primarily SCC) DR thresholds, we found that the proportion of subjective SR exhibitors (3/12) was no different than could occur by chance (i.e. if there was No underlying SR) and was significantly lower than what would be expected from the Weak and Strong underlying SR simulations. There was only one subject who was judged to exhibit SR and also had a statistically significantly lower than baseline minimum DR threshold, which again could have statistically occurred by chance. However, for the inter-aural translation (primarily otolith) task, subjective vestibular SR was exhibited at a proportion (7/11) significantly higher than what could occur by chance, and consistent with simulated Weak SR. The proportion of subjects that also had a statistically significantly lower than baseline minimum DR threshold (6/11) was statistically similar to the proportion of corresponding simulated subjects in the Weak SR case. Although SR was exhibited in the primarily otolith task, the rate of exhibition was slightly less than the rate of SR exhibition when both SCCs and otoliths were stimulated by the upright roll tilt motion (9/12) tested in Experiment 1 (Table 5, See Appendix 10.14 for same table with additional pilot data included.). Comparing across the three motion directions, the average percent changes from baseline at the minimum DR threshold for the subject groups that showed

subjective SR and for those that also had statistically significant decreases were -29% and -39% (upright roll tilt), -25% and -26% (supine roll rotation), and 42% and -46% (inter-aural translation).

Table 5. Summary of experimental and simulated DR threshold with SVS results in ascending order of subjective SR exhibition.

Group	**Frequency (Hz)**	**SCC/ otolith**	**Subjective SR Exhibition**	**Minimum DR threshold significantly lower than baseline ($p<0.05$)**
Supine Roll Rotation	0.2	SCC	3/12 (25%)	1/12 (8%)
Simulations – No SR	-	-	31%	16%
Simulations – Weak SR	-	-	54%	36%
Inter-aural translation	1	otolith	7/11 (64%)	6/11 (55%)
Upright Roll Tilt	0.2	SCC & otolith	9/12 (75%)	6/12 (50%)
Simulations – Strong SR	-	-	96%	93%

In the GVS literature, although there is not a clear consensus as to whether responses to GVS (e.g. perceptual, swaying, eye movements, etc.) are more consistent with SCC or otolith stimulation, there is a common agreement that electrical stimulation applied via surface skin electrodes is non-specific in its target, such that both canal and otolith neurons are being stimulated by the electrical signal. With the same application method, it seems reasonable that the same should hold true with the application of subsensory SVS. Why then would it be that stochastic resonance was not exhibited in a motion task specific to SCC stimulation, but was when the task was otolith specific or involved both SCC and otoliths?

We previously discussed the effect that sleepiness may have had for some of our subjects in the supine roll rotation data set. The testing time was no longer than the upright roll tilt test session however subjects lay in the supine position instead of in an upright position, which may explain the additional sleepiness. As in all of our motion threshold testing, subjects were tested in a dark

room while white noise played in their headphones. These two factors alone can cause sleepiness/boredom; however as subjects were tested in the supine position, they may have been even more prone to sleepiness than when tested upright. No subjective or objective measures of sleepiness were taken during the experiment and therefore a rigorous analysis including measured sleepiness was not possible. However when we attempted to account for this sleepiness factor on an individual subject basis, the SR exhibition proportion only increased by one subject (3/12 to 4/12). The overall rate of SR exhibition was still comparable to simulations with no underlying SR. Our approach for adjusting for sleepiness may be imperfect (i.e. it cannot account for nonlinear effects of sleepiness, such as appeared to occur for S7). However with the limited data (i.e. 5 tests each potentially affected by sleepiness and/or SVS level) and apparent differences between subjects, this simple linear adjustment approach seemed the most appropriate. Additionally, subjects were repeatedly encouraged to report if they were too sleepy and "missed" a trial, which then allowed us to repeat the trial with the direction re-randomized. Most subjects never reported a single miss in the full test session while others would report very few, somewhere around 1-3 within a single test. Subjects were also given breaks between tests during which the lights were turned on and they could get off of the motion device and walk around. We therefore conclude that even though sleepiness may have been a factor for some subjects in the supine roll rotation (primarily SCC) threshold task, there was still very little to no evidence for SR exhibition.

One conceptual framework for thinking about why vestibular SR occurred for upright roll tilt and inter-aural translation, but not supine roll rotation, is to recall the classical definition of SR, which requires: 1) a nonlinear system, 2) a weak (periodic) input, and 3) a nonzero (presumably at or around the optimal) level of noise. Note that Collins et al. (1996) have shown that aperiodic stochastic resonance (ASR) exists both theoretically and in actual mechanoreceptor neuron responses, and therefore a periodic input may not be truly required, regardless of the classic definition.

We begin with the first requirement and ask of each case, is the system nonlinear? It is difficult to define the system involved in vestibular perception, because of the complex and multi site pathways associated with vestibular signal processing within the central nervous system. We can

however think about linearity and nonlinearity in terms of the system output, which in our case is estimated DR thresholds. If the neural systems involved in upright roll tilt, supine roll rotation, and inter-aural translation DR thresholds (prior to the threshold element) were linear, then DR thresholds should simply increase with increasing applied noise. This is certainly not the case in the upright roll tilt or inter-aural translation DR threshold data sets. However, the group average supine roll rotation DR threshold trends upwards as SVS level increases and is significantly higher at 700 μA SVS than 0 μA SVS (paired $t(10)=1.839$, $p=0.048$) (Figure 33A). An attempt to adjust the data for sleepiness does not change the trend of increasing DR threshold with increasing SVS level in this primarily SCC data set. The mean DR threshold is still significantly higher at 700 μA SVS than 0 μA SVS by 0.895 deg/s (paired $t(10)=2.311$, $p=0.022$, See Appendix 10.11 for figure). These results suggest that the vestibular perceptual system being used during supine roll rotation motions has linear characteristics that may contribute to the lack of SR exhibition in this primarily SCC task. The relatively large inter-subject variability in the supine roll rotation data suggests that humans are simply less consistent at making direction specific decisions for this motion. This could be attributed to the fact that humans don't typically encounter supine rotations in normal life. It may be that the pure SCC pathway has more noise in it relative to an otolith pathway and that the level of noise needed for SR exhibition has already been surpassed. This argument aligns with the concept that the SCC system (at least when supine) may have linear tendencies in terms of its response to increasing external noise.

The second requirement is that there should be a weak periodic or aperiodic input. Even though each DR threshold trial is a single cycle sinusoidal acceleration, the otolith utricle, saccule, and SCCs sense different components of the motion stimulus between a upright roll tilt, supine roll rotation, or inter-aural translation motion (Figure 36). We see that the periodic sinusoidal acceleration input is only encoded by the utricle in the inter-aural translation (primarily otolith) motion, however a full periodic cycle must not be necessary for SR exhibition since upright roll tilt motions were very conducive to SR even though neither the saccule, utricle, or SCCs are detecting a periodic cycle of either acceleration or velocity. Because SR exhibition was not present in the predominately SCC supine roll rotation motion, we speculate that perhaps SR is more likely to occur when bidirectional afferent neuronal information is available from each ear, such that on each side of the head, the firing rate both increases and decreases in response to a

single motion. A future study could investigate whether SR requires the afferent firing rate to both increase and decrease unilaterally by measuring supine roll rotation DR thresholds with SVS application where each trial consists of a single cycle velocity, instead of a single cycle acceleration. This would create a motion in which the subject is rotated both left and right and would cause bidirectional stimulation of the SCC afferent neurons on both sides of the head. To account for being moved in two directions, the subject could be asked to report the direction of motion that was perceived first (or second).

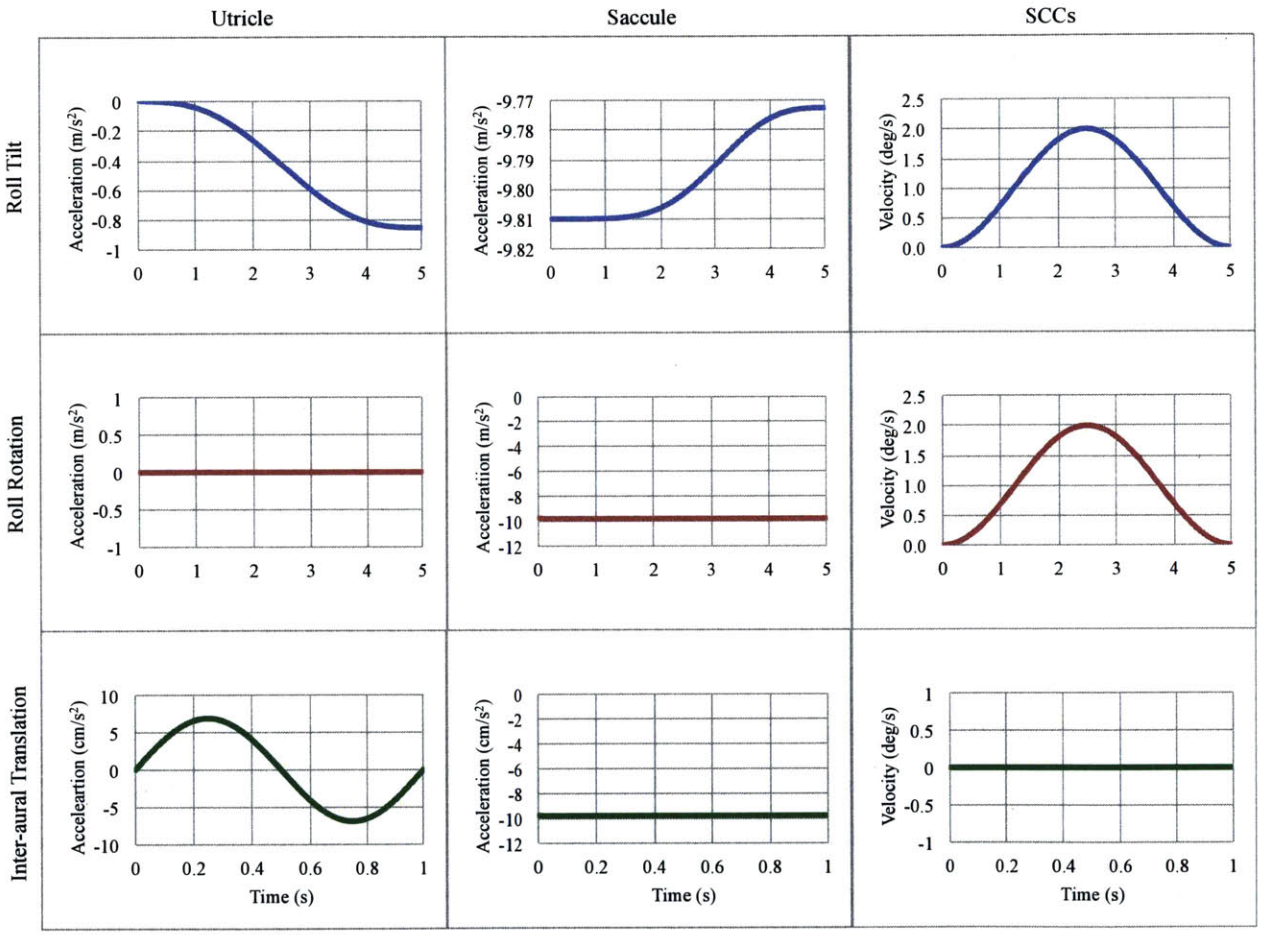

Figure 36. Simplified (assuming purely orthogonal geometry, and pure rotation absent of translation accelerations) accelerations and velocities for the three motion directions tested (upright roll tilt, supine roll rotation, and inter-aural translation) sensed by the otolith utricle, saccule, and semicircular canals (SCCs). Acceleration due to gravity is in the negative direction. Upright roll tilt and supine roll rotation plots correspond to a 0.2 Hz motion while the inter-aural translation example has a frequency of 1 Hz.

In the background section of this thesis, we discussed the differentiation between dynamical and threshold SR. We then chose to use the term SR to broadly refer to noise benefit as suggested by McDonnel and Abbot (2009). However it may be that for our experiment, the dynamic component of the physical stimulus is important to the SR exhibition, a characteristic more consistent with dynamical SR. A pilot study tested "pseudo-static" tilt DR thresholds with varying levels of SVS applied. These motions were upright roll tilts (stimulating the otoliths similarly to the prior 0.2 Hz upright roll tilts), however they differ in that the angular velocity of the tilt is well below SCC threshold. The result is that the tilt direction decision is based primarily on static otolith sensory inputs. Due to the slow rotation rate between tilts, pseudo-static tilt thresholds are tedious to assess (~50 minutes for each of the 5 SVS test levels). Therefore only two subjects were tested, both of whom were SR exhibitors in upright roll tilt (Experiment 1). SR exhibition was not judged to exist in pseudo-static tilt DR thresholds for either subject, tentatively suggesting that noise benefit relies on a dynamic vestibular sensory signal (pilot data shown in Appendix 0).

The third requirement of classic SR is the presence of a nonzero level of noise. Out of the three motion directions tested (Experiment 1 and 2), the two motion axes in which SR was exhibited, upright roll tilt and inter-aural translation, were conducted on the same motion device, a Moog 6-DOF platform that has considerable physical vibrations associated with both positive and negative motions. The supine roll rotation test, in which SR was not exhibited, was conducted on the Eccentric Rotator, which has very low vibrations. A previous study characterized the vibration of the two devices and found that for a one second single cycle acceleration in the yaw direction with a peak velocity of 0.893 deg/s the Moog and Eccentric Rotator devices had peak vibrations of 0.007 m/s^2 and 0.002 m/s^2, respectively (Chaudhuri et al. 2013). It is unknown whether the physical vibrations of the Moog motion device could add noise along the same relevant channel as the electrical stochastic vestibular stimulation. However, if it were possible, this may have contributed to SR exhibition in both motions tested on the higher vibration device while SR was not exhibited on the lower vibration device. It is known that although the predominant inputs to the vestibular nuclei are from the vestibular system (i.e. SCCs and otoliths), there are also neurons that receive inputs from other sources, such as the somatosensory system (Goldberg et al. 2012). Perhaps the net level of nonzero noise in the system was too low

during the low vibration primarily SCC supine roll rotation tests. However, it is important to note that the vibration of the Moog device alone has not been shown to cause a change in direction recognition thresholds. Chaudhuri et al. (2013) tested three subjects in the upright yaw motion direction on both the Moog and Eccentric Rotator devices and found no difference in either the arithmetic or geometric mean in thresholds between the two devices. Additionally, the Moog vibrations quantified represented a magnitude of the three-dimensional acceleration vector. If physical vibration noise could add to the effect of SVS, it may be that only vibrations in the plane of motion, which would be only a fraction of the total vibration, would be relevant. Lastly, Chaudhuri et al. (2013) makes an important point when discussing the possible contributions of non-vestibular sensory cues to recognition thresholds. They cite data from patients with no vestibular function that had DR thresholds 10 times greater than normal for 1 Hz yaw rotations and 5 times greater for 1 Hz inter-aural translations (Valko et al. 2012) as evidence that even with vibrations on the Moog motion device, vestibular signals clearly play a predominant role.

We have collected pilot data for upright head-centered upright roll tilt motions at 1 Hz on the Moog device, the same device that was used in Experiment 1. The 1 Hz frequency is higher than the 0.2 Hz frequency tested in Experiment 1 and primarily stimulates the semicircular canals (Lim et al. 2009). As best we could, given device limitations (i.e. the Moog chair cannot readily perform supine roll rotation), this pilot study tested SR exhibition in a threshold task that predominantly assesses the SCC's sensitivity (similar to the Eccentric Rotator supine roll rotation tests in Experiment 2). But it now includes the vibrations of the Moog chair (similar to the upright roll tilt and inter-aural translation axes where SR was well exhibited). One out of the four subjects (25%) tested had data consistent with SR exhibition, however there was no significant difference between the baseline and minimum threshold (see Appendix 10.13), suggesting with limited data that SR was not present in the primarily SCC task even when measured in the presence of the physical vibrations associated with testing on the Moog device. A future study could collect more data to solidify these results that suggest that even with the vibrations associated with the Moog device, there is no SR exhibition for a primarily SCC task. If physical vibration and electrical stochastic vestibular stimulation do interact with each other in a way that is important to sensorimotor performance, future studies could perhaps investigate the combination of SVS and vibrational tactors on the head or other parts of the body.

Preliminary data collected by Lim et al. (2009) gave evidence that the brain integrates SCC and otolith cues for better self-motion perception than when using either cue individually. Optimal linear sensory integration of the individual SCC and otolith contributions to the upright roll tilt DR threshold, given by $1/\hat{\sigma}^2_{SCC+OTO} = 1/\sigma^2_{SCC} + 1/\sigma^2_{OTO}$ (adopted from Karmali et al. 2014, Ernst and Banks 2002), would predict that if the otolith response was improved with SVS, the upright roll tilt response (SCC + otolith) with SVS would also improve, but would have a lower percentage improvement than that of the individual otolith component. For example, assuming equally weighted SCC and otolith input, a baseline upright roll tilt threshold (SCC + otolith) will be 29% lower than the individual SCC or otolith thresholds. A 25% decrease in just the otolith threshold due to SVS would result in an 11% decrease in the SCC+otolith upright roll tilt threshold assuming no change at all in the SCC response. This pattern is consistent with the experimental data in which we see larger percent changes in the inter-aural translation (primarily otolith) DR thresholds than in the upright roll tilt (SCC + otolith) DR thresholds even though we see similar proportions of SR exhibition for both groups. It remains unknown at this point if vestibular SR follows optimal integration. In order to investigate this further, more pseudo-static DR thresholds need to be collected with the application of SVS, in order to facilitate the necessary comparison between the SCC+otolith response (upright roll tilt at 0.57 Hz) and the relevant otolith response (pseudo-static tilt). As discussed briefly earlier, the current limitation is the time required to collect pseudo-static data sets with multiple levels of SVS, however in the future, testing time could be cut down considerably if only a single SVS level is selected.

If the benefit of SVS is restricted to particular motion directions, it's important to understand which directions are included in order to enable optimal implementation of SVS as a sensorimotor aid in the future. Bilateral bipolar GVS is known to primarily cause perceptions of motion in the upright roll tilt plane, which is why we focused our SVS studies on motions within that plane as well. Based upon GVS studies, one may not expect SR to be exhibited with bilateral bipolar SVS application in yaw, pitch, up/down translation, or forward/aft translation. However, this study showed SR exhibition during otolith related tasks, which was also not expected based on GVS modeling results that suggest GVS should have little to no effect on otolith responses (Fitzpatrick and Day 2004). This suggests that simply stimulating the vestibular organs as a

whole is important, and a net stimulus in any one direction is not required for SVS induced SR, as it is for behavioral responses to GVS. Future SVS studies should include these additional motions directions or even combinations of varying motions that are closer to real life movement. It would be beneficial for future implementation if a bilateral bipolar electrode setup can be effective for motions outside of the coronal plane. Goel et al. (2015) showed an improvement for many healthy subjects in standing balance in both the medio-lateral and anterior-posterior planes with the application of SVS using a bilateral bipolar setup, suggesting that SVS applied in medio-lateral plane can affect vestibular function in other planes. However, this study differed from ours in that it measured responses to self-controlled motions (standing balance corrections) while our study focused on perceptual responses to passive motion. It is therefore unknown if bilateral bipolar SVS can specifically benefit perception of passive motions outside of the anterior-posterior plane. It is known that GVS applied via alternative electrode configurations can effectively elicit motion perception in other planes (Cevette et al. 2012), however expanding this to SVS induced SR has not been done and a complex electrode configuration may be impractical in future SVS applications.

It is also well known that vestibular function is highly frequency dependent. Our tests consisted of only two frequencies (0.2 Hz and 1 Hz). Pilot pseudo-static data also included a ~0 Hz test. Further testing over a range of motion frequencies, along with multiple motion directions would provide the data needed to fully define the characteristics of vestibular perceptual SR due to bilateral bipolar SVS application.

How DR thresholds relate to more natural sensorimotor behaviors such as human posture and locomotion or to more complex sensorimotor performance is still relatively unexplored. A recent study of DR thresholds showed that patients with total bilateral surgical ablation of the inner ears had significantly higher DR thresholds than normal in upright yaw (5.4 to 15.7 x greater), z-translation (8.3 to 56.8 x greater), inter-aural translation (1.7 to 4.5 x greater), and upright roll tilt (1.3 to 3 x greater)(Valko et al. 2012). In our experiment, the changes in DR threshold with SVS in upright roll tilt ranged from a baseline that was 1.1 to 1.9 (SF, SK) times greater than the minimum and the average ratio of baseline to minimum DR threshold in all 10 SR exhibitors was 1.5. In the inter-aural translation direction, the changes in DR thresholds ranged from 1.2 to 2.7

(S7, S8) times greater at baseline than minimum with an average ratio of 1.9 for all 7 subjective SR exhibitors. These changes in DR thresholds due to SVS are therefore on the order of differences in DR thresholds between patients with no vestibular system and normal subjects. However, although these patients had no inner ear, they seemed to be highly functional, with one subject noted as actively competing in triathlons while another had a limp but was able to ride a bicycle. As the CNS is a very adaptable system, it is still unclear how a lowered DR threshold may correspond to functional performance. Whether lowered DR thresholds would be helpful for astronauts with heightened sensorimotor dysfunction due to gravity-transitions also remains an open question because of the uncertain mechanism of the impaired sensorimotor function. Specifically, while balance and locomotion are impaired post-flight (Paloski et al. 2008, Bloomberg et al. 1997), some data suggests linear translation sensitivity is actually improved post-flight (Merfeld, 1996). As discussed earlier there are mixed results concerning changes in x, y, and z body axis thresholds post flight and considerable inter-individual differences (Benson et al. 1986). Whether SVS could lessen that inter-subject variability remains unknown.

7 Experiment 3: The Effect of Stochastic Vestibular Stimulation on Self-Orientation Manual Control

7.1 Background Specific to Experiment 3

Experiments 1 and 2 demonstrated that vestibular perceptual SR occurs in the context of motion direction recognition thresholds, meaning that SVS improved subjects' ability to correctly perceive the directions of small, near threshold motions. Experiment 3 aimed to investigate whether the improvement in vestibular perceptual sensitivity due to SVS can cause measurable improvement in a more operationally relevant manual control task. To date every human-rated space vehicle that is capable of controlled landing (i.e. not landing via parachute) has been landed in a manual control mode with the astronaut pilot using a joystick (Space Shuttle, Apollo Lunar Module). Piloting a spacecraft through entry and landing is one of the most difficult and critical tasks associated with spaceflight and altered gravity and gravity transitions associated with the landing phase of spaceflight missions are associated with impaired manual control performance (Merfeld et al. 1996, Paloski et al. 2008, Clark et al. 2015). Unsuccessful manual control during landing could put crew life at risk and be mission ending and therefore improvements in manual control ability could be valuable for future astronaut piloting. An improvement in manual control capability could also be applicable and valuable to aircraft pilots in terrestrial environments.

In regards to SR theory, this experiment specifically differed from Experiment 1 and 2 in that it investigated whether SVS could be beneficial when the input signal, or physical stimulus in this case, was aperiodic and partially suprathreshold (see Figure 38 for example stimulus profile). Collins et al. (1996) have shown that aperiodic stochastic resonance (ASR) exists both theoretically in responses of single mammalian cutaneous mechanoreceptor neurons. However ASR in the context of vestibular perception has not yet been investigated. Based on our previous results that showed 300 μA SVS was beneficial in lowering upright roll tilt (SCC & otolith) DR thresholds regardless of subject-specific GVS thresholds, we hypothesized that 300 μA SVS would improve manual control nulling performance for a task in the upright roll tilt plane that also elicits both SCC and otolith responses. Additionally, the highest level of subject-specific imperceptible SVS was applied while measuring manual control nulling performance as an

exploratory part of the study. There was no single hypothesis for what this high level of SVS would do to performance. Stocks (2000) suggests that SR in response to suprathreshold input stimuli (suprathreshold SR, SSR) may require that the noise in the system be scaled accordingly, so that a signal to noise ratio is maintained. This idea suggests that the same level of noise that benefits the system's response to near or subthreshold inputs (in our case, DR threshold motions), may be too low to elicit an improvement in the system's response to larger, suprathreshold inputs (in our case, suprathreshold motion stimuli given in the manual control task). Therefore, in terms of this manual control task, if 300 μA SVS proved to not be helpful when motions were relatively large, then it was possible that the higher level of SVS would be. The high SVS level could also not have any effect on performance or could potentially worsen performance relative to the baseline, no SVS, condition.

7.2 Methods Specific to Experiment 3

7.2.1 Subjects

This study originally enrolled 10 participants (6 female) who were healthy, had no known vestibular disorders, and were of average (± one standard deviation) age of 27.1 ± 3.0 years. All subjects signed informed consent forms prior to participating in the experiment. Two subjects (both female) were dropped after the first full test session. The first removed subject struggled with performing the task to a satisfactory and consistent level and the second removed subject showed obvious signs of inattention and sleepiness, such as not making any control inputs for long periods of time. Six out of the eight subjects were tested in previous experiments (See Appendix 10.5 for subject details).

7.2.2 Testing Procedures

Testing was done on the Eccentric Rotator device located in the JVPL at the MEEI. Although the same device was used in both this experiment and for the supine roll rotation thresholds part of Experiment 2, the configuration was different such that in this experiment subjects were seated in the upright position (Figure 37). Subjects were tested on two separate days. Each test session began with the application of electrodes to the mastoid processes as described previously. Also,

like in the previous experiments, the impedance between the electrodes was verified to be less than 1 kΩ before SVS application and any further testing. After electrode application and impedance check, subjects were seated on the motion device. Their body was held in place with a five-point quick release harness, and their head was kept in place between two foam-lined adjustable plates. Shoulder restraints were also put in place to secure the subject and prevent side-to-side motion. A vertical control bar was placed in front of the subject at approximately chest height. The control bar was attached to the device subject chair and therefore did not move relative to the subject. All testing was done in the dark with white noise played through the subject's headphones during all motions, to help eliminate visual and auditory cues, respectively.

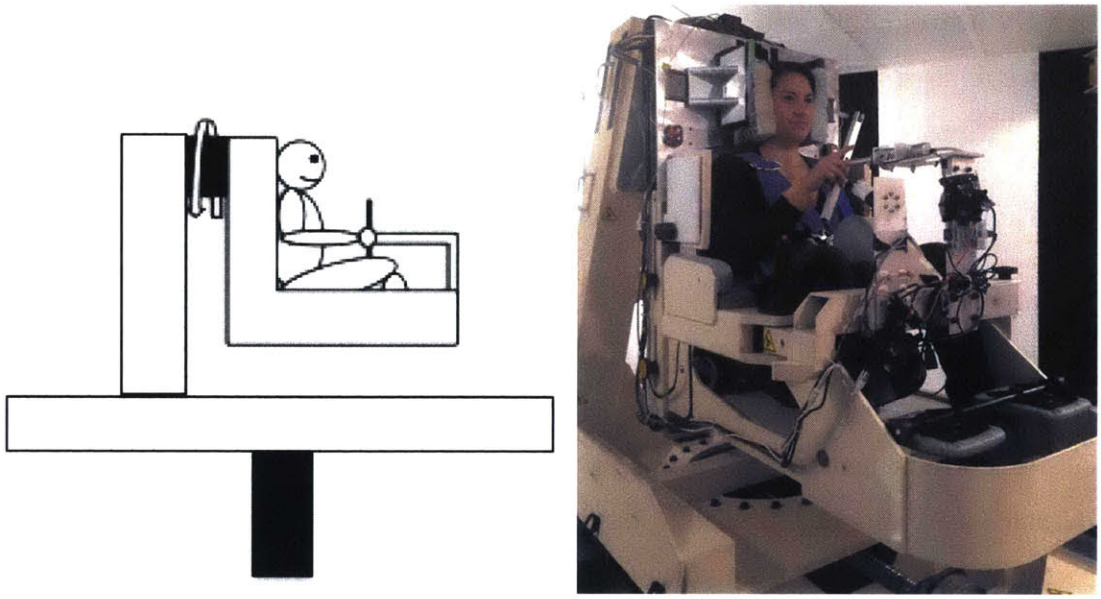

Figure 37. Schematic and photograph of Eccentric Rotator device with subject in testing position. Subject was held in place by a five-point harness, shoulder restraints, and a padded head restraint.

The experiment consisted of repeated manual control trials in which the subject chair was upright roll tilted left and right about a head-centered axis (Profile modified from Clark et al. 2015 and Merfeld et al. 1996, see Appendix 10.15 for more details). The subject was instructed to use the control bar to null out their motion in response to a disturbance. Their goal was to maintain a zero degree tilt, or upright, position. The control bar rotation was physically limited to about ±45 degrees. The control bar deflection angle was converted to an angular velocity command such that 1 degree of deflection commanded 0.44 degrees/s of angular velocity (i.e. in a rate control, attitude hold mode, similar to a helicopter or the Apollo lunar landing vehicle (Hainley et al.

2013)). The velocity command was passed through a discrete time low pass filter with a cutoff frequency of 20 Hz. The commanded chair deflection was limited by software to ±15 degrees added to the maximum motion disturbance deflection of ± 10.9 degrees. Each trial was 2 minutes long. The disturbance profile consisted of a sum of sines (12 sinusoids with different frequencies), designed to appear random to the subject so they could not provide any lead or preparatory control inputs. The amplitude of the individual sinusoids was 2.6472 degrees for the first 6 frequencies less than 0.2 Hz and 0.2647 degrees for the remaining 6 frequencies up to 0.6636 Hz. This step down in amplitude at frequencies above 0.2 Hz was based on pilot data from Merfeld et al. (1996) and Clark et al. 2015, that showed subjects had difficulty nulling out motions at frequencies above 0.2 Hz. The profile had a maximum tilt angle of 10.9 degrees, velocity of 6.7 degrees/s, and acceleration of 11.9 degrees/s^2. Two different motion disturbance profiles were used that were the same trajectory mirrored about zero degrees (described in Table 6 as Right First or Left First). An example of a 'Right First' motion disturbance and nulled out upright roll tilt position can be seen in Figure 38.

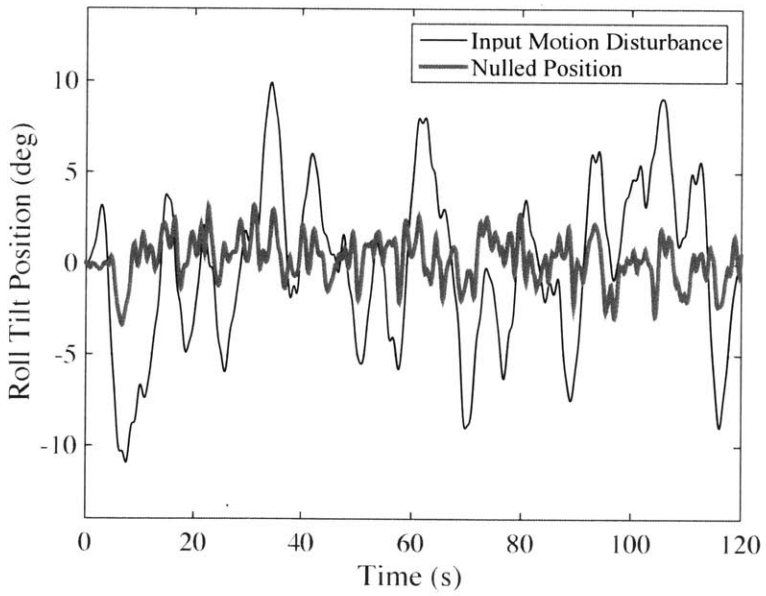

Figure 38. Example of a single manual control trial showing the motion disturbance in black and the actual position resulting from the subject's compensatory control bar commands in grey. As seen, the large amplitude (i.e. 5-10 degrees) disturbances were well nulled such that the subject stayed within +/- 3 degrees of upright through the trial.

Subjects were given at least three full 2 minute practice trials to learn the task and develop a nulling strategy. Using the control bar to null out the tilt motions using rate control proved to be

quite intuitive and most subjects were able to understand the task and perform efficiently very quickly. After practice, the full experiment was conducted including a total of 12 manual control trials, split up into 4 blocks of 3 trials each (Table 6). Although each trial's motion disturbance profile ended at zero degrees, the subject's tilt position was never exactly zero degrees at the end of each trial due to residual manual control error. Therefore, between each trial the subject was tilted back to zero degrees and told when they were upright, but remained in the dark. Between each block subjects were given a 1.5 minute break in which the lights were turned on so that they could maintain alertness and visually reference the vertical.

Based on Experiment 1 which found the optimal level of SVS for upright roll tilt (SCC and otolith) DR thresholds for most subjects was ±300 μA regardless of their GVS threshold, we used ±300 μA as the SVS level for all subjects in the first test session of manual control upright roll tilt nulling. Manual control performance, like measures of balance, can be inherently variable and therefore we chose to have subjects complete many trials at only two SVS levels, rather than fewer trials at many SVS levels. The SVS level that the subject received first was counterbalanced across subjects and the two mirrored motion disturbance profiles were alternated throughout the experiment so that they were given an equal number of times within each SVS level. During the breaks, no SVS was applied.

Table 6. Experiment 3 Test Protocol

Block	Trial	SVS Level (μA)		Motion Disturbance Profile
		Option 1	Option 2	
1	1	0	300	Right First
	2	0	300	Left First
	3	300	0	Right First
BREAK				
2	4	300	0	Left First
	5	0	300	Right First
	6	0	300	Left First
BREAK				
3	7	300	0	Right First
	8	300	0	Left First
	9	0	300	Right First
BREAK				
4	10	0	300	Left First
	11	300	0	Right First
	12	300	0	Left First

The second test session was identical to the first except that the nonzero SVS level given was larger. For each subject, we identified the highest level of SVS that could not be detected (either as motion perception or stimulation sensation at the electrode site) by the subject. We aimed to apply a relatively high level of SVS but still wanted the subject to remain blinded to the presence of stimulation. This level was determined prior to putting the subject on the motion device, by having the seated subject close their eyes and verbally report if they felt any sensations or symptoms beginning with ±1000 μA sinusoidal GVS and stepping down by multiples of 100. In this subject group the undetectable SVS level ranged from 700 to 900 μA (4 subjects at 900 μA, 3 subjects at 800 and 1 subject at 700 μA SVS). Whether the subject received the 0 or high nonzero level of SVS first was counterbalanced across subjects. In this second test session, subjects completed at least two practice manual control trials prior to starting the experiment.

7.2.3 Data Analysis

Data analysis focused on measures of performance related to nulling position over time and by frequency. Chair position data was collected at a 600 Hz sampling rate and was not reduced for any analysis. All testing was done in the dark and although small, we did notice a small drift in the position bias of some subjects within a trial and across trials. Therefore to compare subject performance with and without SVS applied in terms of position, we used the standard deviation of the nulled chair position. The standard deviation, or position variability metric (PVM), quantified the range of tilt position that the subject was able to maintain throughout a trial without penalizing for a potential bias in their non-visual perception of upright. A frequency analysis was also done to determine if differences in subject performance due to varying SVS levels were frequency specific. A nondimensional Scalar Performance Metric (SPM) (Merfeld et al. 1996) was used to define the subject's performance at each of the twelve frequencies in the sum of sines motion profile. The nondimensional SPM was defined as

$$SPM = \frac{\sum_{i=1}^{12}[D_1(i) - \phi(i)]}{\sum_{i=1}^{12} D_1(i)}$$

where $D_1(i)$ and $\phi(i)$ are the amplitude of the input motion disturbance and of the actual tilt position at the ith frequency included in the sum of sines motion disturbance profile. These frequency specific amplitudes were calculated using MATLAB's dft.m function. An SPM of zero represented nulling performance equivalent to if the subject had made no control inputs at all. An SPM of one represented perfect nulling of the motion disturbance. If the SPM was negative, at the particular frequency the actual chair motion was larger than if the subject would have made no control effort at all (i.e. overcompensation or overcontrolling). Our analysis looked at the SPM calculated for each specific motion disturbance input frequency and the SPM over all frequencies (above equation).

The motion disturbance profiles were scaled to ramp up (and down) for the first 5 seconds at the beginning (and end) of the trial to ensure smooth transitions out of and into rest. For our analysis, each trial was split up into two segments. The first segment included only the first 5 seconds of each trial and was used to investigate whether SVS had an effect on manual control performance when the physical stimuli was first transitioning from sub to supra threshold. The maximum

position, velocity, and acceleration of the uncompensated disturbance during the first five seconds were 5.8 deg, 6.2deg/s, 4.9 deg/s^2 (Figure 39).

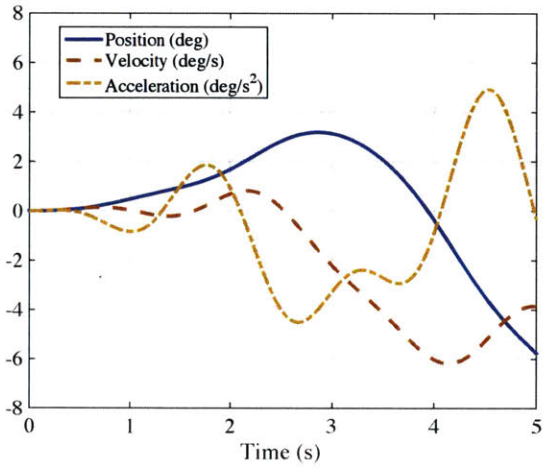

Figure 39. Angular position, velocity, and acceleration for the first 5 seconds of a 'Right First' motion disturbance profile.

The second segment of the analysis excluded the first and last five seconds of each trial. Although this 110 second segment of the trial certainly included disturbances that were sub or near vestibular perceptual threshold, it also included larger, suprathreshold, motions. The PVM was calculated for both the 5 second and 110 second trial segments while the frequency analysis (SPM) was done only for the 110 second segment. The SPM was not calculated for the initial 5 seconds of each trial because the Fourier transform requires data over a substantial amount of time so that all of the input frequencies of the input motion disturbance can be analyzed. We did not assume that task performance with 0 SVS applied was consistent across test days and therefore comparisons were only made between performance with the zero and nonzero SVS conditions within single test days.

Because we hypothesized that 300 μA SVS would improve manual control performance (i.e. lower PVM and higher SPM), Test Session 1 group comparisons between 0 and 300 μA SVS conditions were made using one-tailed paired t-tests and within-subject comparisons used one-tailed two sample t-tests. For the Test Session 2 data, comparisons between 0 and high SVS levels were done with two-tailed t-tests (paired t for group and two sample t for within subject comparisons) because we had no a priori hypothesis concerning the direction of the effect of

high SVS on manual control performance. To ensure normality assumptions were met, t-statistics and p-values reported for the PVM were calculated using log-transformed data. However, we report average differences and percentage changes using the non-transformed values for easier interpretation. We acknowledge that many t-tests were done in this analysis and that no correction for multiple tests was implemented; however we believe that the exploratory nature of this experiment warrants the reporting of unmodified statistical significance.

7.3 Results Experiment 3

7.3.1 Position Variability Metric

Over the first 5 seconds of each trial, the group mean PVM with 300 μA SVS was statistically significantly lower by 0.151 degrees than with 0 μA SVS (one-tailed paired $t(7)=1.991$, $p=0.018$). This decrease corresponded to a -21% change in PVM. Two individual subjects had a significant difference in their PVM with 0 and 300 μA SVS applied. For MC5, the PVM with 300 μA applied was 0.159 degrees less than with 0 μA SVS applied ($t(10)=2.266$, $p=0.023$) and for MC6 the PVM was 0.269 degrees less ($t(10)=2.800$, $p=0.009$). These differences corresponded to a -25% and -41% change for MC5 and MC6, respectively. Additionally, the PVM for MC8 was 0.625 degrees less with 300 μA SVS than with 0 μA SVS, trending towards significance ($t(10)=1.574$, $p=0.073$) and corresponding to a percent change of -38% (Figure 40). These differences can also be visualized in the absolute raw position means and standard deviations for each subject shown in Figure 41. A similar comparison between the mean PVM during the first five seconds when 0 and high SVS were applied in Test Session 2 showed no significant difference between the two conditions. Additionally, there were no significant differences between the 0 and high SVS conditions within any individual subjects (Raw position means and standard deviations for each subject shown in Figure 42).

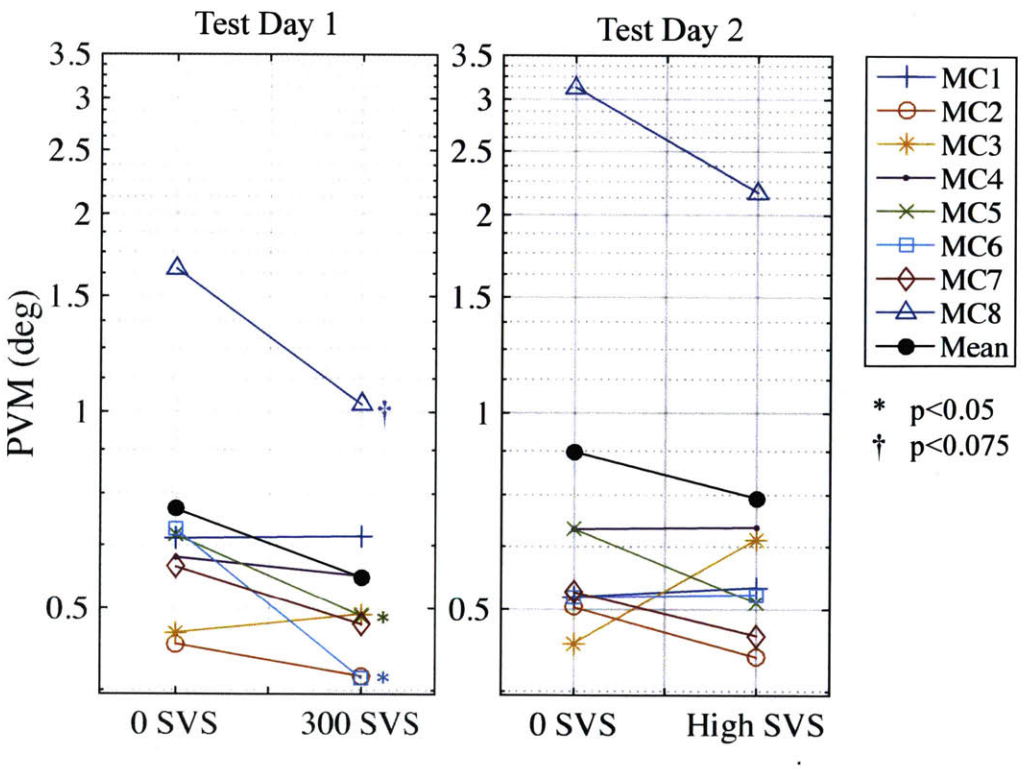

Figure 40. Each subject's PVM for the 5 second trial portion, averaged over six trials and grouped by the 0 and 300 μA SVS conditions (Test Session 1) or 0 μA and a subject specific high level (Test Session 2) SVS conditions. The black filled circles represent the average PVM by SVS condition of all subjects. In the left panel, the * symbols correspond to MC5 and MC6.

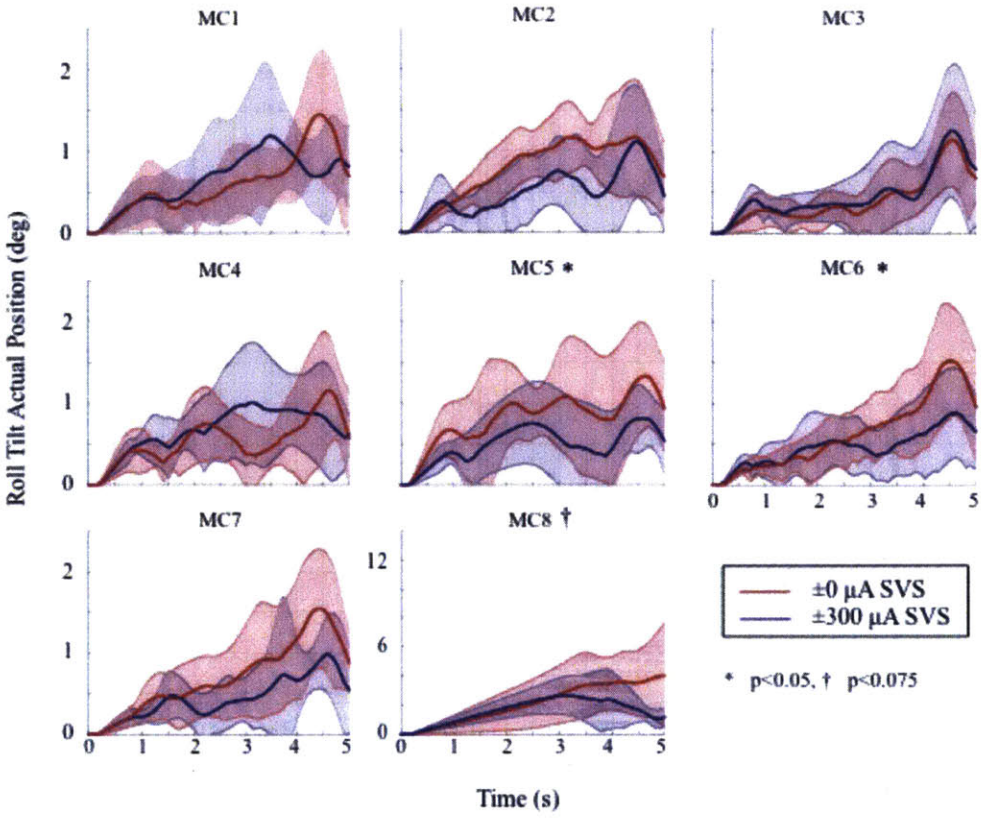

Figure 41. For each subject, mean absolute upright roll tilt position of six manual control trials in which either 0 (red) or 300 (blue) μA SVS was applied. Shaded regions represent the standard deviation of the mean at each point in time. Only the first five seconds of the trials are shown. Subjects (particularly MC5, MC6, and MC8) were able to keep the chair's upright roll tilt angle closer to upright with +/- 300 μA SVS than with no stimulation (see text for statistical tests).

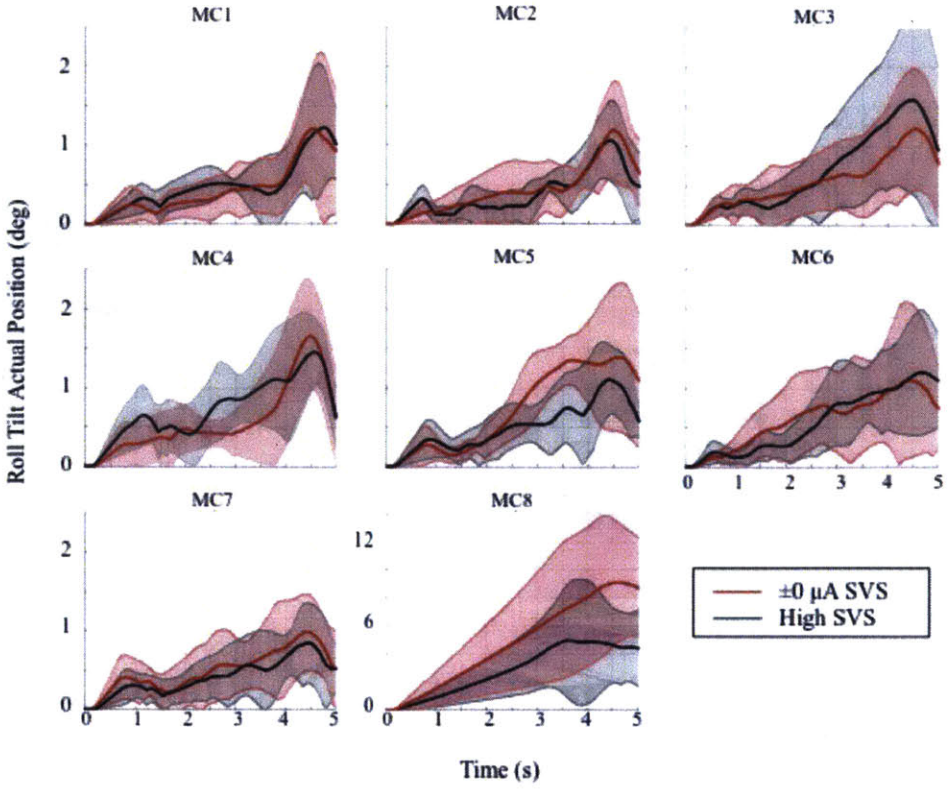

Figure 42. For each subject, mean absolute upright roll tilt position of six manual control trials in which either 0 μA (red) or a subject-specific high (black) SVS level was applied. Shaded regions represent the standard deviation of the mean at each point in time. Only the first five seconds of the trials are shown. High SVS had no significant effect on upright roll tilt nulling early in the trial compared to baseline.

When considering the 110 second segment of the manual control trials that did not include the 5 second scale up at the beginning and scale down at the end, there were no significant difference in PVM between the 0 and 300μA SVS conditions either for the group or within any individual subject (Figure 43). There was also no significant difference in the group mean PVM between the zero and high SVS conditions for this 110 second trial segment from Test Session 2. Analyzing by individual, one subject (MC8), had a significant difference in PVM of -0.693 degrees ($t(10)= 2.560$, $p=0.028$) showing that they performed better at the task by 14% with 800 μA SVS than with 0 μA SVS applied. Subject MC8 also had a significantly higher PVM in the 0 μA SVS condition than the other seven subjects (Mean difference = 3.587 deg, $t(46)=16.077$, $p<0.001$).

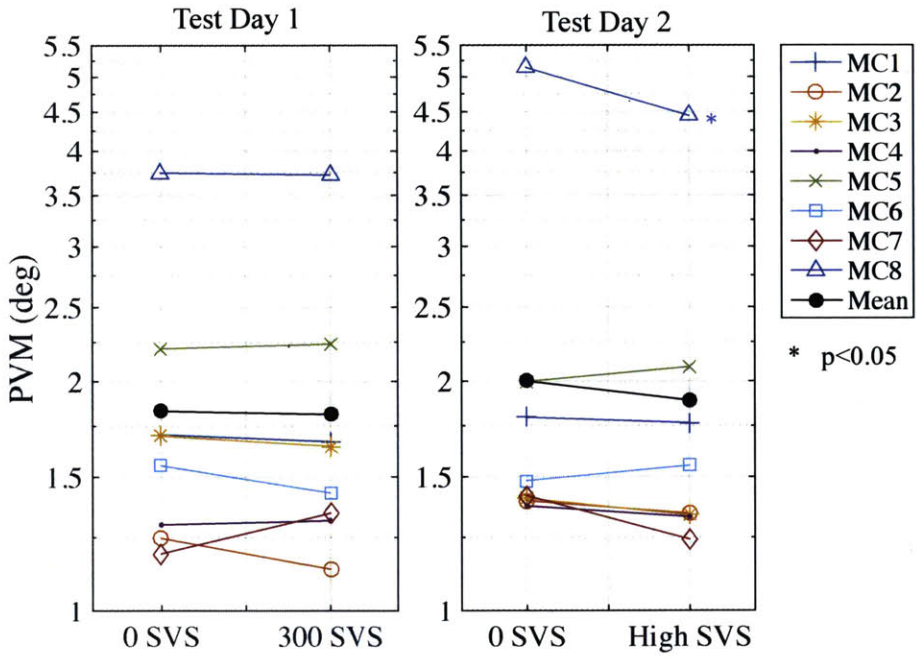

Figure 43. Each subject's PVM for the 110 second trial portion, averaged over six trials and grouped by the 0 and 300 μA SVS conditions (Test Session 1) or 0 μA and a subject specific high level (Test Session 2) SVS conditions. The black filled circles represent the average PVM by SVS condition of all subjects.

7.3.2 Frequency Analysis

Twelve independent sinusoids with different frequencies made up the sum of sines motion disturbance profile in this experiment. The SPM was calculated for each of these 12 frequencies in each of the 12 repeated manual control trials. There was no significant difference between the average SPM (including all frequencies) between the two SVS conditions on either Test Session 1 (0 and 300 SVS) or Test Session 2 (0 and high SVS). However, at a specific mid-frequency (0.209 Hz) in Test Session 1, the group mean SPM with 300 μA SVS was significantly higher (i.e. better nulling performance) by 0.148 (7.7 times greater) than the mean SPM with 0 μA SVS (one-tailed paired $t(7)=1.997$, $p=0.043$). Similarly, the group mean SPM at 0.264 Hz was six times higher with 300 μA than 0 μA SVS applied with a mean difference of 0.173 (paired $t(7)=1.553$, $p = 0.082$). In Test Session 1, 6/8 and 5/8 subjects had higher SPMs with 300 μA SVS at the 0.209 Hz and 0.264 Hz frequencies, respectively. The more consistent SVS effect between subjects at 0.209 Hz allowed for a statistically significant paired-t test result even though the mean SPMs for each of the SVS levels are farther apart at 0.264 Hz (Figure 44 Left).

In Test Session 2, the group mean SPM with 0 μA SVS was not significantly different than the mean SPM when the subject-specific high level of SVS was applied at any particular frequency (Figure 44 Right). This suggests that ±300 μA SVS proves beneficial for manual control performance, specifically at mid-frequencies (0.2-0.26 Hz), while the subject-specific high level of SVS was not beneficial.

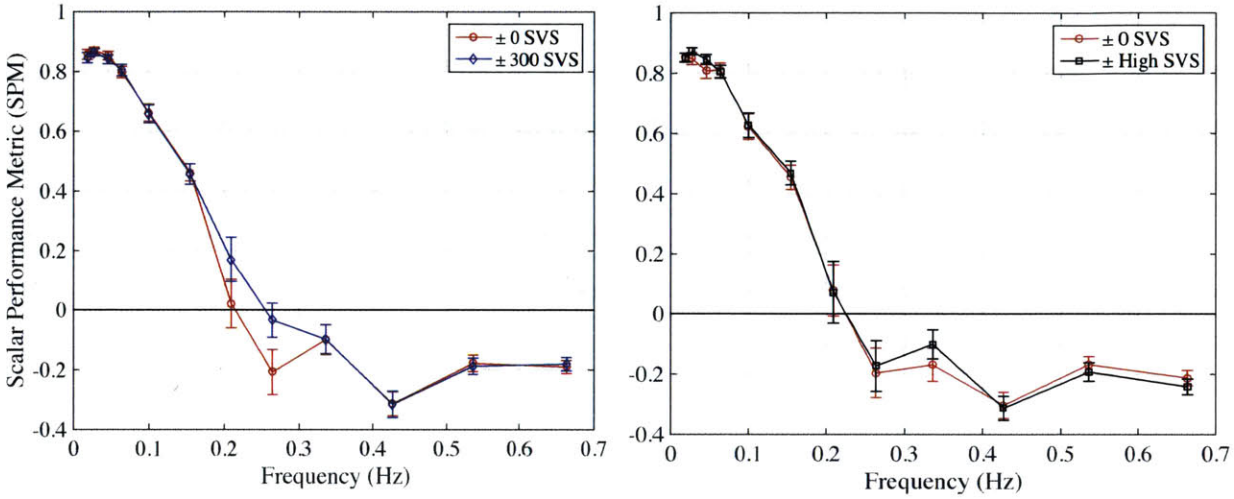

Figure 44. The mean normalized SPM and standard error of all 192 individual trials for all eight subjects split by Test Session 1 (left), Test Session 2 (right), and SVS level within the test session. The horizontal line at SPM=0 represents the point at which nulling performance transitions from better than with no control inputs (SPM>0) to worse than with no control inputs (SPM <0). SVS condition.

In Test Session 1, although 6 out of 8 subjects had a higher SPM with 300 μA SVS at 0.209 Hz, it was not statistically significantly higher for any individual subject (two-sample t-test). At 0.264 Hz, 3 out of the 8 subjects had a statistically significantly higher SPM with 300 μA SVS than with 0 μA SVS, including MC1 (mean diff = 0.263, t(10)=1.95, p=0.040), MC6 (mean diff = 0.333, t(10)=1.9, p=0.043), and MC8 (mean diff = 0.835, t(10)=3.13, p=0.005). In Test Session 2, one subject, MC6, had a statistically significantly different SPM with high SVS than 0 μA SVS at 0.264 Hz (mean diff = 0.676, t(10)-3.70, p=0.004), showing that they performed better with the high level SVS than 0 SVS. This behavior was inconsistent with the rest of the group in Test Session 2. MC4 was another subject who differed from the group in that they displayed a differentiation in performance at low frequencies between SVS levels. See Appendix 10.16 for additional details on MC6 and MC4.

7.4 Summary of Results and Discussion

This experiment aimed to investigate if the phenomenon of SR in vestibular perceptual sensitivity observed among some subjects in Experiments 1 and 2 could be exploited to create a measurable improvement in manual control task performance. Unlike Experiments 1 and 2, the task in this study required subjects to actively translate vestibular perceptual information into appropriate motor commands in order to continuously null out their motion. Understanding the effect of SVS on one's ability to not only perceive motion but also react to that motion is an important step in the advancement of SVS as a potential sensorimotor enhancement tool, particularly for aerospace applications. In this study, subjects were tested repeatedly on a two minute long manual control task with 0 μA, 300 μA (aimed to be optimal SVS), and a subject specific high level of SVS, on two separate test days. SVS levels were set below the subject's SVS stimulus perceptual threshold so that subjects were blind to the SVS level being applied during all manual control testing.

We found that 300 μA SVS improved manual control PVM by 21% for the group and for several subjects individually (ranging from 25 to 41% changes) when the motion disturbances were relatively small, during the first five seconds of each trial in which motions were transitioning from sub to suprathreshold. This level of SVS was however not broadly beneficial (in terms of PVM) when considering the rest of the manual control trial, in which the average velocity and acceleration were at least twice those of the initial five seconds. The application of the highest level of SVS that could be applied while remaining imperceptible to the subject did not help or hurt group mean performance in either portion of the trial. Initially, we were unsure if high level of SVS would impair manual control performance by providing too much added noise to the vestibular sensory channels. Alternatively, we speculated that the higher level of SVS might be necessary to facilitate an improvement in performance when the motion stimuli were considerably larger (Stocks 2000); however this was not the case. Using FitzHugh-Nagumo model neurons, Collins et al. (1995) showed that a summing network of identical units, each subjected to an independent noise source, but common input signal, can exhibit subthreshold SR by better detecting a range of weak signals. They further showed that the noise did not improve nor degrade the networks ability to detect suprathreshold signals. Like the summing network model, we applied a common input signal (the physical motion disturbance). However, unlike

the model, we applied the same, or at least similar, noise source to all units. The end result is likely similar because each vestibular neuron is not identical and has its own variability (spike timing variability in SCCs and otoliths, respectively: Goldberg and Fernandez 1971, Fernandez et al. 1972). Our results are thus phenomenologically consistent with the behavior of the simulated summing network in that with exposure to both sub- and supra-threshold stimuli, low level SVS allowed for the exhibition of subthreshold SR while not degrading the subjects' responses to suprathreshold stimuli.

A frequency analysis of the group data revealed that during the 110 second segment in between the initial and final five seconds of each trial, 300 μA SVS improved performance (higher SPM) at two of the middle range frequencies 0.209 Hz (significantly, increased SPM by 7.7 times) and 0.264 Hz (noticeable trend, increased SPM by 6 times). Previous studies, as well as the current one, found that without SVS, subjects become largely unable to null out motions over 0.2 Hz (Clark et al. 2015, Merfeld et al. 1996). However, in our study, we believe that the 300 μA SVS effectively increased the frequency bandwidth for which subjects were able to null out disturbances. Because we expected little to no nulling capability above 0.2 Hz, we designed our sum of sines motion profile to decrease in amplitude from 2.7 degrees to 0.27 degrees for all frequencies above 0.2 Hz. Perhaps 300 μA SVS would have a measurable effect on overall performance (total SPM or PVM) if more of the input disturbance power were in the frequency range between 0.2 and 0.3 Hz where SVS seemed to be most beneficial. Conversely, it may be that the extension of the frequency range due to SVS only existed because the motion amplitudes were small at those frequencies. The results from this experiment warrant further examination of nulling performance at frequencies above 0.2 Hz with higher amplitude sinusoids in order to determine if in fact the improvement in the frequency domain still persists when then motion amplitudes are large. The finding that SVS can slightly extend the frequency range of vestibular performance could also be further investigated by measuring the effect of SVS on DR thresholds near and just beyond known frequency limits (dependent on motion direction).

The extension of the frequency range at which humans can null out motions may be particularly important for manual control tasks that are on the edge of human performance limitations (e.g. helicopter hovering or planetary landing and piloting tasks). Human manual control ability at it's

limit can be seen in occurrences of pilot induced oscillations, which are often induced by a lag in a pilot's response and are most common in pitch, roll, and yaw at frequencies between 0.16 and 0.8 Hz (Mitchell et al. 2004). Pilot induced oscillations during the 5th flight of the Enterprise Space Shuttle drove a redesign of the control system software. This redesign aimed to counteract the likelihood of pilot induced oscillations at the expense of control sensitivity and even with the redesign there was evidence of a pilot induced oscillation during the landing of STS-3 (Paloski et al. 2008). In the future, if SVS can be proven to reliably extend the frequency range in which pilots can effectively control their aircraft, and if applying SVS could be practically and noninvasively implemented, it may be possible for control system software to be redesigned to give additional control sensitivity back to the pilot.

8 Thesis Conclusion

8.1 Summary of Findings and Contributions

We have found that the application of low level, noisy electrical current to the vestibular system via electrodes placed behind each ear can improve human vestibular perception of low level physical motion stimuli. We believe that this improvement in sensory performance is due to the exhibition of stochastic resonance, in which added noise enables better transfer of information through the nonlinear system. First we investigated the effect of SVS on DR thresholds (i.e. the smallest motion that a person can reliably perceive leftward from rightward motion while in darkness). We used 0.2 Hz head-centered upright roll tilt away from the upright to elicit responses from both vestibular organs - the semicircular canals and the otoliths. We found that SR was exhibited subjectively in 9/12 subjects and statistically in 6/12 subjects, with percent changes in DR threshold as large as -47%. Further, the relationship between DR thresholds and SVS level was consistent with the characteristic SR pseudo bell shaped curve within individual subjects.

Past studies of SR have reported that SR was not exhibited in all subjects tested. In our subject groups there was also less than 100% SR exhibition, however our proportion of subjects that exhibited SR in upright roll tilt was at least as high and often larger than previous SR studies that tested human subject performance. In order to better understand the likelihood of our data indicating the exhibition of SR when in fact there was no underlying SR and conversely of underlying SR existing but not being measured by our methods, we used numerical simulations of our experiment protocol to create a large dataset of simulated subjects with varying (controlled) levels of underlying SR. A comparison between our experimental data and the simulation data further solidified the exhibition of SR in the upright roll tilt motion with SVS application, even when not every subject exhibited SR.

Whether GVS differentially stimulates the SCCS or ototliths has been a topic of debate which to date is not fully settled. Whether SVS differentially affects the two vestibular organs is also unclear and relatively unstudied. Therefore in a second experiment, we investigated the effect of SVS on supine roll rotation and inter-aural translation DR thresholds, which primarily stimulate

the semicircular canals and otoliths, respectively. By again comparing our experimental results to our simulated dataset, we found essentially no SR exhibition in the supine roll rotation data set (subjectively in 3/12 subjects and statistically in 1/12 subjects). We found less ambiguous SR exhibition in the inter-aural translation measurements (subjectively in 7/11 subjects and statistically in 6/11 subjects), with proportions of SR exhibitors comparable to the upright roll tilt subject group from Experiment 1. These results suggest that the otoliths, the vestibular organs that respond to gravity and linear accelerations, are an integral component to vestibular perceptual SR exhibition. The results of our second experiment suggest that although SVS is simply a lower, noisier version of GVS, the effects of SVS and GVS on vestibular perception may not be directly related.

Finally, we aimed to study if SVS could benefit human sensorimotor performance in a task that is operationally relevant in the aerospace field. We studied the effect of a zero, low, and high level of SVS on the ability to null out whole body motion roll disturbances using a manual control bar, a task relevant to piloting. We found that low level SVS (same ± 300 μA level that caused minimal DR thresholds in many subjects in Experiment 1) helped subjects to maintain a smaller range of motion when the input disturbance was near sensory threshold (statistically significant for the group mean, corresponding to a decrease in PVM of 21% and for 2/8 individual subjects with a maximum decrease in PVM of 41%), but not over a longer period of time in which the disturbance was larger and more variable. The high level of SVS tested had no measurable effect on mean manual control performance. Since it is well known that vestibular system function is highly dependent on the frequency of the motion stimuli, we also did a frequency analysis of the manual control data. With the low level of SVS applied, 6/8 subjects were able to null out motions at a mid-frequency (0.2-0.26Hz) that without SVS was out of the controllable frequency range. This difference in SPM was statistically significant for the group mean corresponding to a 7 times increase in SPM. These results suggest that low-level SVS can extend the frequency range in which upright roll tilt motions can be sensed and nulled out in a manual control task. A few individual subjects also showed unique frequency-specific performance changes with the different level of SVS that were inconsistent with the group means, suggesting that subject-specific responses to SVS may be depend on the frequency of the physical motion stimulus.

The results of this thesis are consistent with the concept that SVS is able to extend the operating range of the vestibular perceptual system in some individuals. As such, the future of SVS applications may be broad and far reaching. Future studies should focus on better understanding inter-individual differences in the response to SVS and aim to increase the proportion of subjects that exhibit SR and the reliability of SR repeatability. These practical aspects of SVS are important in ensuring that SVS continue to be considered for future implementation in the aerospace or clinical fields.

The overall goal of this work was to start answering questions about how and when SR occurs in the human subject to progress our current understanding of SVS and better understand how it may be used in the future. The primary contributions of this work include:

1) Demonstration of the existence of stochastic resonance in vestibular perceptual DR thresholds using both subjective and objective measures, including thorough analyses of both group and individual data.
2) The acknowledgement and application of classical SR theory equations to SR in human performance as an additional analysis tool.
3) An investigation into the repeatability of SR exhibition. We found poor repeatability in upright roll tilt DR thresholds across days. This was largely due to poor baseline repeatability that occurred surprisingly often.
4) The development of a simulation based framework for thinking about the likelihood of false positives and negatives in SR data.
5) A comparison of vestibular perceptual SR specific to the two vestibular sensors, the SCCS and otoliths. Our results suggest that the otoliths might be an integral component to the exhibition of vestibular perceptual SR.
6) An investigation into whether SVS induced SR in DR thresholds could translate to a measurable improvement in a task operationally relevant to humans in aerospace. We found that group performance was improved when motion stimuli were small and when motion frequencies were near the limit of human performance.

8.2 Limitations and Future Work Directions

Limited subject pool: Our subjects were all between the ages of 18-35 and had no known vestibular disorders. However, it is possible that the benefits of SVS could be valuable for other groups. A result that was consistent across all three experiments was that the subjects that had relatively worse baseline performance, whether that be in terms of DR threshold or manual control ability, benefited the most from the application of the SVS. This suggests that SVS may be particularly useful for elderly subjects (Bermudez-Rey et al. in preparation), or certain patient groups that have degraded vestibular performance. Because one possibility is that the site of GVS activation is at the spike-trigger zone, which is further down the pathway than the hair cells, the beneficial effects of SVS may be larger for the elderly population in which the hair cell death is naturally occurring (Rosenhall 1973). However, central adaptation is believed to partially compensate for the detrimental effects of aging on the vestibular system (Matsumara and Abrose 2006). The effects of SVS in the elderly should be studied in the future.

After effects of SVS: In this research, we also largely assumed that the effect of SVS on the vestibular system does not remain once the stimulation has been stopped; however to my knowledge, this assumption has not been formally tested. In an attempt to mitigate any potential effect, we randomized the order of the SVS levels applied to each subject however future work could carefully investigate whether the application of SVS at varying levels has an effect on perception and/or performance post-SVS application, within the same day and across several days. For some subjects, results from the repeat test session in our first experiment were surprising in that the baseline DR threshold measure was lower in the second test session than in the first. One interpretation of these results would be that SVS applied on the first test session somehow affected the baseline measure in the second test session. Our experiment was not designed to study this so we cannot claim that an after effect was present however a future study could focus specifically on determining if perception is affected after SVS has previously been applied. Understanding the mechanism and duration of the effect, if it exists, could be beneficial to future sensorimotor training paradigms.

Effect of SVS on perception in other planes: Future work should include testing the effect of bilateral bipolar SVS application on perception of motions not in the coronal plane. This research gave evidence that SR due to SVS does not necessarily correspond to behavioral responses due to GVS. Although bilateral bipolar GVS primarily elicits perceptual and behavioral responses consistent with motion in the coronal plane, it's possible that bilateral bipolar SVS may be effective in inducing SR behavior in other planes. Our finding that otoliths seem to be necessary for SR exhibition suggests that DR thresholds in the yaw motion direction may not be affected since they are primarily SCC related. However SR in DR thresholds in pitch and translation in the x- (anterior-posterior) and z- (superior-inferior) axes may be exhibited with SVS, even though the bilateral bipolar electrode setup is typically associated with coronal plane motion perception.

Differences in inter-individual responses to SVS: Similar to other SR studies, we found that not all subjects were responsive to SVS. Furthermore, we found no correlations between SR exhibition, GVS thresholds, baseline direction recognition thresholds, or measured impedance. Future studies should collect additional subject-specific data to try and find a predictor of SR exhibition. Possible additional measures could relate to visual vs. vestibular dependency or tactile sensitivity. Additionally, it may be beneficial to develop a reliable and repeatable method for measuring an individual's SVS threshold, which could better correlate to the exhibition of SR in response to SVS. Although measured impedance did not seem to correlate to any other measures in our research, it may also be methodologically valuable to better understand what factors effect the impedance across the two electrodes on the mastoids, for an individual. Factors may include hydration, diet, time of day, or previous activities. Better insight into what causes variability in impedance within and between subjects could potentially provide insight into how we can achieve higher proportions of SR exhibitors in future studies.

Development of a wearable for faster and more repeatable don/doff of electrodes: Although we used the same electrode application method for all test sessions, and even though the large area of the electrodes helped to ensure stimulation of the full non-specific area, we could not ensure identical placement of the electrodes for each application. For example, we did not physically mark the subjects to ensure electrodes were placed in the exact same location in their subsequent

test session. Future work could develop a wearable that might enable easier and quicker application and removal of the electrodes and also more precise placement of the electrodes within an individual between test sessions. An initial prototype could be based on a modification to an electroencephalogram (EEG) cap.

The anatomical location of vestibular SR: In this work, we have shown the existence of SR in vestibular perception however it remains unknown where specifically, the SR is taking place. Broadly speaking, the SR phenomenon may occur in the periphery at the end organs and associated afferent neurons. It may also be taking place centrally in brain locations associated with the integration and interpretation of vestibular sensory information. One such area cited as a likely location for spatial orientation internal models is the cerebellum. We have begun work investigating whether vestibular SR is present in cerebellar dysfunctional patients, measuring upright roll tilt DR thresholds with varying levels of SVS applied, as was done in Experiment 1. This is a first step in understanding what parts of the sensory pathway are required for SR exhibition. Future studies could test patients with other localized dysfunctions to better understand where vestibular perceptual SR is occurring. These types of studies should be thoughtful about whether the SVS could be physically reaching the central area of interest (for example the cerebellum) in addition to the vestibular end organs.

The contribution of SVS in the presence of other sensory input: All of our tests were done in complete darkness and with foam padding around the subjects' heads to eliminate visual and tactile cues, and to isolate vestibular contribution to task performance. The minimization of other sensory cues is however not realistic to actual operations of astronauts or pilots. While there are piloting scenarios in which out-the-window visual cues may not be available due to dust blow back (of concern for both lunar landings (Clark et al. 2011) or helicopter landings (Szoboszlay et al. 2010)), pilots are trained to use their flight instruments to maintain situational awareness and spatial orientation. Future studies should investigate whether SVS is beneficial when visual information, such as a cockpit display, is present.

Sensorimotor adaptation with SVS: In the context of human spaceflight, sensorimotor adaptation is a central focus because of the necessity for astronauts to quickly adapt to altered gravity

environments. This body of research did not study adaptation, but instead focused on questions of how SVS fundamentally affects vestibular perception. Bloomberg et al. (2015) suggested that SVS could be used as a pre-spaceflight training aid, by enhancing the vestibular sensory information so that, for example, visually-dependent subjects may learn to use all sensory inputs more effectively. Whether SVS can be used as a post-spaceflight aid remains unknown largely due to the complexities associated with spaceflight induced sensorimotor adaptation. Future experiments using a hypergravity test paradigm could begin to investigate the possible interaction between SVS and performance in altered gravity without requiring astronaut subjects. Transitioning a subject from Earth gravity to hypergravity created by centrifugation is analogous (although certainly not identical) to the transition from spaceflight to Earth (or another planetary) gravity level. To enable a comparison to 1-G normative data collected in this work, a future experiment could measure DR thresholds and manual control nulling ability in hypergravity by centrifugation with varying levels of SVS. Measurements should be made during the G-transition and for some time after the transition to hypergravity is complete in order to understand the effects of SVS in both phases. In a future planetary exploration mission, the phases could correspond to the landing phase in which manual control is most important, and then a post-landing phase in which vestibular perception in terms of balance and locomotion are critical. In terms of atmospheric flight applications, future studies could investigate the effects of SVS on performance during different transient G-level changes such as those that occur during fighter pilot maneuvers.

9 References

Abe, C., Tanaka, K., Awazu, C., and Morita, H. (2009). Galvanic vestibular stimulation counteracts hyper- gravity-induced plastic alteration of vestibulo-cardio- vascular reflex in rats. J. Appl. Physiol. 107, 1089–1094.

Aihara, T., Kitajo, K., Nozaki, D., & Yamamoto, Y. (2008). Internal noise determines external stochastic resonance in visual perception. *Vision research*, *48*(14), 1569–73. doi:10.1016/j.visres.2008.04.022

Aihara, T., Kitajo, K., Nozaki, D., & Yamamoto, Y. (2010). How does stochastic resonance work within the human brain? – Psychophysics of internal and external noise. *Chemical Physics*, *375*(2-3), 616–624. doi:10.1016/j.chemphys.2010.04.027

Akerstedt, T., Gillberg, M (1990). Subjective and objective sleepiness in the active individual. International Journal of Neuroscience, 52:29-37.

Ali, A. S., Rowen, K. A., & Iles, J. F. (2002). Vestibular actions on back and lower limb muscles during postural tasks in man. *The Journal of Physiology*, *546*(2), 615–624. doi:10.1113/jphysiol.2002.030031

Angelaki D, McHenry M, Dickman JD, Newlands S, and Hess B. Compu-tation of inertial motion: neural strategies to resolve ambiguous otolith information. J Neurosci 19: 316–327, 1999.

Arrott AP, Young LR (1986) M.I.T./Canadian vestibular experiments on the Spacelab-1 mission. 6. Vestibular reactions to lateral acceleration following ten days of weight- lessness. Exp Brain Res 64:347-357

Arrott AP, Young LR, Merfeld DM, Lichtenberg BK (1987) Vestibular responses to linear acceleration in weightlessness. In: Proceedings of the D-1 Results Sym- posium. DFVLR Rep (in press)

Arrott, A.P., L.R. Young, and D.M. Merfeld, Perception of linear acceleration in weightlessness. Physiologist, 1991. 34(1 Suppl): S40-42.

Aw, S. T., Todd, M. J., Halmagyi, G. M., Swee, T., Todd, M. J., & Latency, G. M. H. (2006). Latency and Initiation of the Human Vestibuloocular Reflex to Pulsed Galvanic Stimulation. *J Neurophysiol*, *96*, 925–930. doi:10.1152/jn.01250.2005.

Baraduc P, Lang N, Rothwell JC, et al. Consolidation of dynamic motor learning is not disrupted by rTMS of primary motor cortex. Curr Biol 2004;14:252–256. [PubMed: 14761660]

Basner, M., & Rubinstein, J. (2011). Fitness for duty: A 3 minute version of the Psychomotor Vigilance Test predicts fatigue related declines in luggage screening performance. *Journal of occupational and environmental medicine*, *53*(10), 1146–1154. doi:10.1097/JOM.0b013e31822b8356.Fitness.

Bastian, A. J. (2008). Understanding sensorimotor adaptation and learning for rehabilitation. *Curr Opin Neurol*, *21*(6), 628–633. doi:10.1097/WCO.0b013e328315a293.Understanding

Benson AJ, Kass JR, Vogel H (1986) European vestibular experiments on the Spacelab-1 mission. 4. Thresholds of perception of whole-body linear oscillation: modification by space-flight. Exp Brain Res 64: 264-271

Benson AJ, Wetzig J (1987) Thresholds for the detection of the direction of whole-body linear movement: modifica- tion by D-1 space-flight. In: Proceedings of the D-1 Results Symposium. DFVLR Report (in press) 6.

Benzi, R., Sutera, A., & Vulpiani, A. (1981). The mechanism of stochastic resonance. *J. Phys, A: Math*, *14*, 453–457. Retrieved from http://iopscience.iop.org/0305-4470/14/11/006

Benzi, R., Parisi, G., Sutera, A., & Vulpiani, A. (1982). Stochastic resonance in climatic change. *Tellus*, *34*, 10–16. Retrieved from http://onlinelibrary.wiley.com/doi/10.1111/j.2153-3490.1982.tb01787.x/abstract

Bloomberg, J. J., Peters, B. T., Smith, S. L., Huebner, W. P., & Reschke, M. F. (1997). Locomotor head-trunk coordination strategies following space flight. *Journal of Vestibular Research : Equilibrium & Orientation*, *7*(2-3), 161–177.

Bloomberg JJ, Mulavara AP (2003) Changes in walking strategies after spaceflight. IEEE Eng Med Biol Mag 22:58–62

Bloomberg JJ, Peters BT, Cohen HS and Mulavara AP (2015) Enhancing astronaut performance using sensorimotor adaptability training. Front. Syst. Neurosci. 9:129. doi: 10.3389/fnsys.2015.00129

Boyle, R., Mensinger, A. F., Yoshida, K., Usui, S., Intravaia, A., Tricas, T., & Highstein, S. M. (2001). Neural Readaptation to Earth ' s Gravity Following Return From Space Neural. *J Neurophysiol*, *86*, 2118–2122.

Buckey, J.C. (2006). Space physiology. (p.129). New York: Oxford.

Bryanov II, Yemel'yanov MD, Matveyev AD, Mantsev EI, Tarasov IK, Yakovleva IK, Kakurin LI, Kozerenko OP, Myasnikov VI, Yeremin AV, Pervishin VI, Cherepakin MA, Purakhin YN, Rudometkin NM VCI (1976) Space flights in the Soyuz spacecraft: biomedical research. Leo Kanner Associates, Red- wood City

Séverac Cauquil, A., Faldon, M., Popov, K., Day, B. L., & Bronstein, A. M. (2003). Short-latency eye movements evoked by near-threshold galvanic vestibular stimulation. *Experimental brain research.*, *148*(3), 414–8. doi:10.1007/s00221-002-1326-z

Cevette, M. J., Stepanek, J., Cocco, D., Galea, A. M., Pradhan, G. N., Wagner, L. S., Oakley, S. R., et al. (2012). Oculo-Vestibular Recoupling Using Galvanic Vestibular Stimulation to Mitigate Simulator Sickness. *Aviation, Space, and Environmental Medicine*, *83*(6), 549–555. doi:10.3357/ASEM.3239.2012

Chaudhuri, S. E., Karmali, F., & Merfeld, D. M. (2013). Whole body motion-detection tasks can yield much lower thresholds than direction-recognition tasks: implications for the role of vibration. *Journal of Neurophysiology*, *110*(12), 2764–72. doi:10.1152/jn.00091.2013

Chaudhuri, S. E., & Merfeld, D. M. (2013). Signal detection theory and vestibular perception: III. Estimating unbiased fit parameters for psychometric functions. *Experimental Brain Research.*, *225*(1), 133–46. doi:10.1007/s00221-012-3354-7

Clark, T. K., Young, L. R., Stimpson, A. J., Duda, K. R., & Oman, C. M. (2011). Numerical Simulation of Human Orientation Perception during Lunar Landing. *Acta Astronautica, 69*(7-8), 420-428. doi:10.1016

Clark, T. K., Newman, M. C., Merfeld, D. M., Oman, C. M., & Young, L. R. (2015). Human manual control performance in hyper-gravity. *Experimental Brain Research, 233*(5), 1409–1420. doi:10.1007/s00221-015-4215-y

Clement G, Wood SJ (2014) Rocking or Rolling – Perception of Ambiguous Motion after Returning from Space. PLoS ONE 9(10): e111107. doi:10.1371/ journal.pone.0111107

Cohen, B., Yakushin, S. B., & Holstein, G. R. (2012). What Does Galvanic Vestibular Stimulation Actually Activate? *Frontiers in Neurology, 2*(January), 2011–2012. doi:10.3389/fneur.2011.00090

Collins, J., Chow, C., & Imhoff, T. (1995). Stochastic resonance without tuning. *Nature*. Retrieved from http://www.bu.edu/abl/files/stochastic_resonance_without.pdf

Collins, J., Imhoff, T., & Grigg, P. (1996a). Noise-enhanced information transmission in rat SA1 cutaneous mechanoreceptors via aperiodic stochastic resonance. *Journal of Neurophysiology*, 642–645. Retrieved from http://jn.physiology.org/content/76/1/642.short

Collins, J., Imhoff, T., & Grigg, P. (1996b). Noise-enhanced tactile sensation. *Nature; Nature*. Retrieved from http://psycnet.apa.org/psycinfo/1997-02469-001

Collins, J., Imhoff, T., & Grigg, P. (1997). Noise-mediated enhancements and decrements in human tactile sensation. *Physical Review E, 56*(1), 923–926. doi:10.1103/PhysRevE.56.923

Collins, J. J., Priplata, A. a, Gravelle, D. C., Niemi, J., Harry, J., & Lipsitz, L. a. (2003). Noise-enhanced human sensorimotor function. *IEEE engineering in medicine and biology magazine : the quarterly magazine of the Engineering in Medicine & Biology Society, 22*(2), 76–83. Retrieved from http://www.ncbi.nlm.nih.gov/pubmed/12733463

Courtine G, Pozzo T (2004) Recovery of the locomotor function after prolonged microgravity exposure. I. Head-trunk movement and locomotor equilibrium during various tasks. Exp Brain Res 158:86–99

Curthoys, I. S., & Macdougall, H. G. (2012). What galvanic vestibular stimulation actually activates. *Frontiers in Neurology, 3*(July), 117. doi:10.3389/fneur.2012.00117

Dakin, C. J., Son, G. M. L., Inglis, J. T., & Blouin, J.-S. (2007). Frequency response of human vestibular reflexes characterized by stochastic stimuli. *The Journal of physiology, 583*(Pt 3), 1117–27. doi:10.1113/jphysiol.2007.133264

Day BL, Severac Cauquil A, Bartolomei L, et al. Human body-segment tilts induced by galvanic stimulation: a vestibularly driven balance protection mechanism. J Physiol 1997; 500: 661-72.

Day BL and Cole J. Vestibular-evoked postural responses in the absence of somatosensory information. Brain 125: 2081–2088, 2002.

Day B. L., Fitzpatrick R. C. (2005). Virtual head rotation reveals a process of route reconstruction from human vestibular signals. J. Physiol. (Lond.) 567, 591–59710.1113/jphysiol.2005.092544

Della-Maggiore V, Malfait N, Ostry DJ, Paus T (2004) Stimulation of the posterior parietal cortex interferes with arm trajectory adjustments dur- ing the learning of new dynamics. J Neurosci 24:9971–9976.

Dettmer, M., Pourmoghaddam, A., Lee, B.-C., & Layne, C. S. (2015). Effects of aging and tactile stochastic resonance on postural performance and postural control in a sensory conflict task. *Somatosens Mot Res*, (November), 1–8. doi:10.3109/08990220.2015.1004045

Dilda, V., MacDougall, H. G., Curthoys, I. S., & Moore, S. T. (2012). Effects of Galvanic vestibular stimulation on cognitive function. *Experimental brain research. 216*(2), 275–85. doi:10.1007/s00221-011-2929-z

Dinges, D.F., & Powell, J.W. (1985). Microcomputer analyses of performance on a portable, simple visual RT task during sustained operations. Behavior Research Methods, Instruments, & Computers, 17:652-655.

Ditzinger, T., Stadler, M., Strüber, D., & Kelso, J. a. (2000). Noise improves three-dimensional perception: stochastic resonance and other impacts of noise to the perception of autostereograms. *Physical review. E, Statistical physics, plasmas, fluids, and related interdisciplinary topics*, *62*(2 Pt B), 2566–75. Retrieved from http://www.ncbi.nlm.nih.gov/pubmed/11088737

Einstein A. Die Grundlage der allgemeinen Relativit¨ atstheorie. Leipzig: Joh. Ambr. Barth, 1916. English version: The Meaning of Relativity. Princeton, NJ: Princeton Univ. Press, 1945.

Enders, L. R., Hur, P., Johnson, M. J., & Seo, N. J. (2013). Remote vibrotactile noise improves light touch sensation in stroke survivors' fingertips via stochastic resonance. *Journal of Neuroengineering and Rehabilitation*, *10*(1), 105. doi:10.1186/1743-0003-10-105

Ernst MO, Banks MS. Humans integrate visual and haptic information in a statistically optimal fashion. Nature 415: 429–433, 2002.

Fernandez C, Goldberg JM. Physiology of peripheral neurons innervating semicircular canals of the squirrel monkey. II. Response to sinusoidal stimulation and dynamics of peripheral vestibular system. J Neurophysiol 34: 661–675, 1971.

Fernandez, C., Goldberg, J. M., & Abend, W. (1972). Response to Static Tilts of Peripheral Innervating Otolith Organs of the Squirrel Monkey. *Journal of Neurophysiology*, *35*(6), 978–87. Retrieved from http://jn.physiology.org/content/35/6/978.short

Fitzpatrick, R., Burke, D., & Gandevia, S. C. (1994). Task-dependent reflex responses and movement illusions evoked by galvanic vestibular stimulation in standing humans. *The Journal of physiology*, *478 (Pt 2*(1994), 363–72. Retrieved from http://www.pubmedcentral.nih.gov/articlerender.fcgi?artid=1155693&tool=pmcentrez&rendertype=abstrac

Fitzpatrick, R. C., Marsden, J., Lord, S. R., & Day, B. L. (2002). Galvanic vestibular stimulation evokes sensations of body rotation. *Neuroreport*, *13*(18), 2379–2383. doi:10.1097/01.wnr.0000048002.96487

Fitzpatrick, R. C., & Day, B. L. (2004). Probing the human vestibular system with galvanic stimulation. *Journal of applied physiology (Bethesda, Md. : 1985)*, *96*(6), 2301–16. doi:10.1152/japplphysiol.00008.2004

Galica, A. M., Kang, H. G., Priplata, A. A., D'andrea, S. E., Starobinets, O. V., Sorond, F. A., et al. (2009). Subsensory vibrations to the feet reduce gait variability in elderly fallers. Gait Posture 30, 383–387. doi: 10.1016/j.gaitpost.2009.07.005

Galvani, L. (1791). De Viribus Electricitatis in Motu Musculari Commentarius. Institute of Sciences at Bologna, Bologna.

Gammaitoni, L., Hänggi, P., Jung, P., & Marchesoni, F. (1998). Stochastic resonance. *Reviews of Modern Physics*, *70*(1), 223–287. Retrieved from http://journals.aps.org/rmp/abstract/10.1103/RevModPhys.70.223

Gartenberg, D., & Parasuraman, R. (2010). Understanding Brain Arousal and Sleep Quality Using a Neuroergonomic Smart Phone Application. In *Advances in Understanding* (pp. 200–210). Retrieved from http://proactivesleep.com/understanding.brain.arousal.10.pdf

Geraghty MC, Deegan BM, Wood SJ, Serrador JM (2008) Enhancement of vestibular ocular counter-roll with subthreshold stochastic resonance galvanic stimulation. 19th international symposium on the autonomic nervous system, Kauai, Hawaii, October 29–November 1, 2008

Gingl, L.B. Kiss, and F. Moss. Non-dynamical stochastic resonance: theory and ex- periments with white and arbitrarily coloured noise. Europhys. Lett., 29:191–19, 1995.

Goel, R., Kofman, I., Jeevarajan, J., De Dios, Y., Cohen, H. S., Bloomberg, J. J., & Mulavara, A. P. (2015). Using low levels of stochastic vestibular stimulation to improve balance function. *PLoS ONE*, *10*(8), 1–24. doi:10.1371/journal.pone.0136335

Goldberg, J., & Fernandez, C. (1971). Physiology of Peripheral Neurons Innervating Semicircular Canals of the Squirrel Monkey. I. Resting Discharge and Response to Constant Angular Accelerations. *J Neurophysiol*, *34*(4), 635–60. Retrieved from http://www.mbfys.ru.nl/staff/j.vangisbergen/endnote/endnotepdfs/vestibulair/Goldberg_Fernandez_1971.pdf

Goldberg, K. M., Fernandez, C., and Smith, C. E. Responses of vestibular-nerve afferents in the squirrel monkey to externally applied galvanic cur- rents. Brain Res. 252: 156- 160, 1982

Goldberg, J. (1984). Relation between discharge regularity and responses to externally applied galvanic currents in vestibular nerve afferents of the squirrel monkey. *Journal of Neurophysiology*. Retrieved from http://jn.physiology.org/content/51/6/1236.short

Goldberg JM. Afferent diversity and the organization of central vestibular pathways. Exp. Brain Res 2000; 130: 277-97.

Goldberg, J.M., Wilson, V.J., Cullen, K.E. (2012). The Vestibular System: A sixth sense. (pp-73-75). New York. Oxford.

Grabherr, L., Nicoucar, K., Mast, F. W., & Merfeld, D. M. (2008). Vestibular thresholds for yaw rotation about an earth-vertical axis as a function of frequency. *Experimental brain research*. *186*(4), 677–81. doi:10.1007/s00221-008-1350-8

Gravelle, D. C., Laughton, C. a, Dhruv, N. T., Katdare, K. D., Niemi, J. B., Lipsitz, L. a, & Collins, J. J. (2002). Noise-enhanced balance control in older adults. *Neuroreport*, *13*(15), 1853–6. Retrieved from http://www.ncbi.nlm.nih.gov/pubmed/12395078

Hainley, C. J., Duda, K. R., Oman, C. M., & Natapoff, A. (2013). Pilot Performance, Workload, and Situation Awareness During Lunar Landing Mode Transitions. *Journal of Spacecraft and Rockets*, *50*(4), 793–801. doi:10.2514/1.A32267

Harris PA, Taylor R, Thielke R, Payne J, Gonzalez N, Conde JG. Research electronic data capture (REDCap)—A metadata-driven methodology and workflow process for providing translational research informatics support. J Biomed Inform. 2009;42(2):377–81. doi: 10.1016/j.jbi.2008.08.010. pmid:18929686

Harry, J. D., Niemi, J. B., Priplata, A. A., & Collins, J. J. (2005). Aging Technology, Fifth in a series of reports on biomedical engineering innovations. *IEEE Spectrum*, (April), 36–41.

Hartmann, M., Furrer, S., Herzog, M. H., Merfeld, D. M., & Mast, F. W. (2013). Self-motion perception training: thresholds improve in the light but not in the dark. *Experimental Brain Research*, *226*(2), 231–40. doi:10.1007/s00221-013-3428-1

Hullar TE, Minor LB (1999) High-frequency dynamics of regularly discharging canal afferents provide a linear signal for angular vestibuloocular reflexes. J Neurophysiol 82:2000–2005Ivey, C. (1998). Noise-Induced Tuning Curve Changes in Mechanoreceptors. *Journal of neurophysiology*, 1879–1890. Retrieved from http://jn.physiology.org/content/79/4/1879.short

Hullar TE, Della Santina CC, Hirvonen T, Lasker DM, Carey JP, Minor LB (2005) Responses of irregularly discharging chinchilla simicircular canal vestibular-nerve afferents during high-frequency head rotations. J Neu- rophysiol 93:2777–2786.

Jaramillo, F., & Wiesenfeld, K. (1998). Mechanoelectrical transduction assisted by Brownian motion: a role for noise in the auditory system. *Nature neuroscience*, *1*(5), 384–8. doi:10.1038/1597

Johnson, E. G., & Rust, K. F. (1992a). Chapter 5: Population Inferences and Variance Estimation for NAEP Data. *Journal of Educational and Behavioral Statistics*, *17*(2), 175–190. doi:10.3102/10769986017002175

Johnson, E. & Rust, K. (1992b). "Effective Degrees of Freedom for Variance Estimates from a Complex Sample Survey," Proceedings of the Section on Survey Research Methods, American Statistical Association

Karmali, F., Lim, K., & Merfeld, D. M. (2014). Visual and vestibular perceptual thresholds each demonstrate better precision at specific frequencies and also exhibit optimal integration. *Journal of Neurophysiology*, *111*(12), 2393–403. doi:10.1152/jn.00332.2013

Karmali, F., Chaudhuri, S. E., Yi, Y., & Merfeld, D. M. (2015). Determining thresholds using adaptive procedures and psychometric fits: evaluating efficiency using theory, simulations, and human experiments. *Experimental Brain Research*, *234*(3), 773–789. doi:10.1007/s00221-015-4501-8

Karni, A., Bertini, D. (1997) Learning perceptual skills: behavioral probes into adult cortical plasticity. Curr Opin Neurobiol 7:530-535.

Kaufman, G. D., and Perachio, A. A. (1994). Translabyrinthine electrical stimulation for the induc- tion of immediate-early genes in the gerbil brainstem. Brain Res. 646

Kaut, O., Brenig, D., Marek, M., Allert, N., & Wüllner, U. (2016). Postural Stability in Parkinson's Disease Patients Is Improved after Stochastic Resonance Therapy. *Hindawi, 2016*. doi:10.1155/2016/7948721

Kim, J., & Curthoys, I. S. (2004). Responses of primary vestibular neurons to galvanic vestibular stimulation (GVS) in the anaesthetised guinea pig. *Brain research bulletin, 64*(3), 265–71. doi:10.1016/j.brainresbull.2004.07.008

Landi, S. M., Baguear, F., & Della-Maggiore, V. (2011). One week of motor adaptation induces structural changes in primary motor cortex that predict long-term memory one year later. *The Journal of neuroscience : the official journal of the Society for Neuroscience, 31*(33), 11808–13. doi:10.1523/JNEUROSCI.2253-11.2011

Lim K, Nicoucar K, Merfeld DM. (2009). Perceptual direction-detection thresholds for whole body roll tilt about an earth-horizontal axis. Program No. 357.20/AA12. 2009 Neuroscience Meeting Planner. Chicago, IL: Society for Neuroscience, 2009 [Online]

Lim, K., & Merfeld, D. M. (2012). Signal detection theory and vestibular perception: II. Fitting perceptual thresholds as a function of frequency. *Experimental brain research. 222*(3), 303–20. doi:10.1007/s00221-012-3217-2.

Liu A, Duda K, Oman C, Natapoff A. 2002 Effects of parabolic flight zero-gravity onlooming linear vection.. Journal of Vestibular Research 11(3-5): 325

Lobel, E., & Kleine, J. (1998). Functional DRI of Galvanic Vestibular Stimulation. *Journal of ...*, 2699–2709. Retrieved from http://jn.physiology.org/content/80/5/2699.short

MacDougall, H. G., Brizuela, A. E., Burgess, A. M., Curthoys, I. S., and Halmagyi, G. M. (2005). Patient and normal three-dimensional eye- movement responses to maintained (DC) surface galvanic vestibular stimulation. Otol. Neurotol. 26, 500–511.

MacDougall, H. G., Moore, S. T., Curthoys, I. S., & Black, F. O. (2006). Modeling postural instability with Galvanic vestibular stimulation. *Experimental brain research. 172*(2), 208–20. doi:10.1007/s00221-005-0329-y

Marshburn, T. H., Kaufman, G. D., Purcell, I. M., and Perachio, A. A. (1997). Saccule contribution to imme- diate early gene induction in the gerbil brainstem with posterior canal galvanic or hypergravity stimulation. Brain Res. 761, 51–58.

Matsumura, B. A., & Ambrose, A. F. (2006). Balance in the Elderly. *Clinics in Geriatric Medicine, 22*(2), 395–412. doi:10.1016/j.cger.2005.12.007

McDonnell, M. D., & Abbott, D. (2009). What is stochastic resonance? Definitions, misconceptions, debates, and its relevance to biology. *PLoS computational biology, 5*(5), e1000348. doi:10.1371/journal.pcbi.1000348

Merfeld, D. M. Effect of spaceflight on ability to sense and control upright roll tilt: human neurovestibular experiments on SLS-2. J. Appl. Physiol. 81:50-57, 1996.

Merfeld, D.M., K.A. Polutchko, and K. Schultz (1996), Perceptual responses to linear acceleration after spaceflight: human neurovestibular studies on SLS-2. Journal of Applied Physiology. 81(1):58-68.

Merfeld, D. M. (2003). Rotation otolith tilt-translation reinterpretation (ROTTR) hypothesis: a new hypothesis to explain neurovestibular spaceflight adaptation. *Journal of vestibular research : equilibrium & orientation*, *13*(4-6), 309–20. Retrieved from http://www.ncbi.nlm.nih.gov/pubmed/15096674

Merfeld DM and Zupan LH. Neural processing of gravitoinertial cues in humans. III. Modeling tilt and translation responses. J Neurophysiol 87: 819–833, 2002.

Merfeld, D., & Park, S. (2005). Vestibular Perception and Action Employ Qualitatively Different Mechanisms. I. Frequency Response of VOR and Perceptual Responses During Translation and Tilt. *Journal of Neurophysiology*, *02114*, 186–198. doi:10.1152/jn.00904.2004

Mitchell, D., Arencibia, A., & Munoz, S. (2004). Real-Time Detection of Pilot-Induced Oscillations. In *AIAA Atmospheric Flight Mechanics Conference and Exhibit* (pp. 1–12). Providence, Rhode Island. doi:10.2514/6.2004-4700

Moore, S. T., MacDougall, H. G., Peters, B. T., Bloomberg, J. J., Curthoys, I. S., & Cohen, H. S. (2006). Modeling locomotor dysfunction following spaceflight with Galvanic vestibular stimulation. *Experimental brain research*. *174*(4), 647–59. doi:10.1007/s00221-006-0528-1

Moore, S. T., Dilda, V., & MacDougall, H. G. (2011). Galvanic Vestibular Stimulation as an Analogue of Spatial Disorientation After Spaceflight. *Aviation, Space, and Environmental Medicine*, *82*(5), 535–542. doi:10.3357/ASEM.2942.2011

Morse, R., & Evans, E. (1996). Enhancement of vowel coding for cochlear implants by addition of noise. *Nature medicine*. Retrieved from http://www.nature.com/nm/journal/v2/n8/abs/nm0896-928.html

Moss, F., Pierson, D., O'Gorman, D. Stochastic resonance: Tutorial and update. Int. J. Bifurcation Chaos, 4:1383–1397, 1994.Moss, F. (2004). Stochastic resonance and sensory information processing: a tutorial and review of application. *Clinical Neurophysiology*, *115*(2), 267–281. doi:10.1016/j.clinph.2003.09.014

Mulavara, A. P., Feiveson, A. H., Fiedler, J., Cohen, H., Peters, B. T., Miller, C., Brady, R., et al. (2010). Locomotor function after long-duration space flight: effects and motor learning during recovery. *Experimental brain research, 202*(3), 649–59. doi:10.1007/s00221-010-2171-0

Mulavara, A. P., Fiedler, M. J., Kofman, I. S., Wood, S. J., Serrador, J. M., Peters, B., Cohen, H. S., et al. (2011). Improving balance function using vestibular stochastic resonance: optimizing stimulus characteristics. *Experimental brain research*. *210*(2), 303–12. doi:10.1007/s00221-011-2633-z

Mulavara, A. P., Ruttley, T., Cohen, H. S., Peters, B. T., Miller, C., Brady, R., Merkle, L., et al. (2012). Vestibular-somatosensory convergence in head movement control during locomotion after long-duration space flight. *Journal of vestibular research : equilibrium & orientation*, *22*(2), 153–66. doi:10.3233/VES-2011-0435

Nicolis, C., & Nicolis, G. (1981). Stochastic aspects of climatic transitions- Additive fluctuations. *Tellus*, *33*, 225–234.

Nicolis, C. (1982). Stochastic aspects of climatic transitions- response to a periodic forcing. *Tellus*, 1–9. Retrieved from http://onlinelibrary.wiley.com/doi/10.1111/j.2153-3490.1982.tb01786.x/abstract

Oman , C.M., et al., The role of visual cues in microgravity spatial orientation, in The Neurolab Spacelab Mission: Neuroscience Research in Space, L.C. Buckey and J.L. Homick, eds. 2003, NASA, Houston, TX, pp. 69-82.

Paige GD, Tomko DL (1991a) Eye movement responses to linear head motion in the squirrel monkey. I. Basic characteristics. J Neurophysiol 65:1170–1182.

Pal, S., Rosengren, S. M., & Colebatch, J. G. (2009). Stochastic galvanic vestibular stimulation produces a small reduction in sway in Parkinson's disease. *Journal of vestibular research : equilibrium & orientation*, *19*(3-4), 137–42. doi:10.3233/VES-2009-0360

Paloski WH, Reschke MF, Black FO, Doxey DD, Harm DL (1992) Recovery of postural equilibrium control following spaceflight. Ann N Y Acad Sci 656:747–754

Paloski W, Oman CM, Bloomberg JJ, Reschke MF, Wood SJ, et al. Risk of sensory-motor performance failures affecting vehicle control during space missions: a review of the evidence . J Gravit Physiol 2008 ; 15 : 1 – 29 .

Parker, D.E. et al., Otolith tilt-translation reinterpretation following prolonged weightlessness: Implications for pre- flight adaptation training, Aviation, Space, and Environmental Medicine 56 (1985), 601–605.

Parker, D. et al., Vestibulo-ocular reflex changes following weightlessness and prelight and adaptation training, in: Pro- cesses in Visual and Oculomotor Systems, E. Keller and D. Zee, eds, 1986, Pergamon Press: Oxford.

Pastor M, Day B, Marsden C (1993) Vestibular induced postural responses in Parkinson's disease. Brain 116:1177–1190.

Pavlik, A., Inglis, J., & Lauk, M. (1999). The Effects of Stochastic Galvanic Vestibular Stimulation on Human Postural Sway. *Experimental brain Research*. Retrieved from http://onlinelibrary.wiley.com/doi/10.1002/cbdv.200490137/abstract

Piana, M., Canfora, M., & Riani, M. (2000). Role of noise in image processing by the human perceptive system. *Physical review. E, Statistical physics, plasmas, fluids, and related interdisciplinary topics*, *62*(1 Pt B), 1104–9. Retrieved from http://www.ncbi.nlm.nih.gov/pubmed/11088566

Priplata, A., Niemi, J., Salen, M., Harry, J., Lipsitz, L., & Collins, J. (2002). Noise-Enhanced Human Balance Control. *Physical Review Letters*, *89*(23), 238101. doi:10.1103/PhysRevLett.89.238101

Priplata, A. a, Niemi, J. B., Harry, J. D., Lipsitz, L. a, & Collins, J. J. (2003). Vibrating insoles and balance control in elderly people. *Lancet*, *362*(9390), 1123–4. doi:10.1016/S0140-6736(03)14470-4

Priplata, A. a, Patritti, B. L., Niemi, J. B., Hughes, R., Gravelle, D. C., Lipsitz, L. a, Veves, A., et al. (2006). Noise-enhanced balance control in patients with diabetes and patients with stroke. *Annals of neurology*, *59*(1), 4–12. doi:10.1002/ana.20670

Purkyne J. Commentatio de examine physiologico organi visus et systematis cutanei. In: Opera Selecta Joannis Evangelistae Purkyne, edited by Laufberger V and Studnicka F. Pragae: Spolek ceskych le ´karu, 1819

Reisine H, Simpson JI, and Henn V. A geometric analysis of semicircular canals and induced activity in their peripheral afferents in the rhesus monkey. Ann N Y Acad Sci 545: 10-20, 1988.

Reschke, M.F.,Bloomberg, J.J., Harm, D.L., Paloski, W.H., Layne, C.S., and McDonald, P.V. "Posture, locomotion, spatial orientation, and motion sickness as a function of space flight," Brain Res. Rev., vol. 28, pp.102-117, 1998.

Reynolds, R. F., & Osler, C. J. (2012). Galvanic vestibular stimulation produces sensations of rotation consistent with activation of semicircular canal afferents. *Frontiers in Neurology*, *3*(June), 104. doi:10.3389/fneur.2012.00104

Riani, M., & Simonotto, E. (1994). Stochastic Resonance in the Perceptual Interpretation of Ambiguous Figures: A Neural Network Model. *Physical Review Letters*, *72*(19), 3120–3123. doi:10.1097/01.NURSE.0000425876.00812.7d

Richardson, K. a., Imhoff, T. T., Grigg, P., & Collins, J. J. (1998). Using electrical noise to enhance the ability of humans to detect subthreshold mechanical cutaneous stimuli. *Chaos (Woodbury, N.Y.)*, *8*(3), 599–603. doi:10.1063/1.166341

Roll, R., Gilhodes, J. C., Roll, J. P., Popov, K., Charade, O., & Gurfinkel, V. (1998). Proprioceptive information processing in weightlessness. *Exp Brain Res*, (122), 393–402.

Rosenhall U. Degenerative patterns in the aging human vestibular neuro-epithelia. Acta Otolaryngol 76:208-220, 1973.

Ross, M.D., and J. Varelas, Ribbon synaptic plasticity in gravity sensors of rats flown on Neurolab, in The Neurolab Spacelab Mission: Neuroscience Research in Space, J.C. Buckey and J.L. Homick, eds. 2003, NASA, Houston, TX, pp.39-44.

Ross, S. E., Linens, S. W., Wright, C. J., & Arnold, B. L. (2013). Customized noise-stimulation intensity for bipedal stability and unipedal balance deficits associated with functional ankle instability. *Journal of Athletic Training*, *48*(4), 463–470. doi:10.4085/1062-6050-48.3.12

Rouvas-Nicolis C, Nicolis G (2007) Stochastic resonance. Scholarpedia 2: 1474.

Russell, D. F., Wilkens, L. A., & Moss, F. (1999). Use of behavioural stochastic resonance by paddle fish for feeding. *Nature*, *402*, 291–294.

Sadeghi SG, Minor LB, and Cullen KE. Response of vestibular-nerve afferents to active and passive rotations under normal conditions and after unilateral labyrinthectomy. J Neurophysiol 97: 1503-1514, 2007b. doi:10.1152/jn.00829.2006.

Samoudi, G., Jivegard, M., Mulavara, A. P., & Bergquist, F. (2015). Effects of stochastic vestibular galvanic stimulation and LDOPA on balance and motor symptoms in patients with Parkinson's disease. *Brain Stimulation*, *8*(3), 474–480. doi:10.1016/j.brs.2014.11.019

Satterthwaite, F. E. (1941). "Synthesis of Variance," Psychometrika, 16, 5, 309-316.

Schneider E, Glasauer S, Dieterich M (2002) Comparison of human ocular torsion patterns during natural and galvanic vestibular stimulation. J Neurophysiol 87:2064–2073

Schmidt L, Utz KS, Depper L, Adams M, Schaadt AK, Reinhart S, et al. Now You Feel both: Galvanic Vestibular Stimulation Induces Lasting Improvements in the Rehabilitation of Chronic Tactile Extinction. Frontiers in human neuroscience. 2013; 7:90. doi: 10.3389/fnhum.2013.00090 PMID: 23519604; PubMed Central PMCID: PMC3602932.

Scinicariello, A. P., Inglis, J. T., & Collins, J. J. (2003). The effects of stochastic monopolar galvanic vestibular stimulation on human postural sway. *Journal of vestibular research : equilibrium & orientation*, *12*(2-3), 77–85. Retrieved from http://www.ncbi.nlm.nih.gov/pubmed/12867666

Serrador, J., Blatt, M. Wood, S. (2014). A novel paradigm that restores vestibular function using imperceptible GVS stimulation. Journal of Vestibular Research 24 (2-3). Abstracts from the XXVIII Bárány Society Meeting. Buenos Aires, Argentina. May 25–28, 2014

Simonotto, E., Riani, M., Seife, C., & Roberts, M. (1997). Visual perception of stochastic resonance. *Physical Review Letters*, *256*, 6–9. Retrieved from http://link.aps.org/doi/10.1103/PhysRevLett.78.1186

Smith, C.E., Goldberg, J.M. (1986). A stochastic afterhyperpolarization model of repetitive activity in vestibular afferents. Biol Cybern 54:41-51.

Songer, J.E., Eatock, R.A. (2010). Frequency characterisitics of the mammalian saccular epithelium, NASA Human Research Program Investigators' Workshop. February 3-5, 2010. Houston, TX.

Steinz JA (1980) The Sled programme. ESA Bull 22:59- 66

Stocks, N. (2000). Suprathreshold stochastic resonance in multilevel threshold systems. *Physical Review Letters*, *84*(11), 2310–3. doi:10.1103/PhysRevLett.84.2310

Szoboszlay, Z. P., McKinley, R. A., Braddom, S. R., Harrington, W. W., Burns, H. N., & Savage, J. C. (2010). *Landing an H-60 helicopter in brownout conditions using 3D-LZ displays*. Paper presented at the Proceedings of the American Helicopter Society 66th Annual Forum.

Tukey JW. Bias and confidence in not quite large samples. Ann Math Sci 29: 614, 1958

Valko, Y., Lewis, R. F., Priesol, A. J., & Merfeld, D. M. (2012). Vestibular labyrinth contributions to human whole-body motion discrimination. *The Journal of Neuroscience : The Official Journal of the Society for Neuroscience*, *32*(39), 13537–42. doi:10.1523/JNEUROSCI.2157-12.2012

Ward, L.M., Desai, S., Rootman, D., Tata, M.S., Moss, F. (2001). Noise can help as well as hinder seeing and hearing. Bull Am Phys Soc 46:N23.002. Full paper at: http://www.aps.org/meet/MAR01/baps/vpr/layn23-002.html.

Wilkinson, D., Nicholls, S., Pattenden, C., Kilduff, P., & Milberg, W. (2008). Galvanic vestibular stimulation speeds visual memory recall. *Experimental brain research*, *189*(2), 243–8. doi:10.1007/s00221-008-1463-0

Yamamoto, Y., Struzik, Z., Soma, R., Ohashi, K., & Kwak, S. (2005). Noisy vestibular stimulation improves autonomic and motor responsiveness in central neurodegenerative disorders. Annals of Neurology, 58, 175–181.

Young LR (1974) Perceptions of the body in space: mechanisms. In: Handbook of physiology: The nervous system III, Chap 22, pp 1023– 1066.

Young LR, Oman CM, Watt DGD, Money KE, Lichtenberg BK (1984) Spatial orientation in weightlessness and readaptation to Earth's gravity. Science 225:205–208.

Young, L.R. et al., M.I.T./Canadian vestibular experiments on the Spacelab-1 mission: 1. Sensory adaptation to weightless- ness and readaptation to one-g: an overview, Experimental Brain Research 64 (1986), 291–298.

Zeng, F. G., Fu, Q. J., & Morse, R. (2000). Human hearing enhanced by noise. *Brain research*, *869*(1-2), 251–5. Retrieved from http://www.ncbi.nlm.nih.gov/pubmed/10865084

Zenner, H. P., Reuter, G., Hong, S., Zimmermann, U., & Gitter, A. H. (1992). Electrically evoked motile responses of mammalian type I vestibular hair cells. *J. Vestib. Res.-Equilib. Orientat.*, *2*(3), 181–191.

Zenner, H. P., and Zimmermann, U. (1991). Motile responses of vestibular hair cells following caloric, electrical or chemical stimuli. Acta Otolaryngol. 111, 291–297. doi: 10.3109/00016489109137390

10 Appendices

10.1 Classic SR theory concept applied to DR Thresholds

Although we used classical dynamical SR theory to fit curves to our subject data, we have yet to explicitly define the specific equation parameters and what they may represent. We purposefully did not focus on the fit parameters because there is not an obvious physiological interpretation, but rather we aimed to use the SR equation to quantify the shape of the SR trend in our data. The SR equation used represents the amplitude of the periodic response of a Brownian particle moving within a bi-stable potential well system in the presence of both weak periodic external forcing and noise. In our experiment, we might think about the bi-stable potential well as a two decision potential well in which one well represents a perception/decision of leftward motion and the other of rightward motion. Although vestibular perception also allows for the perception of no tilt, in our forced-choice task, a 'no motion' response is not an option making a bi-stable decision well appropriate. When the subject goes from zero tilt to a left tilted position for example, the depth of the left potential well may become slightly larger than that of the right potential well such that the barrier height between the right potential well and the center is less than that between the left potential well and center. Perhaps the decision variable is analogous to the Brownian particle, in that it experiences a small push into the left well from the physical motion, but it has its own noisy behavior such that it does not always end up falling into the left well. When the optimal level of noise is added to the system, it becomes more likely that the decision variable falls into the left well, resulting in more correct responses with smaller physical stimuli.

10.2 Measured Impedance

Impedance between the two electrode leads was measured prior to the GVS threshold test done at the beginning of each test session and before each DR threshold test in Experiment 1. This data is provided in Table 7 below to show that generally the measured impedance within a test session stayed relatively constant or decreased slightly over time. The time between the GVS test and the first DR threshold test was approximately 30 minutes and the time between each subsequent measurement was approximately 40 minutes.

Table 7. Impedance prior to DR threshold test (kΩ) for Experiment 1

Subject	Test Session 1						Test Session 2			
	Pre-GVS	1	2	3	4	5	Pre-GVS	1	2	3
SA	0.5	0.4	0.4	0.4	0.4	0.4	0.9	0.8	0.8	0.7
SB	0.6	0.4	0.4	0.4	0.4	0.4	0.6	0.4	0.4	0.4
SC	0.9	0.9	0.6	0.6	0.6	0.5	0.6	0.4	0.4	0.4
SD	0.7	0.5	0.5	0.5	0.5	0.5	0.7	0.6	0.6	0.6
SE	0.5	0.4	0.4	0.4	0.4	0.4	0.8	0.7	0.7	0.7
SF	0.2	0.2	0.2	0.2	0.2	0.2	0.3	0.3	0.3	0.3
SG	0.3	0.3	0.3	0.3	0.3	0.3	0.4	0.4	0.4	0.4
SH	0.7	0.6	0.6	0.5	0.5	0.5	0.6	0.5	0.4	0.4
SI	0.8	0.8	0.8	0.8	0.7	0.7	0.8	0.8	0.8	0.8
SJ	0.7	0.7	0.8	0.8	0.8	0.8	0.5	0.5	0.5	0.5
SK	0.6	0.5	0.5	0.4	0.4	0.4	0.5	0.2	0.2	0.2
SL	0.3	0.5	0.5	0.4	0.4	-	0.4	0.3	0.3	0.4

10.3 SCC and Otolith Integration

The following section discusses how the SCC/otolith crossover frequency is determined and why it is important. This data were collected (after Experiment 1 and 2 in this research) in the JVPL at MEEI in which DR thresholds were measured for 14 subjects in many motion directions and at multiple frequencies (Clark et al. in preparation). Tests included supine roll rotation (primarily SCC) at 0.1, 0.2, 0.5, 1 and 2 Hz, upright roll tilt (SCC + otolith) at 0.2 and 1 Hz, and pseudo-static tilt (primarily otolith). From this set of DR thresholds, each subject's crossover frequency was calculated as the frequency at which the DR threshold for pseudo-static tilt equals that for supine roll rotation. The crossover frequency for a single subject denoted by the black diamond in the left plot in Figure 45.

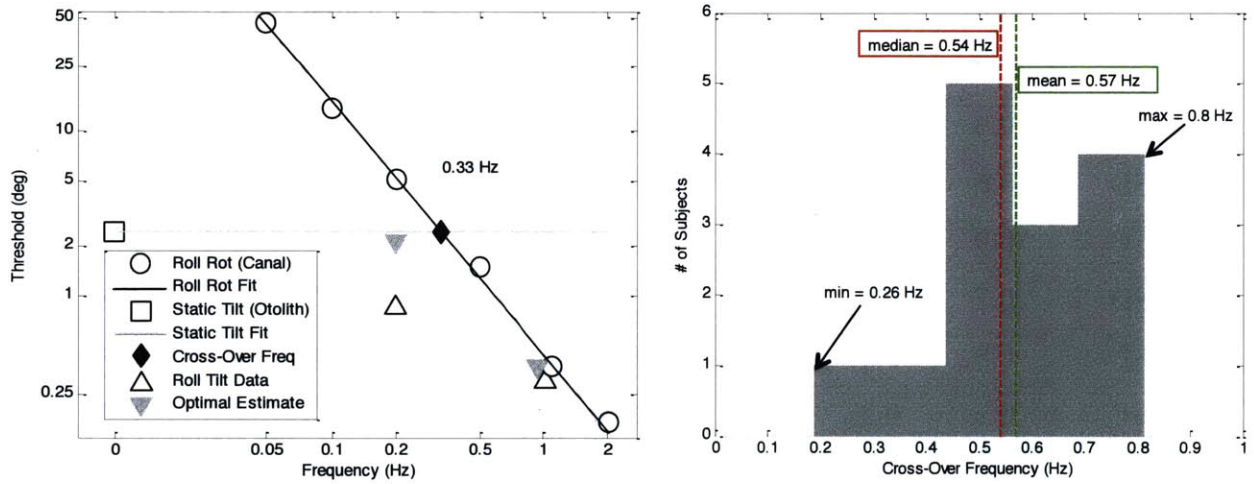

Figure 45. Crossover frequency data. Left: Thresholds over many frequencies and motions for a single example subject who has a crossover frequency of 0.33 Hz. Right: Histogram of cross over frequencies for 14 subjects.

The group mean crossover frequency was 0.57 Hz (right plot in Figure 45). This crossover frequency was higher than we originally thought when designing Experiment 1, which was meant to specifically test subjects at a frequency in which both the SCCs and otoliths contribute approximately equally to perception (by optimal integration theory, two cues should be weighted equally when they each have the same sensitivity, or threshold). The upright roll tilt frequency used in Experiment 1, 0.2 Hz, is lower than any single subject's crossover frequency tested in this subject group. However the SCC + otolith integration does not abruptly start and stop at a single frequency. In this dataset, at 0.2 Hz, 12/14 subjects' crossover ranges had at least begun.

However, the crossover data suggests that otolith contribution was probably larger than the SCC contribution at the 0.2 Hz frequency tested in Experiment 1 for the majority of subjects.

10.4 Moog and Eccentric Rotator Photographs

This section is meant to give a more detailed description of the motion devices used in Experiment 1 and 2. The left picture below (Figure 46) shows the Moog device used in upright roll tilt and inter-aural translation DR threshold tests. The subject is restrained by a 5-point harness and a modified helmet, which can be tightened around the subject's head. In this picture the subject is using an iPad to enter their responses, although in some test session, subjects were asked to use simple buttons held in each hand to indicate their perceived direction of motion. The right picture below shows the Eccentric Rotator Device configured in the supine position, used in supine roll rotation DR threshold tests. In this setup subjects were restrained by a 5-point harness, shoulder restraints, and an adjustable padded head plate restraint. It is not shown in the picture but subjects used hand held buttons to report their perceived motion direction. The main rotation motor (used typically for centrifugation) was employed for supine roll rotation DR threshold tests, rather than the tilt motor, which has a limited range of motion. Unlike in the pictures, testing on both devices was done in complete darkness and subjects always wore long sleeves and pants.

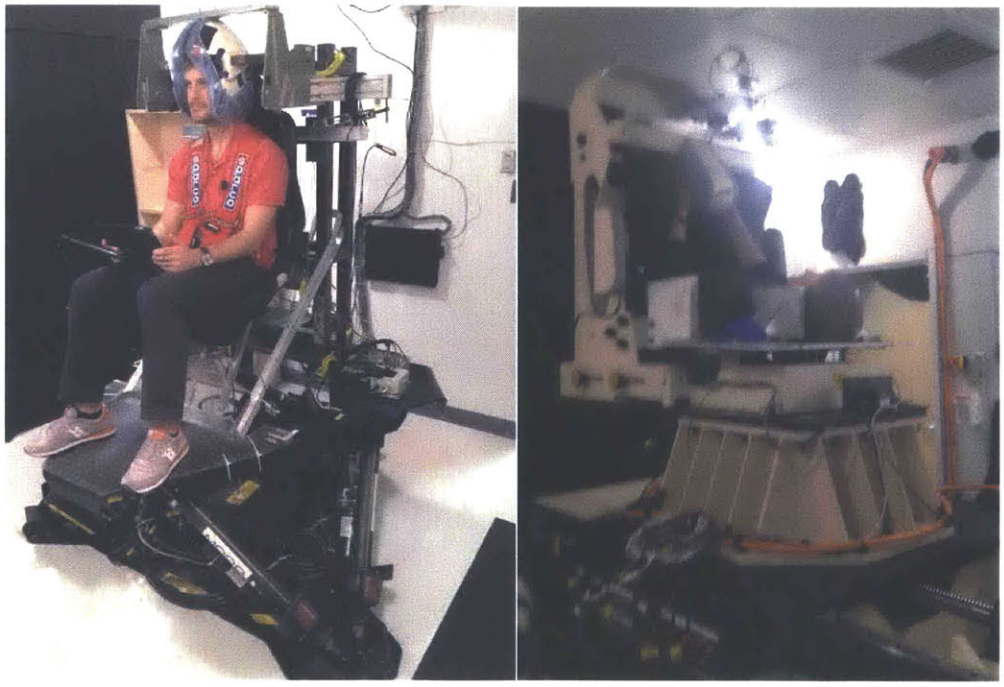

Figure 46. Photographs of the motion devices. Moog motion device (left) was used in upright roll tilt and inter-aural translation threshold tests and eccentric rotator (right) in the supine configuration used in supine roll rotation threshold tests.

10.5 Subject Codes Across Experiments

To enable a within subject comparison across experiments, Table 8 below gives the subject codes for each of the three experiments. If the cell is blank then the subject did not participate in the corresponding experiment.

Table 8. Subject codes across all three experiments.

Count	Exp. 1	Exp. 2	Exp. 3
1	SA	S1	
2	SB		
3	SC	S6	MC2
4	SD	S7	
5	SE	S8	MC6
6	SF	S9	
7	SG		
8	SH	S10	
9	SI		MC8
10	SJ		MC7
11	SK		
12	SL	S12	
13		S2	MC1
14		S3	
15		S4	
16		S5	
17		S11	MC5
18			MC3
19			MC4

10.6 Number of Trials Tested and Lapse Detection Rates

This section aims to provide details on the number of trials tested in each experiment, and the number of lapses that were identified and removed post-hoc during the DR threshold estimating process. In Experiment 1 (Test Session 1 and 2), all DR threshold tests included 150 trials. However, subject SI had relatively large roll tilt thresholds, which caused the motion device to attempt motion velocities that were outside of the range in which is was able to provide pure head-centered roll tilt motions. Using the Moog data acquisition system, we determined that velocities over 3.2 deg/s included motions outside of the roll tilt plane for the 0.2 Hz frequency being tested. We therefore omitted all subject reports for motions above 3.2 deg/s, removing 116 trials from the 750 trials collected on Test Session 1 for SI. In the supine roll rotation tests, 4/12 subjects were given 110 trials per DR threshold while the remaining 8 completed 150 trials per test. Subject S5 completed only 122 trials in the first test within the test session due to a technical issue that prevented completion of the full 150 trials. The first 15 trials were removed from SR11's data set because they reported after the test that they felt that they were still "getting used to the task" during the first 15 trials, even though they had completed the standard training prior to beginning the test session. In the inter-aural translation test sessions, all subjects completed 150 trials per DR threshold measurement. The number of lapses identified and removed from the data for the full subject groups are given in Table 9 below. The total number of lapses was relatively small, with the maximum percentage for any given test within a session of 1.3 %.

Table 9. Number of Lapses / Total number of trials for all subjects in all DR threshold test sessions from Experiments 1 and 2.

Motion	Number of Subjects	Test in Session				
		1	2	3	4	5
Upright Roll Tilt Test Session 1	12	6/1795	16/1797	9/1772	23/1747	11/1773
Upright Roll Tilt Test Session 2	12	8/1800	9/1800	16/1800		
Supine Roll Rotation	12	9/1582	14/1640	10/1640	20/1640	12/1640
Inter-aural Translation	11	10/1650	13/1650	14/1650	9/1650	11/1650

10.7 Confidence Interval Details

Calculating 95% confidence intervals (CIs) for DR thresholds is not a completely straightforward task because it is not clear what the degrees of freedom should be for a single DR threshold estimated from N number of trials. In this section we will review three methods for calculating the degrees of freedom from jackknife derived standard error of a DR threshold estimate. We choose to focus on jackknife standard errors instead of standard errors calculated from a bootstrapping method because of the necessity for symmetric error bars in calculating confidence intervals and performing statistical comparisons via t-tests.

Literature related to data from the National Association of Educational Progress (NAEP) addressed how to calculate degrees of freedom for similar data with jackknife derived standard errors in order to do a t-test between two measures. They used the Satterthwaite equation (Satterthwaite 1941), $df = \frac{\left(\sum_{k=1}^{2} SE_k^2\right)^2}{\sum_{k=1}^{2} \frac{SE_k^4}{df_k}}$ to pool the degrees of freedom from two estimates and an equation for the effective degrees of freedom $df_k = \left[\frac{\left(\sum_{j=1}^{N}(\hat{\sigma}_{jk}-\hat{\sigma}_k)^2\right)^2}{\sum_{j=1}^{N}(\hat{\sigma}_{jk}-\hat{\sigma}_k)^4}\right]$ (Johsnon and Rust 1992a), but found that this method had a downward bias such that it consistently underestimated the degrees of freedom, resulting in overly strict t-tests. Therefore, Johnston and Rust (1992b) empirically derived an adjusted equation for the effective degrees of freedom, $df = \left(3.16 - \frac{2.77}{\sqrt{N}}\right)\left[\frac{\left(\sum_{j=1}^{N}(\hat{\sigma}_{jk}-\hat{\sigma}_k)^2\right)^2}{\sum_{j=1}^{N}(\hat{\sigma}_{jk}-\hat{\sigma}_k)^4}\right]$.

To better understand if either the original or empirically derived adjusted formula for the effective degrees of freedom was appropriate to apply to our data, we ran simulations to compare three different methods. Each method used 1000-3000 simulations each estimating a threshold and CI. We then looked at how many times the underlying threshold lay outside the CI of the simulated threshold. The percentage of misses should be close to 5% if the degrees of freedom are reasonably accurate. The three methods included:

Method 1 (Blue line in Figure 47): Assume the data matches a z-distribution. Multiply the jackknife derived standard error by 1.96 to define the 95% CIs.

Method 2 (Red line in Figure 47): Use the Johnson and Rust (1992a) equation for effective degrees of freedom. Use Matlab's tinv(p,df) function to back calculate the 95% CIs.

Method 3 (Purple line in Figure 47): Use the Johnson and Rust (1992b) adjusted equation for effective degrees of freedom. Use Matlab's tinv(p, df) function to back calculate the 95% CIs.

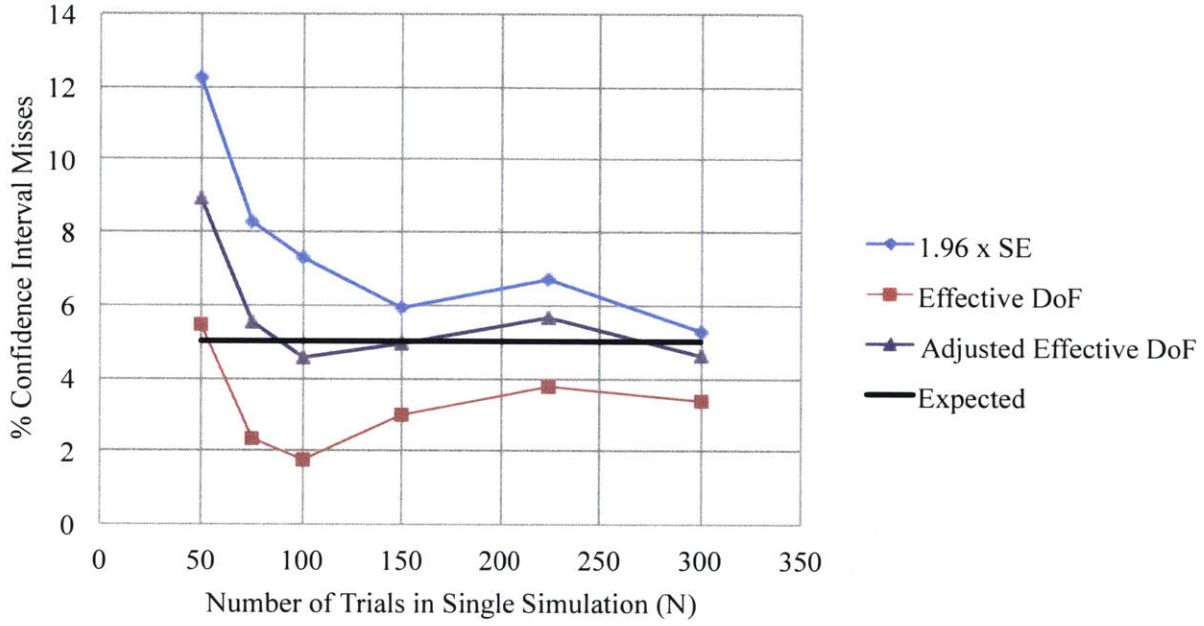

Figure 47. Percentage of 95% confidence intervals misses for three methods of calculating confidence intervals. For N<225, percentage is out of 3000 simulations, for N=225, percentage is out of 2000 simulations, for N=300, percentage is out of 1000 simulations.

The unadjusted effective degree of freedom equation underestimates the degrees of freedom for N at least equal to 75, making the CI's too large and resulting in too few misses (Figure 47). The adjusted degrees of freedom equation seems to properly adjust for this for N at least equal to 75. The difference between the percentage of misses between the 1.96 multiplier (z-assumption) and the adjusted degrees of freedom is small, especially for larger N, but the adjusted formula still provides a more accurate CI estimate.

As we were unaware of the Johnson and Rust (1992b) method at the time that we created the simulations, the CI's plotted on the figures used in the simulation judging task were calculated using the z-distribution, 1.96 multiplier. The t-tests used to determine if the minimum DR threshold was significantly lower than the baseline employed the adjusted effective degrees of freedom formula in all three experimental data sets (upright roll tilt, supine roll rotation, and inter-aural translation) in both Experiments 1 and 2.

10.8 Repeatability Experiment Sleepiness Data

This section aims to provide additional detail on the sleepiness metrics collected during the preliminary DR threshold repeatability experiment (Clark et al. in preparation). Subjective (KSS, Akerstedt and Gillberg 1990) and objective (short PVT-type test, Dinges and Powell 1985, Gartenberg and Parasuraman 2010) measures of sleepiness were taken before and after each DR threshold test during the repeatability experiment. The data discussed in this section includes upright roll tilt DR thresholds measured four times a week, for four weeks and then once per week for another 8 weeks. Each test day consisted of an upright roll tilt test and an upright yaw test (not discussed). The order of the two tests was counterbalanced such that the upright roll tilt test was first in half of the test sessions. Each upright roll tilt test consisted of 75 trials. Figure 48 below shows the subjective sleepiness score (KSS) before and after each DR threshold test. All four subjects subjectively felt sleepier after an upright roll tilt test than before. Although subjects felt sleepier after a test, their objective (PVT) sleepiness did not change.

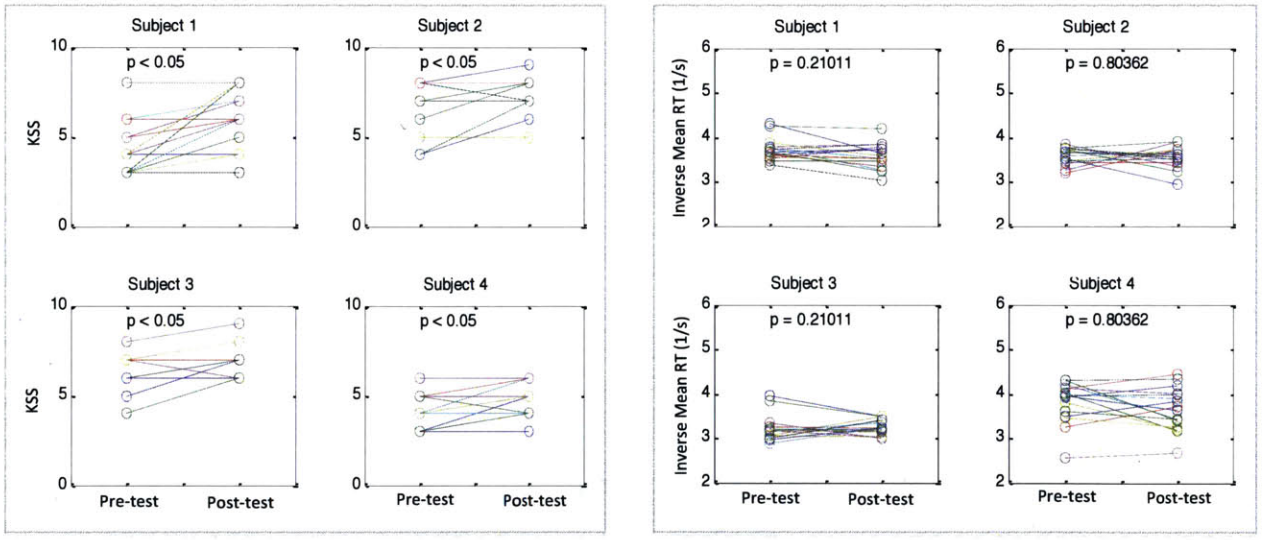

Figure 48. Pre and post test sleepiness data including subjective KSS (left) and objective PVT measure (right) measured during the preliminary repeatability experiment.

We also investigated if the subjective and objective measures of sleepiness correlated with the measured DR thresholds. If subjects were feeling or behaving sleepier, did their task performance worsen so that their DR thresholds increased? Figure 49 below shows the measured DR thresholds plotted against the post-test subjective sleepiness score (1-9 rating). The linear fit

slope was not significantly different than zero for any individual subject. The right set of plots in Figure 49 shows a similar comparison but now with the post-test objective measure of sleepiness, the mean inverse response time for the short PVT-like task. Again, we saw no significant relationship between measured DR thresholds and our objective sleepiness measure. When compared to the pre-test subjective and objective sleepiness measures, only one subject showed a significant trend. Subject 4 had a significantly negative relationship between their pre-test subjective sleepiness and DR thresholds, suggesting that for Subject 4 the more tired they felt, the better their thresholds were. Together, these results indicate that even when subjects reported feeling sleepier, or objectively behaved as if they were sleepier, we were unable to demonstrate that their DR thresholds increased.

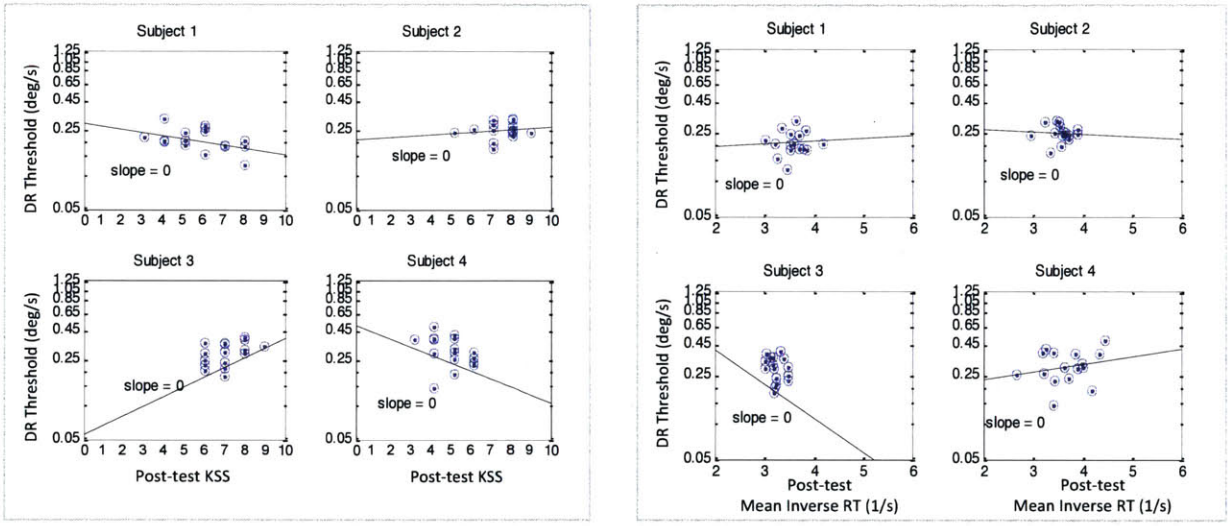

Figure 49. Sleepiness data from preliminary repeatability experiment. DR thresholds are shown against the subjective KSS scores (left) and objective PVT measures (right).

10.9 Matlab Code for SR Equation Fit

This section provides the Matlab code used in the SR equation fitting method in Experiments 1 and 2. Below are the lines of Matlab code that calls the fmsinsearchbnd function used to fit the SR equation to the data. X is a vector of SVS levels tested (can be normalized by GVS threshold, but not required). Y is the vector of measured DR thresholds for the corresponding SVS levels in vector X. These vectors need not be in order of ascending SVS level.

```
% Initialize parameters
params_init = [A0, omega0, lambda, baseline];
options = optimset('MaxFunEvals', 2000,'MaxIter',2000);
% Use fmsinsearchbnd function with lower bounds = zero and no upper bounds
params_est = fminsearchbnd(@(params) SR_eqn(params,X,Y), params_init,…
      [0,0,0,0], [-inf,-inf,-inf,-inf],options);
% Define estimated parameters from fit output.
A0_est = params_est(1);
omega0_est = params_est(2);
lambda_est = params_est(3);
baseline_est = params_est(4);
```

Below is the SR_eqn.m file called in the fminsearchbnd process above:

```
function J = SR_eqn(params, X, Y)
A0=params(1);
omega0=params(2);
lambda=params(3);
baseline=params(4);

% The 4 lines below were necessary for proper scaling
if max(X)<100
    divider=100;
else divider=1000;
end

% Equations from SR literature
rq2 = (sqrt(2)*pi)^-1.*exp(-lambda^2./(2.*(X/divider)));
y_eqn = -A0*lambda./(X/divider).*(rq2./(rq2.^2+(omega0^2./4)).^.5);
% Shifting parameter (baseline) included to allow for varying DR threshold
% baselines between subjects
y_pred = y_eqn+baseline;
% Minimize the error to find the best solution
J = sum((Y2-y_pred).^2);
```

10.10 Roll Tilt Test Session 2 DR Thresholds with Pooled Baseline

This section provides additional analysis pertaining to Experiment 1 Test Session 2 results. Because our repeatability test data was so consistent across days without SVS applied (Section 5.1.1), we analyzed the Test Session 2 upright roll tilt data with a baseline measure estimated using pooled baseline data from both test days. Pooling the baselines from the two test days changed the proportion of subjects that had a decrease in DR threshold with SVS (normalized by the optimal SVS level from Test Session 1) compared to baseline from 4/12 to 8/12. However, the proportion of subjects that had a statistically significant decrease in DR threshold using the pooled baseline did not change from 3/12 subjects (labeled by * in Figure 50).

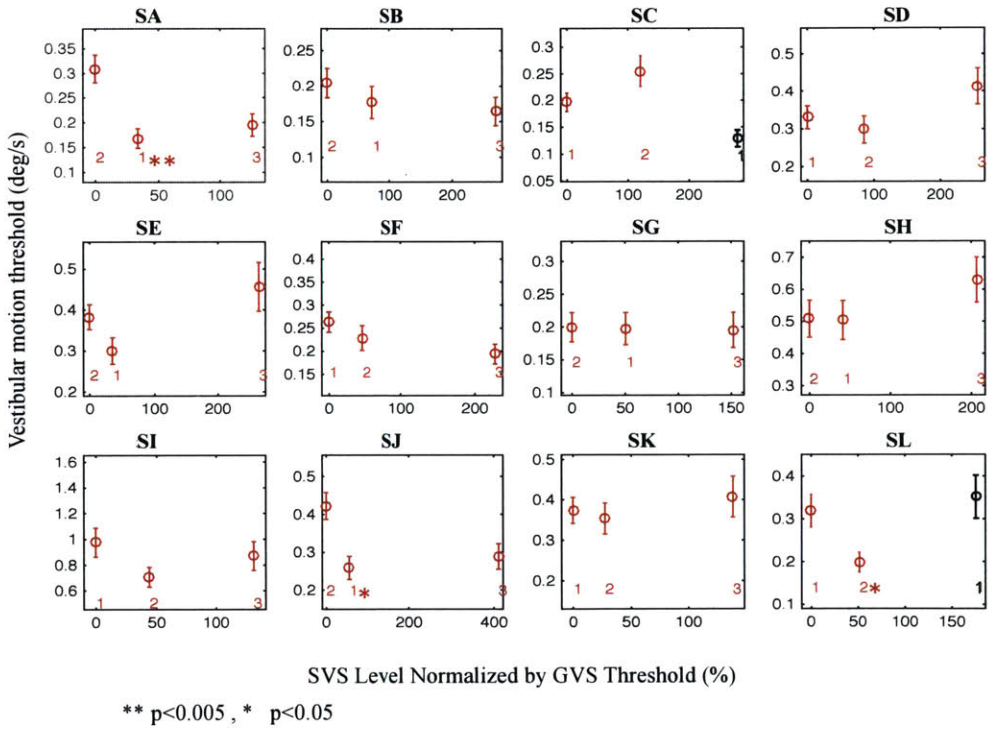

Figure 50. DR thresholds for the repeat Test Session 2 with the no SVS DR threshold estimated from baseline data pooled from both Test Session 1 and Test Session 2. Numbers represent the order of the test within the test session.

10.11 Roll Rotation Sleepiness Adjustment

This section provides additional detail on the supine roll rotation data and the linear sleepiness adjustment that was made an ultimately unsuccessful to account for the possibility that some subjects were affected by sleepiness in ways that increased their DR thresholds. Figure 51 shows the upright roll tilt DR thresholds in the order that they were collected. A simple linear fit is overlaid in orange on the data. If the linear fit was not positive, it was set to a slope of one so that a sleepiness adjustment was not made for that individual subject.

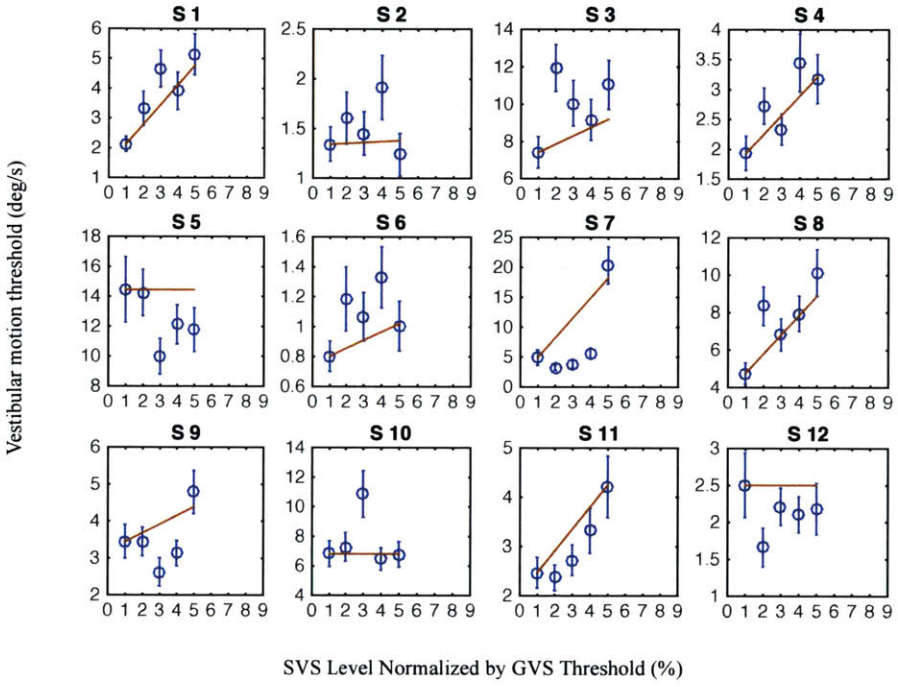

Figure 51. DR thresholds by test order in the supine roll rotation motion direction. Line represents the best linear fit to the data. If the best linear fit was negative, it is plotted as a line with slope = 0.

The linear fits were used to adjust the data, by subtracting out the effect for the particular DR threshold measurement ($\sigma_{adj} = \sigma_i - mi$), where m is the slope of the linear fit and i is the test number from 1 to 5. The adjusted DR thresholds can be seen in orange overlaid on the original data. When a reasonable fit was possible, an SR curve was fit to the adjusted data (orange lines in Figure 52).

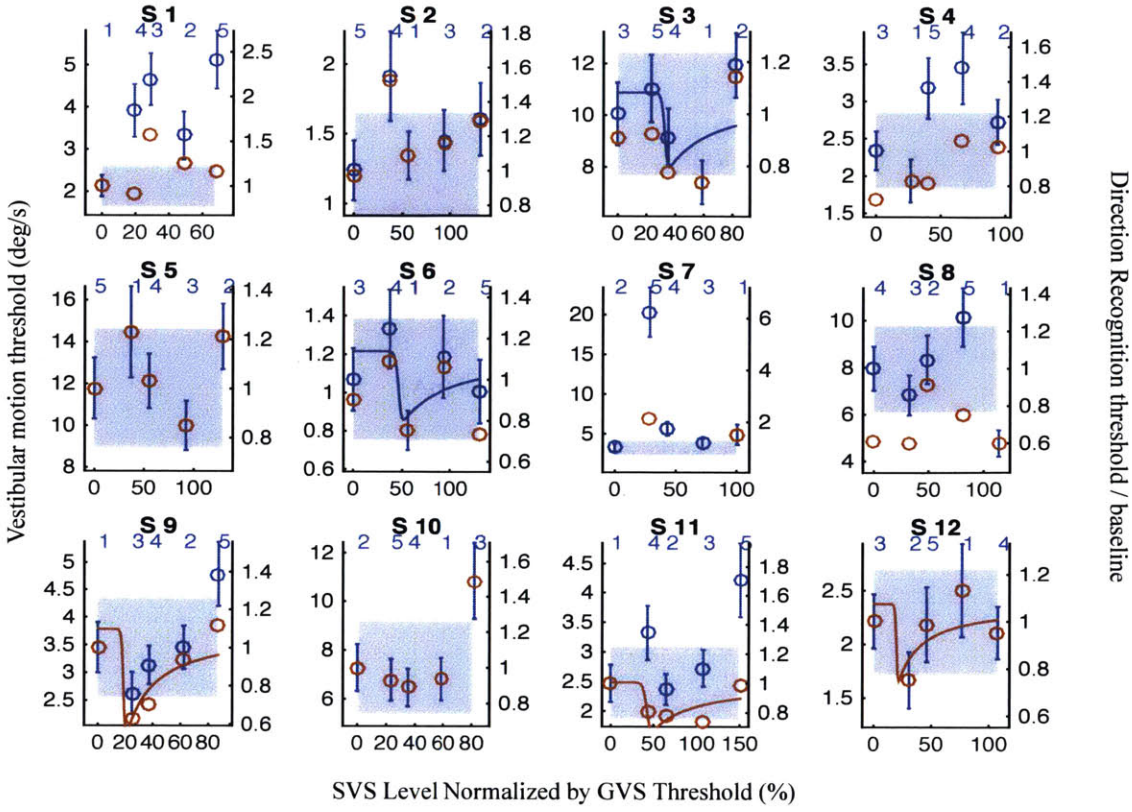

Figure 52. Supine roll rotation DR thresholds with sleepiness adjusted data and corresponding SR fit overlaid in orange.

The group data is shown in Figure 53. S7 was excluded from the following figures because their adjusted DR thresholds were negative due to the steepness of the sleepiness linear adjustment fit. Using the sleepiness adjusted data, the mean DR thresholds increase with increasing SVS level. Additionally, only five subjects had a minimum DR threshold that occurred at an SVS level other than zero. We conclude that adjusting the data with this method did not improve the proportion of SR exhibition in the supine roll rotation data set.

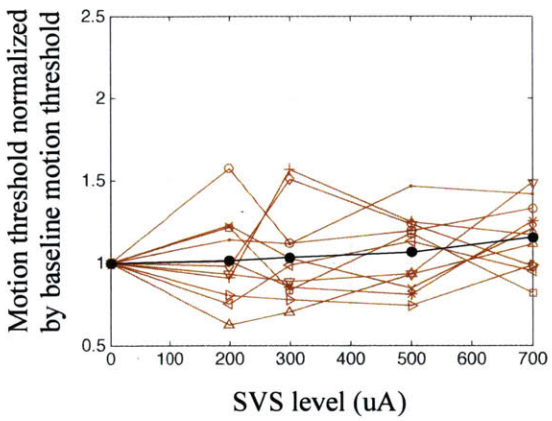

Figure 53. Group supine roll rotation sleepiness adjusted DR thresholds.

10.12 Pilot Data - Pseudo-static DR Threshold

This section provides the pilot data collected for the pseudo-static upright roll tilt DR thresholds with SVS applied. The pseudo-static upright roll tilt is a primarily otolith related motion that matches the otolith stimulation in the upright roll tilt (0.2 Hz) motion tested in Experiment 1. Pseudo-static DR thresholds with 5 levels of SVS were collected for two subjects (SC/S6 and SL/S12, left and right in Figure 54, respectively). There was considerable variability in DR thresholds with the test session however the relationship between DR threshold and SVS level did not subjectively match a characteristic SR shape for either subject.

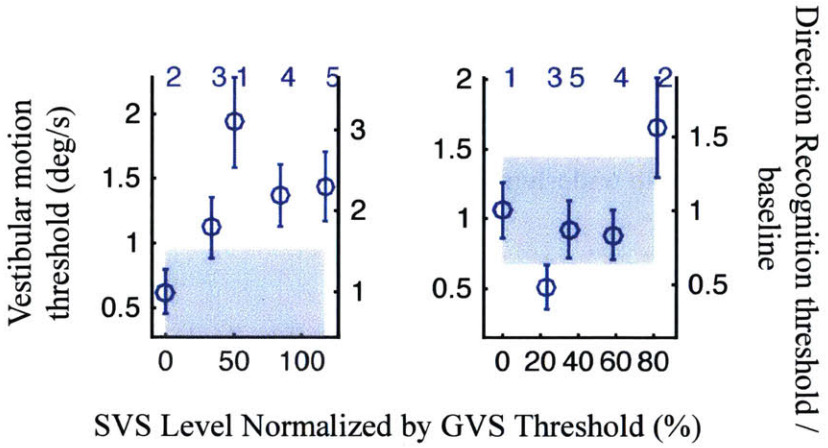

Figure 54. Pseudo-static DR thresholds for two pilot subjects. Blue shaded area represents the 95% confidence interval of the baseline, or zero SVS, DR threshold.

10.13 Pilot Data - Roll Tilt 1 Hz DR Thresholds

This section provides the pilot data collected for the 1 Hz upright roll tilt DR thresholds with SVS applied. This motion and frequency is a primarily SCC related motion like the supine roll rotation data from Experiment 2. However, it is tested in the upright position and on the same motion device as the upright roll tilt motion was in Experiment 1. Upright roll tilt DR thresholds at 1 Hz with 5 levels of SVS applied were collected for four subjects. These DR thresholds were measured on the Moog device so subjects were exposed to the same device vibrations that were present during 0.2 Hz upright roll tilt and 1 Hz inter-aural translation motions on the same device. A single subject (third in Figure 55) exhibited characteristic SR behavior however there was no statistically significant difference between the baseline and minimum DR threshold. Although only four subjects are included here, the total proportion of subjective SR exhibition, 25%, is most consistent with No underlying SR.

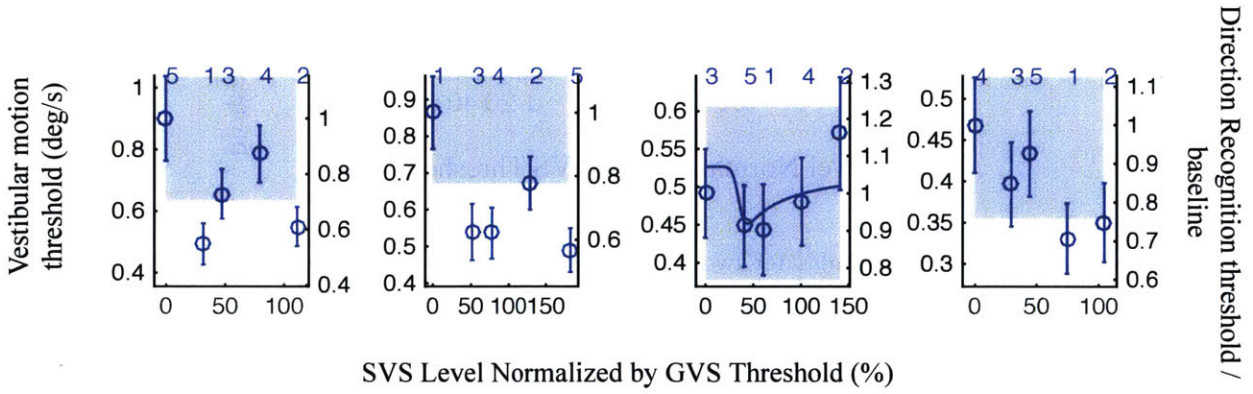

Figure 55. Upright roll tilt (1 Hz) DR thresholds for four pilot subjects. Blue shaded area represents the 95% confidence interval of the baseline, or zero SVS, DR threshold.

10.14 DR Threshold Full Test Comparisons

Table 10 below gives a summary of subjective SR exhibition for all of the experiments conducted in this research effort including pilot data collected for two subjects in pseudo-static tilt and four subjects in upright roll tilt on the Moog device at 1 Hz. The pseudo-static results are inconsistent with the higher percentage of SR exhibition found in the other primarily otolith inter-aural translation motion, however, with only two subjects it is difficult to make definitive conclusions. The rate of subjective SR exhibition in the upright roll tilt 1 Hz motions is consistent with no SR exhibition when compared to simulations suggesting that there was no true underlying SR in the primarily SCC task. Although only four subjects were tested, these results suggest that the vibrations associated with motions on the Moog device are not responsible for SR exhibition found in the upright roll tilt or inter-aural translation motions, also tested on the Moog device.

Table 10. Summary of DR threshold findings across all motion directions and frequencies tested, including pilot test data collected.

Group	**Frequency (Hz)**	**SCC/otolith**	**Subjective SR Exhibition**	**Minimum DR threshold significantly lower than baseline ($p<0.05$)**
Pseudo-static Tilt	~0	otolith	0/2 (0%)	0/12 (0%)
Roll Tilt	1	SCC	1/4 (25%)	0/4 (0%)
Roll Rotation	0.2	SCC	3/12 (25%)	1/12 (8%)
Simulations – No SR	-	-	31%	16%
Simulations – Weak SR	-	-	54%	36%
Inter-aural translation	1	otolith	7/11 (64%)	6/11 (55%)
Roll Tilt	0.2	SCC & otolith	9/12 (75%)	6/12 (50%)
Simulations – Strong SR	-	-	96%	93%

10.15 Manual Control Input Motion Disturbance Profile Details

Table 11 below gives the details of a single manual control input disturbance motion profile used in Experiment 3. The disturbance profile was a pseudo-random sum of 12 sinusoids with the listed frequencies, amplitudes, and phase shifts. There were two profiles used in the experiment that were identical but mirrored about zero ("Left First" and "Right First"). These profiles were based on those used in previous studies (Merfeld 1996, Clark et al. 2015).

Table 11.Manual control motion profile details

Test Profile			
Duration: 120 seconds			
Max rotation: 10.94 deg			
Max velocity: 6.6953 deg/s			
Max acceleration: 11.874 deg/s/s			
Sinusoid #	**Frequency [Hz]**	**Amplitude (deg)**	**Phase (deg)**
1	0.0182	2.6472	344.7292
2	0.0273	2.6472	333.387
3	0.0455	2.6472	348.5783
4	0.0636	2.6472	261.5477
5	0.1	2.6472	153.912
6	0.1545	2.6472	131.0171
7	0.2091	0.2647	226.6798
8	0.2636	0.2647	312.0295
9	0.3364	0.2647	232.9258
10	0.4273	0.2647	165.3185
11	0.5364	0.2647	70.30396
12	0.6636	0.2647	68.71478

10.16 Manual Control Individual Subjects

In Experiment 3, we primarily discussed the group mean SPM (scalar performance metric) values for the various SVS conditions (0, 300, high SVS levels). Figure 56 (Left) shows the SPMs for Subject MC4 who, unlike the other subjects, displayed performance differentiation between SVS levels at the lower frequencies in the motion profile. For this subject, the average SPM was significantly lower in the three frequencies below 0.1 Hz with 300 μA than with 0 μA SVS, indicating poorer nulling performance with the 300 μA SVS, contrary to our hypothesis (mean difference = 0.039, t(34)=3.450, p=0.002).

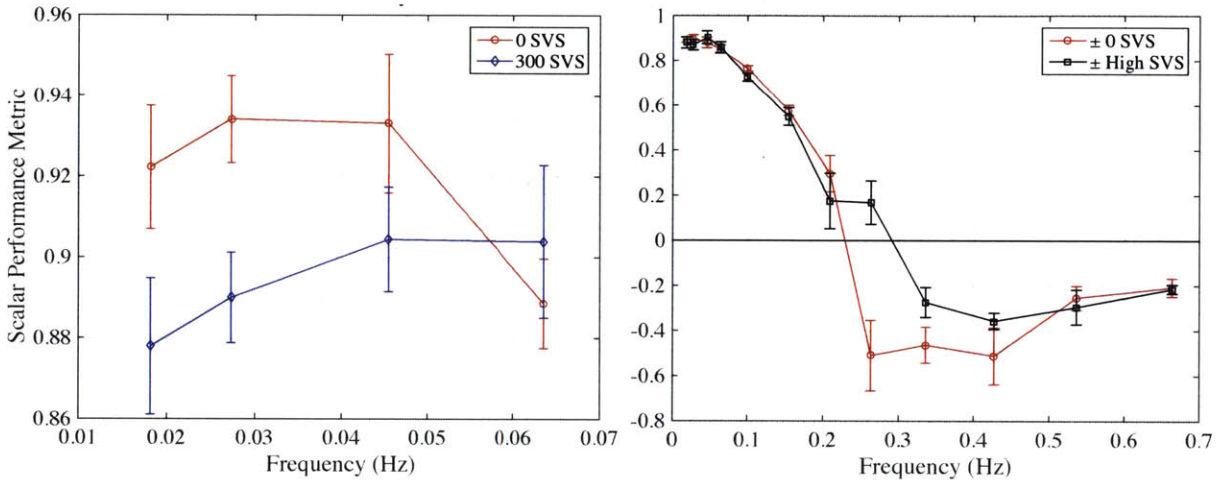

Figure 56. Average SPM and standard error for six trials in each SVS condition for Subject MC4 in Test Session 1 at low frequencies (Left) and for Subject MC6 in Test Session 2 (Right) for all frequencies. Both subjects exhibited unique behavior relative to the rest of the group.

Another subject (MC8) did exhibit an improvement in performance in PVM with the high level of SVS (Left panel in Figure 43). This subject also had considerably larger PVM (at least 2 times higher) than the other subjects. Although it is worth noting that this significant difference is primarily due to a very high PVM with no SVS in Session 2 (i.e. much higher than in session 1) as opposed to a markedly reduced PVM with the high level of SVS. As we have seen in our other experiments, the subjects that have the worst baseline performance tend to benefit most from SVS. Therefore it is also possible that our task was not difficult enough to elicit measurable differences in performance outside of the near threshold beginning stage for the majority of the subjects.

Although MC8 had an improvement in PVM with the high level of SVS, their SPM was not different between the two SVS levels. Subject MC6 however did exhibit unique behavior in Test Session 2 (Figure 56, Right) such that their SPM was significantly higher (indicating better nulling performance) with the high SVS level than with 0 SVS at 0.264 Hz. The results in this section indicate that there are subject-specific responses to SVS across particular frequencies of motion disturbances. Future studies could investigate this further and try to better understand the origin of these differences.

10.17 Health Screen Questionnaire

Below is the health screen questionnaire that was given to all subjects (via MEEI's online REDcap system) prior to testing in all three experiments. Completed questionnaires were reviewed by a MEEI lab member who was approved by the IRB to handle the personal health information. If necessary, this lab member consulted with a physician in order to either approve or disapprove subject participation. No subjects recruited for the three experiments in this research were excluded due to their health screen questionnaire results. The subject that was excluded in Experiment 2 after having completed the supine roll rotation test session was excluded from the subsequent inter-aural translation test due to a reason listed on this questionnaire. However, the subject informed the experimenter verbally rather than through the questionnaire.

Health Screen Questionnaire

Please complete the survey below.

Thank you!

Massachusetts Eye and Ear Infirmary
243 Charles Street
Boston, MA 02114

Title: Vestibular Screening Repository
HSC Protocol #: 13-087H
Principal Investigator: Daniel Merfeld, PhD

==========

DESCRIPTION AND EXPLANATION OF PROCEDURES:

The purpose of the vestibular research studies performed at Massachusetts Eye and Ear Infirmary (MEEI) is to learn how information from different sensory systems, including the vestibular system (the portion of the inner ear that measures both motion and orientation of the head), is used by the brain. One of our goals is to improve diagnostic testing. To determine your eligibility to participate in a vestibular research study (or studies), you are being asked to complete a health questionnaire. We will use the health questionnaire responses to determine if you are eligible to continue the screening process for any of our studies. If found eligible, you may also be asked to complete up to five more surveys: -Beck anxiety inventory, dizziness handicap inventory (DHI), Motion Sickness Susceptibility Questionnaire Short-form (MSSQ-Short), Epworth Sleepiness Scale, and/or the Headache Impact Test - 6 (version 1.1). If you are not eligible for any of our active studies, you will not need to perform any additional steps at this time; but if you qualify for a future study, you may be contacted at that time.

RISKS AND DISCOMFORTS

There is a small risk that information provided on this form could become known to others. This risk is small. For evaluation purposes, information from this health questionnaire will be placed into a database that is stored in a secure partition provided by MEEI. This information will not be deleted if you do not qualify for this study, but, as noted above, the information will remain coded your name will never be included as part of your data. Furthermore, only a limited number of qualified individuals approved by the MEEI human studies committee will ever be authorized to review these secure records.

POTENTIAL BENEFITS:

Our research projects will contribute new information on vestibular function and spatial orientation and may lead to improved vestibular diagnostics. There is no direct benefit to you for participating in this screening.

ALTERNATIVE TREATMENTS:

You may choose not to participate in this study.

CONFIDENTIALITY:
Information derived from this study may be used for research purposes that may include publication and teaching. However, information used for publication and teaching will not disclose your identity. Because this research is regulated by the Food and Drug Administration (FDA), and funded by the National Institutes of Health, the FDA or the Office of Human Research Protections (OHRP) may inspect records related to this research, which may include your protected health information or other information about you derived or maintained as part of this study.

We are required by the Health Insurance Portability and Accountability Act (HIPAA) to protect the privacy of health information obtained for research. This is an abbreviated notice, and does not describe all details of this requirement. During this study identifiable information about you or your health will be collected and shared with the researchers conducting the research. In general, under federal law, identifiable health information is private. However, there are exceptions to this rule. In some cases, others may see your identifiable health information for purposes of research oversight, quality control, public health and safety, or law enforcement. We share your health information only when we must, and we ask anyone who receives it from us to protect your privacy.

RIGHT TO WITHDRAW:
Your participation in this study is entirely voluntary, and you may withdraw from the study. The quality of care you will receive at MEEI will not be affected in any way if you decide not to participate or if you withdraw from the study.

RIGHT TO ASK QUESTIONS:
You are free to ask any questions you may have about the study or your treatment as a research subject. Further information about any aspect of this study is available now or at any time during the course of the study from the principal investigator, Dr. Daniel Merfeld, at (617) 573-5595. Additionally, you may contact the Office of Research Administration at (617) 573-3446 if you have any questions or concerns about your treatment as a research subject.

COSTS AND COMPENSATION FOR PARTICIPATION
There are no costs to you for this screening. You will not be paid to take part in this screening.

CONSENT
The purpose and procedures of this screening process simply involve filling out questionnaires/surveys. The possible risks and benefits have been fully and adequately explained to me in the above text, and I understand them. Specifically, I am being asked to fill out the attached health screening questionnaire now. I understand that I may later be asked to fill out up to five more additional short surveys for this research project. I voluntarily agree to participate as a subject in these questionnaires/surveys and understand that by completing this questionnaire, I am indicating that agreement. I have been provided an electronic copy of this form.

Age _____

FIRST NAME _____

MIDDLE NAME (preferred, but optional) _____

LAST NAME _____

Have you ever had problems with any of the following

- ☐ Dental
- ☐ Neck
- ☐ Jaw
- ☐ Joints
- ☐ Back

If yes, please explain

_____

Have you ever had any of the following

- ☐ High blood pressure
- ☐ Heart rhythm disturbance
- ☐ Stomach/intestinal disease
- ☐ Cancer
- ☐ High cholesterol
- ☐ Neurological disorder
- ☐ Heart disease
- ☐ Lung disease
- ☐ Diabetes
- ☐ Thyroid disease
- ☐ Panic attacks and/or depression
- ☐ Other

If yes, please explain

_____

Have you ever had any of the following symptoms

- ☐ Change in hearing
- ☐ Pain/pressure in ear
- ☐ Migraine headaches
- ☐ Loss of vision
- ☐ Vertigo (sense of spinning)
- ☐ Illusion that visual world is moving
- ☐ Tinnitus (noise in ear)
- ☐ Headaches
- ☐ Blurred vision
- ☐ Double vision

If yes, please explain

_____

Does anyone in your extended family have problems with dizziness, imbalance or hearing loss?

- ○ Yes
- ○ No

If yes, please explain

_____

On a scale of 1-10 (1 being none and 10 being severe), how would you rate your motion sickness susceptibility?

○ 1 ○ 2 ○ 3 ○ 4 ○ 5 ○ 6 ○ 7 ○ 8 ○ 9 ○ 10

If your answer is greater than a 1, please explain

_____

On a scale of 1-10 (1 being none and 10 being severe), how would you rate your tendency for claustrophobia?

○ 1 ○ 2 ○ 3 ○ 4 ○ 5 ○ 6 ○ 7 ○ 8 ○ 9 ○ 10

If your answer is greater than a 1, please explain

_____

Do you ever have panic attacks?

○ Yes
○ No

If yes, please explain

_____

Have you ever been hospitalized?

○ Yes
○ No

If yes, please explain

_____

Do you use any medications?

○ Yes
○ No

If yes, please list all current medications

_____

What company provides your health care insurance? _____

Have you ever?

☐ Smoked
☐ Used alcohol
☐ Used other drugs

Do you wear glasses or contacts?

○ Yes
○ No

WOMEN ONLY
What is your menstrual status?

○ Postmenopausal
○ Premenopausal
○ Pregnant
○ Other

If other, please explain

_____

WOMEN ONLY
Please list any birth control prescription(s) that you use _____

Height _____

ft/in or cm?

○ ft/in ○ cm

Weight _____

lbs or Kg?	○ lbs ○ Kg
Gender	○ Female ○ Male
Please click calendar icon to select your BIRTH DATE	_____
Hispanic or Latino	○ No ○ Yes
Ethnicity	○ American Indian/Alaska Native ○ Asian ○ White ○ Native Hawaiian or Other Pacific Islander ○ Black or African American ○ More than one race
If you checked More than one race, please choose all that apply	☐ American Indian/Alaska Native ☐ Asian ☐ White ☐ Native Hawaiian or Other Pacific Islander ☐ Black or African American

Note: To keep the information you have provided on this form secure, we ask that you return this form to us by mail at the address immediately below or in person. You can also choose to return this form by fax (available upon request) or email (available upon request) but neither email nor fax are guaranteed to be secure.

Mailing address:

Subject Recruiter

Jenks Vestibular Physiology Lab

MEEI Room 421.

243 Charles St

Boston MA 02114

AFTER YOU HIT SUBMIT, IT COULD TAKE UP TO 1 MINUTE FOR PROCESSING. PLEASE DO NOT CLOSE YOUR BROWSER.